Techneau 2.4.
JUNE 2007

MODELLING OF MICROPOLLUTANT REMOVAL BY OZONATION AND CHLORINATION IN POTABLE WATER TREATMENT

BIBLIOGRAPHIC REPORT

MODELLING OF MICROPOLLUTANT REMOVAL BY OZONATION AND CHLORINATION IN POTABLE WATER TREATMENT

BIBLIOGRAPHIC REPORT

Colophon

Title
Modelling of micropollutant removal by ozonation and chlorination in potable water treatment

Author
Pierre Mandel

Quality Assurance
Béatrice Balannec
University of Rennes
Pascal Roche
Anjou Recherche, Veolia Water
Dominique Wolbert
National School of Chemistry, Rennes

Urs von Gunten (WP leader)
EAWAG

Deliverable number
D 2.4.2.6. First report on the development of the modeling software developed by Anjou

This report is: **PU** = Public

Summary

In regards of increasingly stringent rules on toxicity, prediction engines for potable water treatment have become a necessity. This particularly applies to oxidation steps, where micropollutants should be removed and where potentially harmful by-products may be formed, and has therefore lead to the building up of a new simulator for both chlorination and ozonation.

This first report aims at giving a clear overview on the investigation fields related to modelling of oxidation for water purification. Different aspects are thus developed in the following pages. Besides kinetics and hydraulics, special topics on informatics and applied mathematics are discussed as well, presenting simulators that exist and specific calculation procedures. The originality of the modelling lies namely in its adaptability to on site conditions, which implies specific numerical methods to be implemented.

Basing on the bibliographic review (illustrated by first numerical examples), the present work finally will exhibit the challenges to be faced during development.

Table of contents

Introduction

Management of oxidation steps involved in the treatment of potable waters is presently based on few measurements, partially collected at the outlet of the processes, as residual ozone. Now, the vast majority of oxidation simulators that have been developed perform their calculation downstream assuming the whole initial state, i.e. the inlet, to be known.

Considering this contradiction, we therefore propose to build up an innovative simulator adapted to on-site conditions: simple and effective, provided only with few measurements (from the inlet or the outlet), its indications should insure a good level of disinfection combined with an acceptable by-products formation rate. Presently, such a tool already exists ($SimO_3$), predicting concentration profiles (including micropopollutant removal); on the base of the knowledge of the inlet composition though. Our aim is hence to ameliorate and develop it further, adapting its calculation procedures to on site conditions.

Such a task implies a multi-disciplinary approach of the problem: figure **1** illustrates the research fields (and their overlapping zones) associated with it. Our aim is to give here a clear and concise overview of these topics, presenting the four main aspects of the bibliographic work: Kinetics, Hydrodynamics, Applied Mathematics and Informatics.

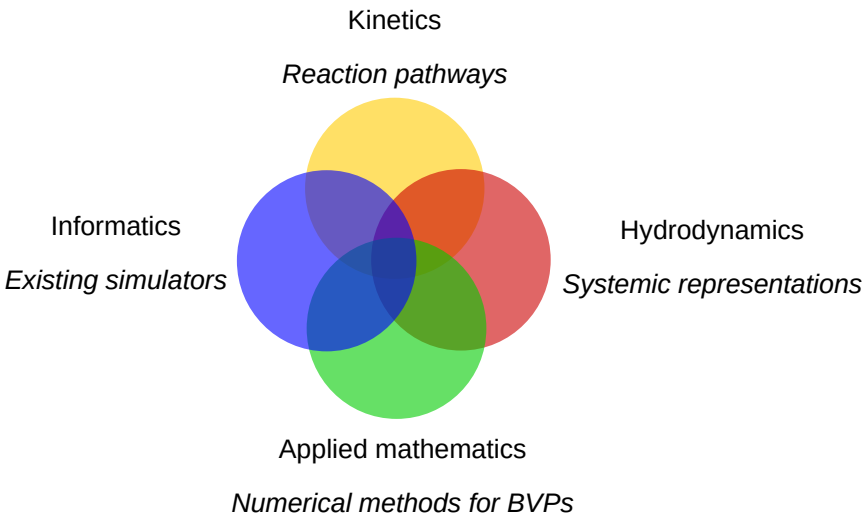

Figure 1 Schematic overview of the bibliography

Since the purpose of a bibliographic report is to refine the investigation field, we shall ask the questions:

"What has been done? What can be adapted? What is still to be developed?"

These questions will concern the knowledge or techniques involved in each research field: *existing simulators, reaction pathways*, *systemic representations*,

numerical methods for BVP[1]s. Finally, basing on the answers to the previous questions, we will exhibit the challenges to be faced during the development of our simulator.

In continuance of this introduction, readers not familiar with potable water treatment are invited to examine the next section, a more precise presentation of the context of the PhD work: the role of oxidation steps in water treatment is explained, the working of the process itself is detailed, the legal frame is set. The list of micropollutants taken into account in this study is given as well.

[1] BVP : Boundary Value Problem

1. PRELIMINARY PRESENTATION OF THE CONTEXT

In this introductory section, our goal is basically to set the frame of the study, letting appear the first difficulties one faces when modeling oxidation steps. We shall therefore present the main physical and chemical aspects involved in the treatment of potable water, focusing on the oxidation steps.

1.1. Water treatment steps

A summarizing scheme for water treatment works is given in Figure **1.1**. Each step of a typical potable water treatment is now briefly described, following the water stream from the intake source to the distribution network.

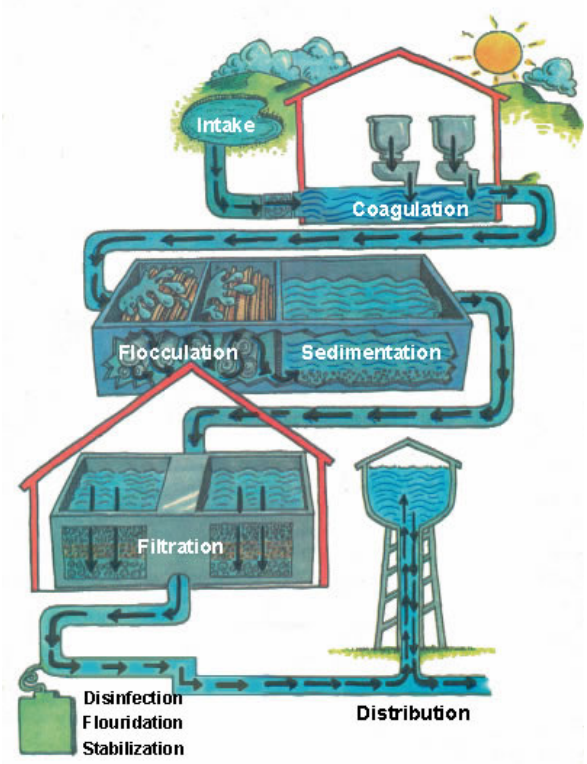

Figure 1.1 Schematic overview of a potable water treatment works (source: city of Longmont, Colorado, USA)

1.1.1. Coagulation and flocculation: the clarification

First stage in water treatment, coagulation (combined with flocculation) removes dirt and other particles suspended in water, "gluing" them together, so that they settle out of the water or stick to sand or other granules in a granular media filter.

Naturally, most of the suspended water particles bear a negative electrical charge, which keeps particles dispersed (similar particles repel each other). Coagulation works by eliminating the natural electrical charge of the suspended particles so they attract and stick together during flocculation. The so formed "flocs" are then heavy enough to settle during sedimentation.

The selected coagulants aim to destabilise the particles, thus allowing as many particles to collide as possible, generating large and robust flocs. Aluminium sulphate is a widely used coagulant, which reacts with water to form flocs of aluminium hydroxide. Iron (II) sulfate and iron (III) chloride are other common coagulants - unfortunately not effective with many source waters. Cationic and other polymers can also be used as coagulant aids in conjunction with other inorganic coagulants.

1.1.2. Sedimentation

Water exiting the flocculation basin may next enter the sedimentation basin, also called clarifier or settling basin. Designed as a large tank with slow flow, allowing floc to settle to the bottom, the sedimentation basin can be in the shape of a rectangle, where water flows from end to end, or circular where flow is from the centre outward. The amount of floc that settles out of the water is dependent on the water residence time and on the depth of the basin (a deep basin will allow more floc to settle out than a shallow one). The retention time of the water must therefore be balanced against the cost of a larger basin - normally, the minimum clarifier retention time is about 4 hours.
An increasingly popular method for floc removal is dissolved air flotation. How does it work? A proportion of clarified water, typical 5-10% of throughput, is recycled and air is dissolved in it under pressure. The biphasic mixing is then injected at the bottom of the clarifier tank where tiny air bubbles are formed that attach themselves to the floc particles and float them to the surface. A sludge blanket is formed, periodically removed using mechanical scrapers. This method is very efficient for floc removal and reduces loading on filters, however it is unsuitable for water sources with a high concentration of sediment.

1.1.3. Filtration

Water shall afterwards be filtered in order to remove remaining suspended particles and unsettled floc. Most commonly, the rapid sand filter is employed: water passes vertically (downward) through a sand layer often covered with a deposit of activated carbon or anthracite coal. The top layer removes organic compounds, which contribute to taste and odour. The major part of the particles passes through surface layers but is then trapped in pore spaces or adheres to sand particles. Undeniably, effective filtration extends into the depth of the filter: if the top layer were to block all the particles, the filter would quickly clog.
To clean the filter, water is passed quickly upward through it, opposite the normal direction (called backflushing or backwashing) to remove embedded particles. Prior to this, compressed air may be blown up through the bottom of the filter to break up the compacted filter media to aid the backwashing process: this is known as air scouring.

1.1.4. Disinfection (by means of oxidation)

Disinfection is generally the last step in purifying drinking water. Its goal: to kill or inactivate any pathogens[2], which have passed through the filters. Its means: mostly oxidation, though techniques involving other physico-chemical phenomena exist (e.g. W radiation, ultrasound, ultrafiltration, reverse osmosis…). Aside from the disinfection itself, public water supplies are in addition required to maintain a residual disinfecting agent throughout the distribution system, in which water may remain for days before reaching the consumer.

Aiming to model the oxidation steps of drinking water treatment, we shall mainly present two disinfection techniques: chlorination and ozonation. UV processes will only be mentioned.

1. Chlorination: the most common disinfection method uses chlorine, a strong **oxidant** that kills many micro-organisms, or its associated compounds chloramine or chlorine dioxide.

For safety reasons (toxicity of the chlorine gas), sodium hypochlorite can be preferred to chlorine. However, in both cases, there are remaining drawbacks. One drawback to the use of gaseous chlorine or sodium hypochlorite is their potential reaction with organic compounds present in water to form harmful chemical by-products **THMs** (TriHaloMethanes) and **HAAs** (HaloAcetic Acids), both of which are carcinogenic in large quantities and regulated by sanitary authorities (e.g. USEPA (U.S. Environmental Protection Agency), European Council). A way to minimise the formation of THMs and HAAs is the preventive removal of organics from the water prior to chlorine addition. As for chlorine as a disinfectant, although effective in killing bacteria, it has limited effectiveness against protozoans that form cysts in water (*Giardia lamblia* and *Cryptosporidium*, both of which are pathogenic).

Chlorine dioxide - another fast-acting disinfectant - is rarely used, due to the excessive amounts of chlorate and chlorite potentially created. Chlorine dioxide also poses extreme risks in handling: not only is the gas toxic, but it may spontaneously detonate upon accidental release to the atmosphere.

Though being weaker oxidant agents as chlorine gas or sodium hypochlorite, chloramines are of interest because less prone to form THMs or HAAs. Their use remains however limited.

2. Ozone (O_3) is a relatively unstable molecule of oxygen, which readily gives up one atom of oxygen providing a powerful **oxidising agent**, toxic to most water borne organisms. Widely used in Europe, it is an effective oxidant to inactivate harmful protozoans that form cysts. It also works well against almost all other pathogens.

Ozone is produced by passing oxygen through ultraviolet light or a "cold" electrical discharge. To use it as a disinfectant, it must be created on site and added to the water; generally the transfer occurs through bubble contact. The use of ozone induces some advantages: among them, the production of relatively fewer dangerous by-products (in comparison to chlorination) and the absence of taste and odour produced by ozonation. Nevertheless, it has

[2] such as viruses; bacteria, including *Escherichia coli* and *Campylobacter*; *protozoans*, including *G. lamblia* and other *Cryptosporidia*

been discovered that the ozonation is susceptible to produce a small amount of the suspected carcinogen **bromate** (BrO_3^-), even if small amounts of bromine (Br^-) are present in raw water. Moreover, due to its instability in water, ozone does not persist, thus leaving no disinfectant agents for the water still to be purified on its way to the consumer (no remanence phenomenon).

The list of micropollutants considered in this study will therefore include the bromate ions, the THMs and HAAs, and also some pesticides of growing interest (such as atrazine). Further, other compounds will also be investigated: deethylatrazine, deisopropylatrazine, alachlor, sulfamethoxazole, carbamazepine, MTBE.

3. UV radiation (light) is very effective at inactivating cysts, as long as the water has a low level of colour so the UV can pass through without being absorbed. The main disadvantage to the use of UV radiation is that, like ozone treatment, it leaves no residual disinfectant in the water.

Because neither ozone nor UV radiation leaves a residual disinfectant in the water, it is sometimes necessary to add an end-of-pipe residual disinfectant. This is often done through the addition of chlorine or chloramines, discussed above as a primary disinfectant. When used in this manner, chloramines provide an effective residual disinfectant with very little of the negative aspects of chlorination.
In the following, we will only consider the two techniques involving oxidation, but let us now have a closer look at one oxidation process: ozonation, presenting in brief some relevant technical aspects (chlorination processes will not be considered since they can be compared to ozonation contact chambers, see following).

1.2. Ozonation process: the ozone contactor

Basically, an ozonation system comprises three different units: the ozone generator, the ozone contactor, and an ozone destruction device. Only the ozone contactor shall be discussed here.
Disinfection will take place all the better if ozone is brought into the water and dispersed as finely as possible. This is accomplished generally through fine bubble diffusers located in baffled chambers (see Figure **1.2**), transfer column or in a turbine type contactor. Baffled chamber diffusers seem to be most prevalent, and the number of chambers, their geometry, the diffuser systems, and their operation differ from plant to plant and are subject to the experience of the design engineers.
Not represented on figure **1.2** following, a typical ozone contactor usually has several compartments in series with bubble diffusers at the bottom. In the first compartment, the water flows downward against the rising bubbles, and in the second compartment the water flows upward. The chambers are covered to prevent the escape of ozone and to increase the partial pressure of the ozone in the contactor. Additional chambers follow to guarantee a contact time between the ozone and the water. These are subsequently called "contact chambers" or "clear wells" and allow the disinfecting action to complete.

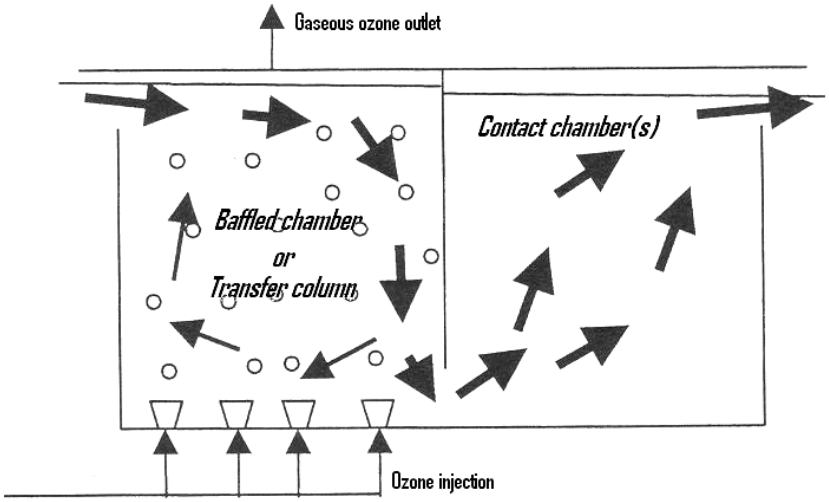

Figure 1.2 Scheme of an ozonation process (for clarity reasons, we only represented one chamber of each type: transfer and contact), adapted from [Savary, 2002]

As it can be seen on figure **1.2**, passing from tank to tank, the water flow is submitted to changing conditions. Indeed, whereas mixing and stirring are highly desirable during the transfer in order to disperse ozone effectively, the optimal conditions for a complete disinfecting action approach those reigning in a PFR (Plug Flow Reactor) – i.e. with no recirculation. Modeling an ozonation process by means of CFD (Computational Fluid Dynamics) or systemic models (see **Appendix C**), one will thus have to modify the hydrodynamic representation between transfer and contact chambers.
Ozone concentration measurements are usually performed at the outlet, thus providing residual ozone. This value is then used to calculate the product of concentration and retention time to get the required CT ((concentration of

residual ozone)*(exposure time)) value[3]. A more precise evaluation of disinfection can be achieved when each of the chambers has sampling ports so that the ozone concentration profile throughout the process is known (*more explanation on CT concept available in* **Appendix B**).

[3] according to the USEPA guidelines, which have set the CT values to be respected, the last chamber should still have an ozone concentration of 0.1 ppm.

1.3. Legal frame for DBPs[4]

Although widely used, chlorine (or its related compounds) and ozone as powerful oxidising agents have shown their limits. Actually, as mentioned above, brought into natural water, these species, reacting with naturally occurring organic substances, are prone to form so-called DBPs (Disinfection By-Products), potentially harmful.
The USEPA regulatory instance has therefore set levels of authorized contamination for various species. The main target compounds with their limits are listed in Stage 1 Disinfectants and Disinfection By-Products Rule (Stage 1 DBPR), which was issued in 1998 (see Table **1.1**). Moreover, draft drinking water regulations in the U.S. have specified MRDLs (Maximum Residual Disinfectant Levels) for chlorine and chloramines of 4.0 mg/L as Cl_2; the MRDL for chlorine dioxide is 0.8 mg/L.
The Stage 1DBPR (Disinfection By-Products Regulation) regulates four DBPs. Since DBPs can continue to form as long as the organic substances and disinfectant are present, the highest concentrations are usually found at the farthest points of the system. The MCLs (Maximum Contaminant Levels) for DBPs are as follows

Table 1.1 Level of authorized contamination – 1DBPR (source: USEPA)

Contaminant	MCL (mg/L)
Total Trihalomethanes (TTHM)	0.080
Five Haloacetic Acids (HAA5)	0.060
Bromate	0.010
Chlorite	1.0

These norms already entered in force: indeed, every affected system had to develop a system-specific monitoring plan to be available for inspection by January 31, 2004.
With a slight delay, the European Instances followed the American position. So, the European Council emitted on November 3, 1998 the 98/83/EC directive on the quality of water intended for human consumption, which regulates water quality at the tap [Roccaro et al., 2005], [Duguet et al., 2006]. Here are the European MCLs

Table 1.2 Level of authorized contamination – 98/83/EC (source: European Portal, http://europa.eu)

Contaminant	MCL (mg/L)	
	December 25, 2003	December 25, 2008
Total Trihalomethanes (TTHM)	0.150	0.100
Bromate	0.025	0.010
Chlorite	0.200	

[4] More generally, the European legislation for disinfection can be found in **Appendix A**; see also **3.1.3.** for the US legislation on *Giardia* cysts and viruses removal

Having defined the context of the study in this introductory section, the first following remarks can be expressed

- Oxidation processes only represent a way to achieve water disinfection, the last step in potable water treatment
- Considering the hydrodynamics, the changing flow conditions discredit a too simple modelling approach
- Running an oxidation process, one has to conceal two antagonist aspects: a good disinfection and few by-products
- Micropollutants considered herein follow: bromate ions, HAAs, THMs, atrazine, deethylatrazine, deisopropylatrazine, alachlor, sulfamethoxazole, carbamazepine, MTBE.

2. ALREADY EXISTING SIMULATORS

All the existing water treatment plant simulators, be it for potable water or wastewater propose, more or less, the same functionalities: design, process optimisation, operator training, educational purposes, automation. Some of them, such as GPS-X (wastewater treatment simulator developed by Hydromantis), also include cost savings investigation modes.
Furthermore, the simulators are very similar in their use. The interface allows building up one's own model and then to run the simulation, having specified certain characteristics (regarding the water, the processes etc…). Table **2.1** gives an overview of the most common simulators currently available.

Table 2.1 Comparison of water treatment works simulators

Name	Developed by	Use	Highlights/ Strenghts	Drawbacks/ Weaknesses	Chemical models
OTTER	WRc	Potable water	Readily extensible by users familiar with FORTRAN/C/C++	Excessive data needs	Semi-empirical relations
Stimela	TU Delft	Potable water	Online access	Simplistic oxidation models	Semi-empirical relations (see next)
Metrex	University of Duisburg	Potable water	Particle removal	Not tested on site	Mechanistic + correlations
Watpro	Hydromantis	Potable water	Disinfection-DBPs	Long calibration time: 1 year of data!	USEPA correlations
WTPmodel	USEPA	Potable water	Removal of NOM-DBPs	Limited validity domain	Empirical relations
BioWin	Envirosim	Wastewater	Activated sludge	No oxidation module	ASM (IWA)
WEST	Hemmis	Wastewater	Editing model mode	Simplistic oxidation models	ASM (IWA)

Contrary to the simulator to be developed, all the simulators present in the table **2.1** are not oxidation-specific. They all aim at simulating a whole water treatment works, for potable water or wastewater. This is why, even though focalising on disinfection problematics (DBPs), their use has given evidence of the lack of precision in their predictions for single processes [Dudley and Dillon, 2005]. Taking into consideration the increasingly drastic legislation, a new tool must therefore be proposed.
As it appears in the above table, the main drawback of common simulators lies in their poor adaptability to specific on-site conditions. When adaptable, the simulators require a very long calibration period. This is mainly imputable to the choice of basing the models on correlations or empirical relations, of which role is not to be physically valid but to fit simulation results to experimental data. Obviously, one cannot simply eliminate such correlations (one could only think at the role of the NOM (Natural Organic Matter)), but our efforts will be directed towards reducing their number.
Additionally, the over-mentioned simulators only offer limited possibilities regarding hydrodynamic modelling. In fact, the single way to "tailor" an

already designed reactor to a real process is often to change the number of CSTRs (Completely Stirred Tank Reactors). Such representation appears at first sight to be insufficient, however, this will be under discussion and we should investigate the impact of the hydraulic representation (as a systemic model) so as to assess how refined a hydraulic model should be.
Finally, one should as well keep in mind on site specificities: (i) only few measurements, (ii) available at various locations of the process (inlet, outlet). This aspect, totally beyond the scope of the over-listed simulators, will have to be a key feature of ours.
We shall now detail the modelling platforms we could use as basis or work with: OTTER and Stimela, also involved in TECHN'EAU (WP 5.4.) and $SimO_3$, simulator developed at the National School of Chemistry in Rennes (ENSC-R).

2.1. OTTER

2.1.1. Generalities

OTTER is a commercial process tool developed by WRc (http://www.wrcplc.co.uk) designed to dynamically simulate the performances of potable water treatment works.
The OTTER software contains models of most common potable water treatment processes that can be linked together via a GUI (Graphical User Interface) to form a model of the whole treatment works. Hence, the user may simulate individual treatment processes or a complete treatment plant. Dynamical in nature, the OTTER package calculates the evolution of variables throughout the plant, but can also predict the impact of rapid changes in the inlet characteristics (water quality, flux modifications, process parameters) all along the installation.
Typical uses of the software include operational decision support, works optimisation, plant design and operator training.

2.1.2. How it works

Regarding the computational device, the mathematical models representing the individual processes are coded in FORTRAN; regarding the user tool, the Microsoft Windows GUI is written in Microsoft Visual Basic. The latter proposes a processes toolbox, which contains icons for each of the available models. The user "drag-and-drop" technique, widely found in many Windows packages, enables the user to put together a model of the whole treatment works on a flowsheet (figure **2.1**).
The data capture of the initial values for the variables is done filling variable fields in a dialog box. When all the data has been entered and a time frame specified, the simulation is run, generating results files for each stream and process.

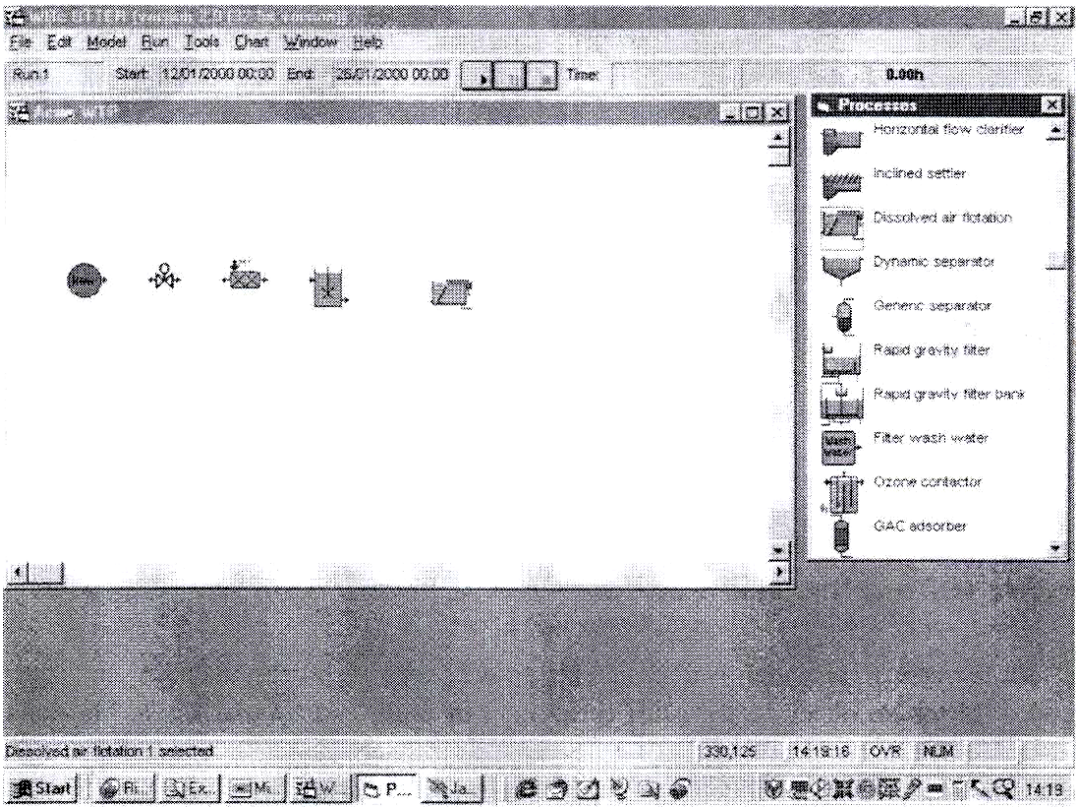

Figure 2.1 Building up a new flowsheet under OTTER

Version 2 of the OTTER package includes [Dudley and Dillon, 2005]

- Chemical floc formation and pH adjustment
- Clarification (floc blanket clarifiers, dissolved air flotation, sedimentation tanks, lamella settlers)
- Rapid gravity filtration
- Granular activated carbon adsorption
- Ozonation
- Disinfection
- Sludge treatment

Concerning ozonation, the software was designed to determine by-products concentrations (bromate ions) and model pesticides oxidation. However, we do not have enough information on the modelling procedures to qualitatively assess OTTER's capabilities. Since a range of different disinfectants is modelled in OTTER – including chlorine, chloramine, chlorine dioxide and ozone – the software can also be used to assess strategies for the reduction of by-products (e.g. using alternative disinfectants, performing enhanced precursor removal…).

2.2. Stimela

2.2.1. Generalities

This software was developed by the T.U. (Technical University) of Delft and DHV (Dutch consultancy firm). As OTTER, it is a PC-based package that enables the user to model at different scales: from the individual unit to the whole treatment works. Hence, the coded models are dynamic (explanations can be found in section **2.4.1.**).
The application field is very close to OTTER's: management and design of water treatment works, analyse and research, operator and students training [van der Helm and Rietveld, 2002].

The user has also the possibility to build the installation he wishes to simulate on a flowsheet (see figure **2.2**). Fields in dialog boxes have then to be filled with the values of the physico-chemical parameters (including all the initial state concentrations). The conceivers have chosen the GUI Simulink, which is the "natural' extension of Matlab™, the programming language of Stimela. From the user's point of view, the main difference to OTTER should be (except the number of values to be specified, surely larger with OTTER) the accessibility of Stimela via an internet platform (http://www.stimela.com). One will however note the limitations of the available online version (see next paragraph).

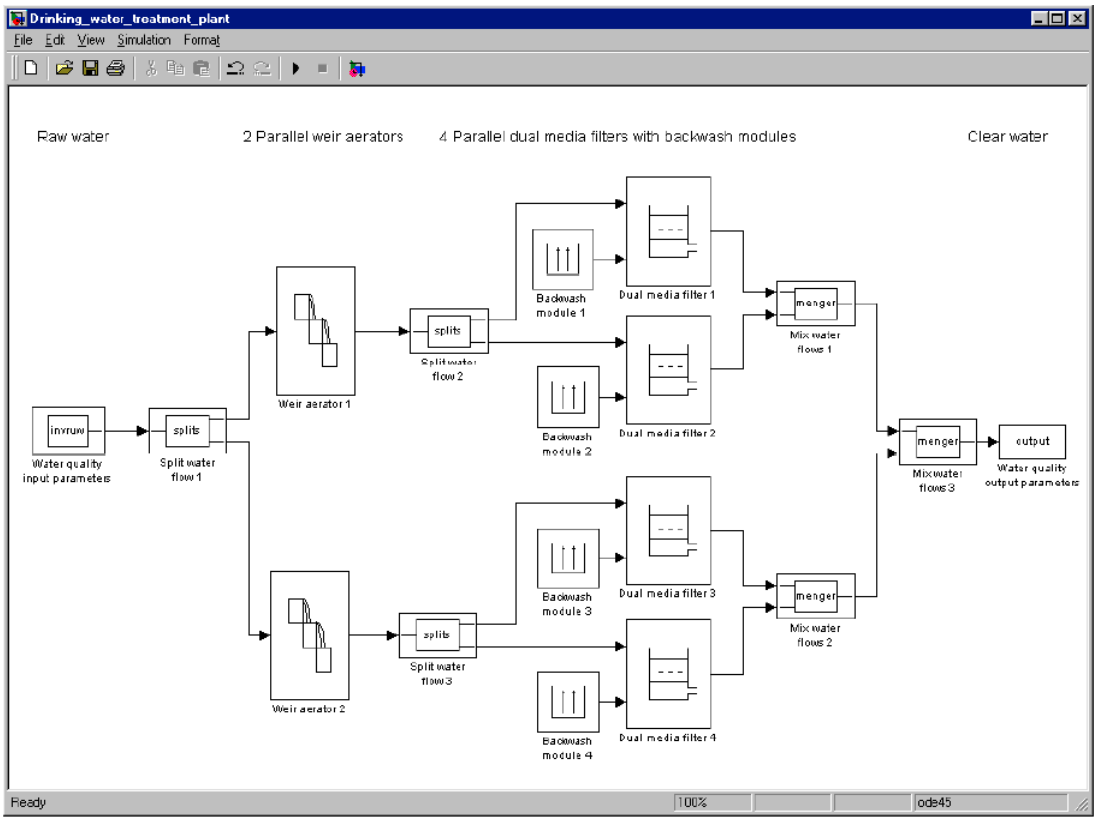

Figure 2.2 Example of a Stimela flowsheet

The Stimela-package includes several processes

- Aeration (cascades, towers, plates, sprayers)
- Filtration (single layer, double layer, continuous, biological)
- Granular activated carbon filtration
- Softening and conditioning
- Ozonation (bubble column and contact chambers)
- Flocculation

Generally speaking, Stimela models dissolved compounds such as gasses (CH_4, CO_2, O_2, O_3), inorganic compounds (HCO_3^-, NH_4^+, CO_3^{2-}, Ca^{2+}) and organic compounds (DOC, organic micropollutants, UV_{254}, AOC). In addition, floc removal is modelled by filtration [Dudley and Dillon, 2005].

2.2.2. The online ozonation step

The online ozonation version gives the user the profiles of dissolved ozone (in a bubble column – the transfer chamber - and in the successive contact chambers), of UV absorbance at 254 nm and of bromate concentration (the latter not fully available).

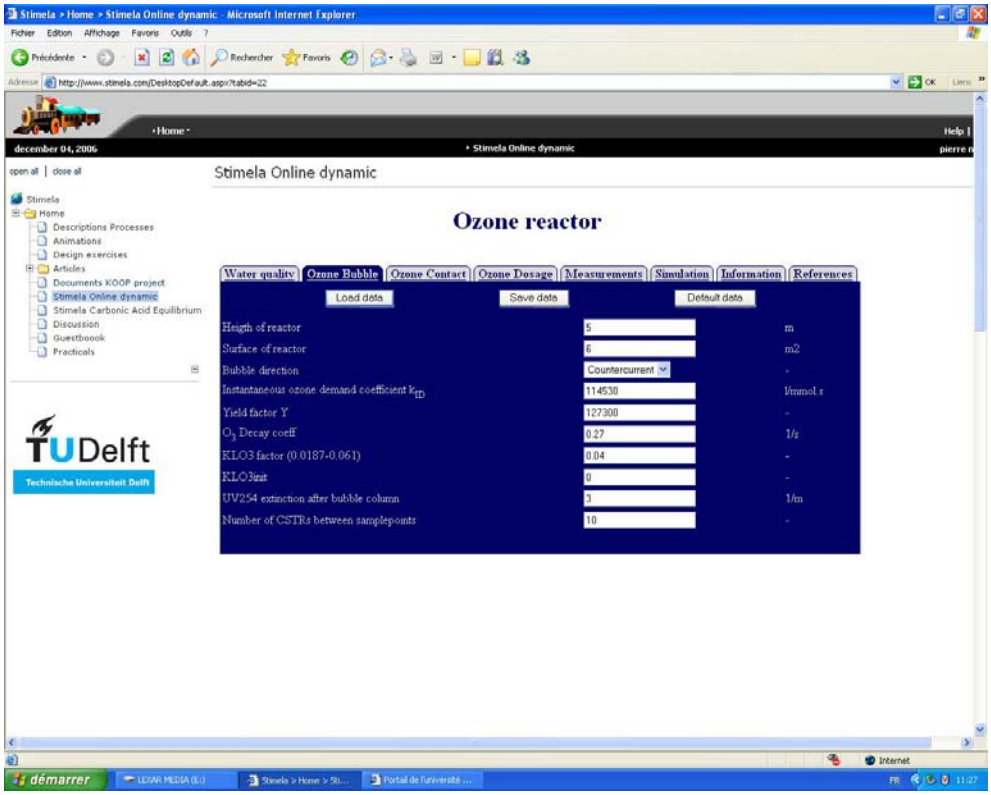

Figure 2.3 Fields to be filled before the simulation is run

The main information to give concerns the quality of the water to be treated (temperature, DOC, ozone concentration, oxygen concentration, total nitrogen, initial UV absorbance), the process parameters (design, operating conditions), the simulation conditions (measurement points, number of CSTRs) and the values of the physico-chemical constants (figure **2.3**).

We give here the results of two simulation runs: those obtained with the default values of the software, with a co- or counter-current bubble column for the transfer (figures **2.4 (a)** and **2.4 (b)** respectively). The characteristics of the installation are clearly to be seen on the graphs: a 30 m^3 bubble transfer column (modelled by a series of 10 CSTRs) followed by four 30 m^3 contact chambers (each of them modelled by a 3 CSTRs series). The (red) stars mark the end or beginning of each contact chamber.

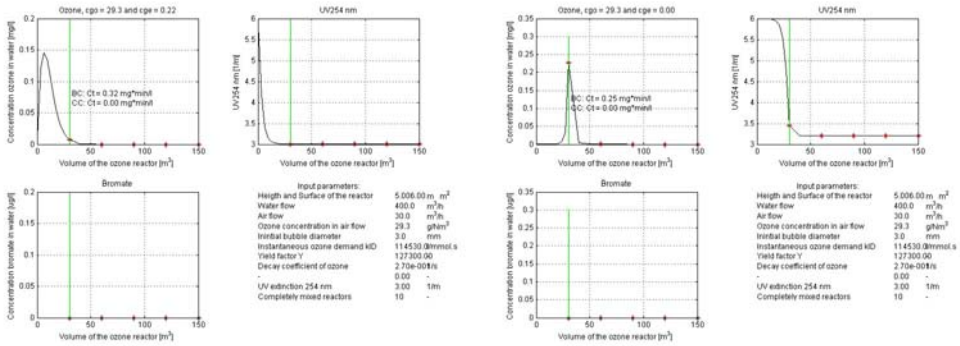

Figures 2.4 (a) and (b) Concentration profiles (dissolved ozone, bromate ions) and 254 nm UV absorbance calculated by Stimela. (a) default vales, co-current transfer; (b) default values, counter-current transfer

As it is to be remarked on the above figures, the bromate concentration profiles cannot be exploited. A formation model could not be found in the literature on Stimela.

2.2.3. Kinetic aspects

The online reaction pathway and that has been proposed in Rietveld's thesis tend to be extremely simple in order to be solved simply. One should keep in mind the ozonation is only a part of Stimela's possibilities.

The online platform does not allow an access to the chemical equations behind the model, neither to alter nor to replace them. However, comparing the results of different runs, the following equations were first guessed, then confirmed by Alex van der Helm

$$\text{(2.1)} \quad \frac{d[O_3]}{dt} = K_{L(O_3)} \cdot (C_{ref} - [O_3]) + \frac{k_{ID}}{Y} \cdot (UV_{final} - UV) \cdot [O_3] - K_{O_3} \cdot [O_3] + A$$

$$\text{(2.2)} \quad \frac{dUV}{dt} = k_{ID} \cdot (UV_{final} - UV) \cdot [O_3]$$

with $A>0$

Where $C_{ref}=p/H_{O_3}.f.[O_{3,g}]$

With p gas pressure
H_{O_3} Henry's constant for ozone
$[O_{3,g}]$ gaseous ozone concentration
f correction factor to convert molar fractions into concentrations

$[O_3]$ aqueous ozone concentration
$K_{L(O_3)}$ mass transfer coefficient for aqueous ozone
UV UV absorbance at 254 nm
UV_{final} final value for UV absorbance

No bromate formation model can be suggested.

Concerning ozone (equation **2.1**), the first term corresponds to the transfer from the gaseous to the liquid phase; the second to the instantaneous ozone demand. Physically, the rapid drop of absorbance in the water matrix is, that way, related *grosso modo* to double bound elimination, aromaticity decrease and immediate oxidisation of certain mineral species. A final value for the UV absorbance must be set *a priori*.
The third term is that of ozone long-term consumption by species less reactive. Generally speaking, the constants stand for a variety of physico-chemical aggregated phenomena. Hence, the chemical model remains quite trivial.

2.3. $SimO_3$

2.3.1. Generalities

This software was proposed by [Savary, 2002] in her thesis. Inspired directly by the works of [Dumeau de Traversay, 2000] regarding the hydrodynamic modelling through a systemic approach, she selected and developed a new chemical pathway of reactions leading to by-products and implemented it in a simulator: $SimO_3$.

Its inner structure makes it easy to adapt to various situations. Indeed, the chemical reactions can be entered (without any restriction concerning reactant- or reaction number), as well as the hydrodynamics, that can be coded in form of a systemic scheme. $SimO_3$ was developed using the FORTRAN 77 programming language.

2.3.2. Hydraulic aspects

Preliminary to its use on a specific site, a systemic scheme has to be set up. This is done calibrating the scheme in comparison to RTD (Residence Time Distribution) curves and/or numerical experiments done with CFD, Computational Fluid Dynamics, (using Fluent for instance; see **4.2.2.**).

To give a clear example, we reproduce here the simple oxidation process of **1.2.** comprising a transfer and a contact chamber with its systemic representation (**figures 2.5** and **2.6**). The gas is introduced only in the first compartment through porous diffuser located at the bottom of the tank. A phenomenon of recirculation loops occurs often in such installations.

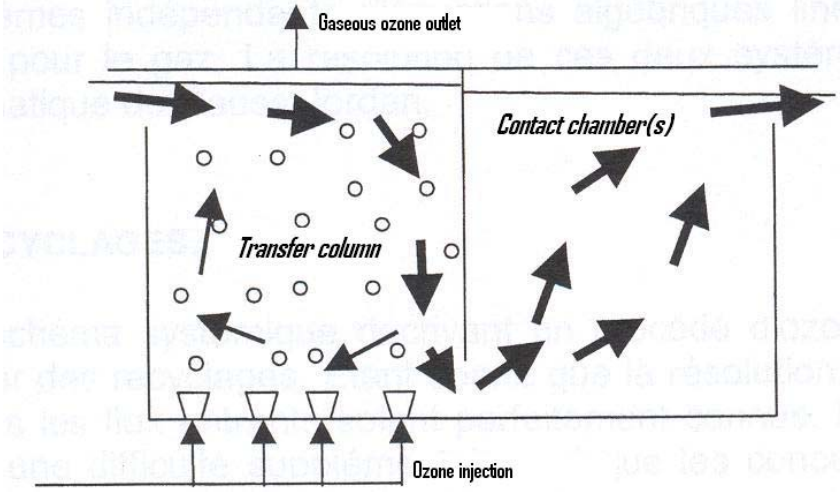

Figure 2.5 An example of a simple oxidation process (adapted from [Savary])

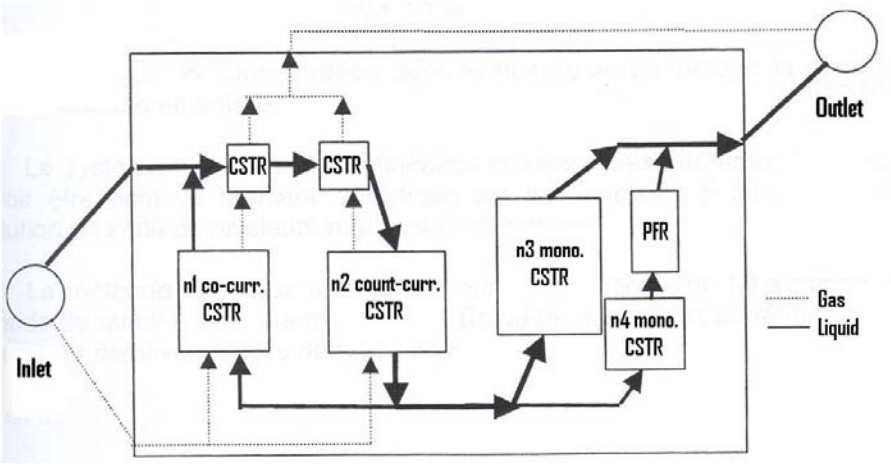

Figure 2.6 Corresponding systemic scheme (adapted from [Savary])

2.3.3. Kinetic aspects

$SimO_3$ is neither specific to a particular reaction mechanism, nor to ozonation. It was designed to simulate biphasic reactions occurring during oxidation steps and can therefore be used as well to model chlorination for instance. In this section however, we shall briefly present the common set of reactions engaged during ozonation. It comprises

- a formation mechanism for hydroxyl radicals
- a formation mechanism for $CO_3^{-\bullet}$ radicals
- formation mechanisms for bromate ions, both molecularly and trough radicals
- reactions representing the TOC contribution to formation and scavenging of hydroxyl radicals that must be calibrated

Besides, the long-term ozone consumption is also considered. As usual, it is represented by a pseudo-first order law, for which the constant value can be determined by previous empirical studies. The general expression is

$$r_{O_3} = w \cdot [O_3] = -\frac{d[O_3]}{dt} \qquad (2.3)$$

Various authors furnish, within a validity domain, the evolution of *log(w)* in function of global parameters such as pH, TOC, alkalinity or 254 nm UV absorbance. The ozone instantaneous demand can also be implemented according to the empirical relation established by [Muñoz Ramirez, 1997].

2.3.4. Results

$SimO_3$ has been calibrated on a lab-scale reactor with micropollutants like atrazine (pesticide). It has been used afterwards on a continuous system (i) with water from the distribution network having already been disinfected by ozonation and (ii) on pilot-scale units located directly at water treatment works.

The results were usually satisfactory, though predictions were not as accurate for the bromate formation as for pesticides [Savary, 2002]. This is mostly due to calibration procedures: whereas pesticides formation was directly

calibrated, the bromate formation mechanism is solely adjusted for the reactions involving NOM. Indeed, the most part of the reactions originates from the literature, guaranteeing a large validity domain wherein the error on the kinetic constants values can represent on the other hand 10 to 20 % and even more.
However, these remarks are more imputable to the chemical reaction pathways chosen and the hydraulic systemic models built (hence, we refer the reader to the sections **3.2.4.4.** and **4.2**). $SimO_3$, as a calculus engine, has to be considered separately. Examining it that way, some reserves can be expressed since:
-$SimO_3$ performs calculations downstream, making it unsuitable to solve our BVP. It represents nonetheless a powerful numerical device, which could be used to check the validity of calculations that would have been done on a BVP
-it remains a research tool, only accessible to scientists used to work with it. The use has actually revealed the difficulties to get insight into it. This situation could easily be overcome with the implementation of a GUI

After this more in-detail overview of three simulators involved within the TECHN'EAU package, some elements of comparison are given in the next section. In doing so, we stress out relevant topics, especially for a future coming together between the participants in TECHN'EAU.

2.4. Elements of reflexion

2.4.1. Dynamical mode

As rightly formulated by [Gimbel and Rietveld, 2002], steps like oxidation, sedimentation or flocculation are stationary and thus do not necessitate to be treated dynamically. The available simulators generally aim to simulate a whole treatment works and are hence dynamic.

OTTER is a predictive tool designed to be a supervisory control device, performing dynamic calculations. This implies it has to work with time-dependent state vectors. These vectors are grouped in a matrix whose coordinates could be defined as follows: (variable, time). For example, let name the matrix A; the concentration of the i^{th} species at time j is $a_{i,j}$.

Passing from process to process, the matrix is gradually modified. At the end of each process one obtains the response to changes at the inlet in form of a new response matrix. It is not always easy to proceed that way dealing with recirculations, especially when the inlet characteristics evolve faster than the recirculation time (in the inverse case, one can handle such a situation as a succession of quasi-steady modes). A solution to this situation is to up-scale the problem: the process submitted to a recirculation loop is no more considered, but is included in a more global process, which includes the recirculation loop (figure **2.7**), converting thus external into internal recirculations. This kind of transformation can be problematic (expansion of the vector sizes, more difficult resolution…), as mentioned by [Head et al., 2002].

At quasi-steady state, the process 1 is considered, with its external recirculation loop. In dynamical mode, recirculations have to be included within the processes (process 2).

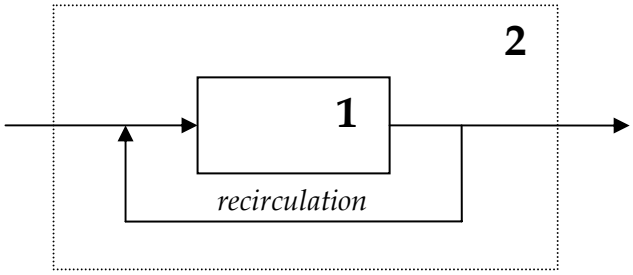

Figure 2.7 Recirculations in steady-state and dynamic modes

Nevertheless, as over-mentioned, regarding such processes as ozonation or chlorination, it does not seem a necessity to opt for a dynamical model, at least for the oxidation processes of potable waters. This choice is justifiable in the case of decantation, which reaches its steady state well afterwards, or in the cases of dynamical processes like filtration or adsorption. Simulating only oxidation processes, one prefers therefore to work in a quasi-steady mode [Savary, 2002].

2.4.2. Data acquisition

Simulating with on-site conditions, one hardly disposes of all the parameters required by the simulator to perform calculations. For example, OTTER is a simulator that does not necessarily need to be coupled to SCADA (Supervisory Control And Data Acquisition) system, yet it has to be calibrated and even run with a large amount of data (the same remark can be made

regarding Metrex [Dudley, 2006]). This was expressed in various reservations [Dudley and Dillon, 2005] [Head et al., 2002] arguing the simulator to be used only on very "data-rich" sites. Besides, the data furnished has to be reliable (on the limited robustness of OTTER, see [Butt et al., 2002]).
Besides, as Stimela, OTTER does not propose any mode of resolution taking into account outlet concentrations, as it will have to be for our simulator. In the case of a parameter choice to meet certain criteria (as outlet concentrations for instance), the software explores all the possible scenarios. Example: if alarms are detected, a prognosis algorithm is run to determine the causes and possible preventive actions scanning a variety of combination. This process is not combined with any cost function yet, and thus cannot be termed "optimisation".

2.4.3. Towards a new modelling platform

The conceivers of OTTER and Stimela (WRc and the TU Delft) have decided to join their efforts to build up an European platform for modelling drinking water treatment processes inside the TECHN'EAU framework. We therefore met several times (at Kiwa on January 31, at the TU Delft on March 30 and at EAWAG on May 9) in order to get a better idea of what will be done and give impetus to possible cooperation.
To achieve the simulator within the time schedule provided, the teams decided to split the tasks as follows: physico-chemical models will be first formulated, tested and validated by the TU Delft (PhD candidate Petra Ross assisted by associate professor Luuk Rietveld), then implemented in the simulator structure, i.e. the calculation core and the GUI, constructed by WRc (Jeremy Dudley and Glenn Dillon).

The final product shall fulfil various demands. WRc and TU Delft agree for the most part upon the following requirements

- Possible communication with other platforms
- Access via web
- Extendable
- Equipped with a GUI
- Documentation and help facilities

Concerning its accessibility, some qualifications were also expressed

- Free use for end users (this disqualifies the package Matlab/Stimela)
- No open source for users
- No commercial package involved: this point could be problematic in case of collaboration. It seems namely that, on our side, such packages could be necessary if we implement an already existing routine for solving BVPs. The problem could possibly be tackled by redeveloping (less efficiently) BVP solvers. This implies however a non-negligible investment.

The three last criteria guided the choices upon the programming languages. So, the framework shall be written in FORTRAN 90 and the models coded in C. The interface, accessible via internet, should be built with a .net language (VB.net for instance).

Even though the new simulator will be designed to model processes not present yet, neither in OTTER, nor in Stimela (e.g. slow sand filtration, UV/H_2O_2 disinfection, membrane filtration…), it shall keep the main features of the original simulators (possibly including also models developed by IWW for Metrex); these are: aeration, coagulation/flocculation, sedimentation/flotation, rapid sand filtration, ozonation, GAC/PAC, softening, chlorination and conditioning.

There remains to say but a few words on the current progress of the simulator and on our possibilities to integrate. After having issued a state-of-the-art review [Dudley and Dillon, 2005] and agreed upon the above topics, both teams have come to the development of the software, presenting a 0 version at the last conference of TECHN'EAU WA 5 held at EAWAG in Zürich (May 9, 10, 11). We attended the meeting and had the opportunity to exchange views on a possible collaboration.
Presently, the simulator is still in its infancy: it simulates two processes and does not provide information to the user; the results are not saved and the interface remains extremely basic. However, some important facts were emphasised that were remained unclear after the first sittings in Holland. So, and after having met several times, essential points can be summarised in the following statements

- We got to know each other. Important fact to understand who is working on what…
- Even if the future simulator will be dynamic, a static module could be inserted, which would recreate dynamic conditions from a sequence of steady-state solved problems
- Regarding the programming language, the only restriction seems to lie in the format of the compiled codes for the processes (dll), which are basic binary files
- In our case, the use of commercial packages (to solve BVPs for instance) could be problematic, unless we decide to redevelop such solvers, what means investments
- Another point, which needs to be clarified concerns the list of parameters that pass from process to process

3. Chemical aspects

Operation of disinfection processes commonly involves the application of the CT concept (see **1.2** and **Appendix B**), where C is the ozone residual concentration in the contactor and T is usually represented by t_{10} (defined as the detention time for ten percent of the water to pass through a disinfection contactor [USEPA, 1991]). The CT approach is a simple way to evaluate disinfection treatment efficiency; nevertheless, it has two major drawbacks. Indeed, both (i) hydraulics and (ii) chemical kinetics are described by a single parameter, a single value. Such an approach ignores the underlying factors governing hydrodynamic behaviour [Dumeau de Traversay, 2000] as well as the main components which may affect the efficiency of disinfection. The latter include mass transfer (in the case of ozone), oxidant demand and decay, microbial inactivation, and DBPs formation kinetics. This chapter is conceived as a presentation of the latter phenomena, with exception of mass transfer; in the next chapter, we shall concentrate on hydrodynamics.

3.1. Chlorination

Chlorine and its compounds are the most commonly used disinfectants for water treatment. Chlorine's popularity is not only due to lower cost, but also to its higher oxidising potential, which provides a minimum level of chlorine residual throughout the distribution system and protects against microbial recontamination.

The disinfection process is affected by different physico-chemical and biological factors and its efficiency can be characterised by dose and intensity [Sadiq and Rodriguez, 2004]. Generally, inactivation of organisms increases with increasing CT. The pH has different effects on different disinfectants, but in general, at lower pH, chlorine is more effective against organisms than in alkaline conditions. Generally CT required for inactivating microorganism is lower in warm water than in cold water. For a specific contact time, required chlorine doses for disinfection are consequently higher in winter than in summer conditions. However, in most drinking water utilities, the application of an excess of disinfectant (such as chlorine) maintains adequate residuals to avoid the reappearance of microorganisms in the water distribution system. The disinfectant residuals deplete rapidly when the water temperature is high, what explains the difficulty of maintaining minimum residual level in large distribution systems during summer. Also microbial activity within distribution systems is higher in warm than in cold waters [Sadiq and Rodriguez, 2004]. To maintain an adequate level of residual disinfectant in the distribution system, higher disinfectant doses are applied during the summer. Usually, the conditions affecting the disinfection efficiency and the requirements to maintain disinfectant residuals in the distribution systems simultaneously affect the formation of DBPs.

Due to the complexity of the reactions that take place during chlorination of potable water, a vast majority of authors has abandoned the approach of an exhaustive mechanistic description, preferring a more pragmatic modelling.

This leads to various combinations, from semi-empirical models to empirical correlations.

3.1.1. Chlorine decay

- 3.1.1.1. Semi-empirical models

Chlorine decay is often considered to occur in two steps. As for ozone, some species may react very quickly, whereas others tend to have much slower kinetics. This was observed in numerous studies (see for instance [Lu et al., 1999]).
The fast initial decay corresponds to reactions with highly reactive species present in the water matrix, mostly inorganic compounds such as iron (II), but also with organic compounds. The duration of this short term chlorine consumption depends on many factors including initial chlorine concentration, TOC addition, treatment type… [Vieira et al., 2004]. During the second, slow and longer decay, chlorine is consumed by less reactive compounds such as organic species (e.g. humic substances and proteins). The time scales are obviously dependent on the nature of the water; therefore the duration of each phase varies significantly from study to study. Considering the several authors who have reported on these differentiated decays [Qualls and Johnson, 1983], [Jadas-Hécart et al., 1992], [Lu et al., 1999], one can expect the first phase to be finished within seconds or minutes or hours, the second within minutes or hours or days before completion…

Additionally to the reactions involving chlorine and other compounds, a phenomenon of self decomposition is likely to take place, though at a much lower rate than the other reactions. This reaction may thus become significant in the second phase of the decay, and after long contact times [Vieira et al., 2004], resulting in an enhanced decay rate.

Slow chlorine decay is often modelled by a first order law - actually a *pseudo*-first order law - although it inherently assumes reactive material to be always in excess, which may not be the case. Therefore, overall second-order, two component models are also proposed that take into account the chlorine demand. Table **3.1** summarises some of the most current models for chlorine decay.

Table 3.1 Some semi-empirical models for chlorine decay

Authors	Rapid decay		Slow decay	
Noack and Doer, 1977	2nd order, 0-7 h.		1st order, 7 h.-7 d.	
WTP model (see Chapter **2**), 1992	0 order, 0-5 min.	2nd order, 5 min.-5 h.	1st order, t>5 h.	
Dugan et al., 1995 and Koechling et al., 1998[5]	Michaelis-Menten		Michaelis-Menten	
Clark, 1998[1]	2nd order		2nd order	
Qualls and Johnson, 1983	2nd order, 0-30 s.	2nd order, 30 s.-5min.		
Jadas-Hécart et al., 1992			2nd order, t>4 h.	
Lu et al., 1999			1st order, 2 h.<t<7 h.	

As illustration to the precedent table, we give here some brief information about two models presented.

1. [Qualls and Johnson, 1983] have studied the **short-term** chlorine decay, basing on the consumption of fulvic acids in natural fresh waters. In accordance to their results, they divided chlorine decay as follows: a first very rapid step (<30s) and a second one, lasting longer than five minutes. These two steps were associated to two second order kinetic laws. Hence,

$$\frac{d[Cl_2]}{dt} = k_1[Cl_2][F_1] + k_2[Cl_2][F_2] \qquad (\mathbf{3.1})$$

with k_1: reaction rate constant for the fast chlorine decay ($M^{-1}.s^{-1}$)
k_2: reaction rate constant for the slow chlorine decay ($M^{-1}.s^{-1}$)

F_1 and F_2 are the concentrations of the specific reactive sites towards chlorine involved in fast and slow decay, respectively ($mol.L^{-1}$).
It was decided to relate the *a priori* unknown concentrations F_1 and F_2 to TOC via

$$\begin{cases} [F_1] = x_1[TOC] \\ [F_2] = x_2[TOC] \end{cases} \qquad (\mathbf{3.2\ a}\text{ and }\mathbf{b})$$

x gives a measure of the number of reaction sites available per mol of C. According to the authors, a graphical method can be employed to assess x_1, x_2, F_1, F_2. If calibrated, this model gives good indications.

2. Like many researchers, [Jadas-Hécart et al., 1992] decompose chlorine decay also in two phases. The first phase is termed 'initial demand' and covers chlorine decay from t = 0 to t = 4h. Jadas-Hécart assumes then the **long-term** consumption to obey a second order kinetic law. Hence, beyond the limit of four hours, the chlorine decay is expressed as

[5] As cited by [Boccelli et al., 2003]

$$\frac{d[Cl_2]}{dt} = -k(a-x)^{\alpha}(b-\frac{x}{n})^{\beta} = -\frac{dx}{dt} \quad (3.3)$$

with *a*: residual chlorine concentration after the fast decay
b: potential chlorine consumption for the slow phase
x: chlorine consumption during the slow phase
n: reaction stoichiometry

The results from the model are fitted to the experimental curves, adjusting *a, β, n, k, b*. These highly depend on the seasonal water composition, on pH (chlorine speciation) and on temperature.

- 3.1.1.2. A mechanistic model

We present here a very simple reaction pathway that has been designed to model chlorine decay. In a recently published paper (2003), [Gang et al., 2003] presented namely a chlorine decay model founded on possible reaction pathway. The chemical mechanisms were then implemented in a mathematical model developed to investigate chlorine decay in natural waters. The following assumptions were expressed [Gang et al., 2003]

1. In the presence of inorganic demand, chlorine follows a rapid first order decay (5 reactions involving Fe^{2+}, Mn^{2+}, S^{2-}, Br^-, NH_3 + hypochlorite decomposition).

2. Two distinct types of reactive functionalities exist in NOM resulting in two parallel first order reactions. One NOM_R functionality, possibly attributed to aldehyde and phenolic hydroxyl groups, results in a very rapid rate of chlorine consumption. The other NOM_S functionality is less reactive, such as expected for activated double bonds and methyl groups, and results in a slow, long-term chlorine consumption.

3. The long-term chlorine demand follows slow first order decay.

4. A fixed proportion of the chlorine follows rapid first order decay while the remaining proportion decays at slower first order rate for specific water.

Correspondingly to assumptions 2-4, two chemical reactions for the consumption of chlorine by NOM are proposed (2 reactions, with NOM_R and with NOM_S).

Three parameters (k_R: reaction rate constant for rapid reactions involving NOM, k_S: reaction rate constant for slow reactions involving NOM, *f*: fraction of the chlorine consumed by the rapid first order reaction) have then to be adjusted to fit the model to the experimental points.

Experimentally, both alum treated and raw waters from different locations in the U.S. were investigated. The results are satisfactory for every site (good correlation between experiments and simulations). Nevertheless, the measures were performed only once for each water, what hampers a more global view of the stability for the adjusted coefficients (seasonal measurements would have provide more information concerning the possibility to implement this model on site). Moreover, this study concerned only surface waters; thus, the variability of the adjusted constants could not be evaluated with regards to the water origin.

Now, mechanistic models often contain modules for DBPs formation, and can thus be regarded as complete sets for chlorine disinfection. We shall present in the following (section **3.1.2.3.**) two of them.

3.1.2. DBPs formation

On DBPs in drinking water and the predictive models for their occurrence, an excellent review is given by [Sadiq and Rodriguez, 2004]. *We therefore present only two models of importance in this section that are not discussed in the previous article.*

- 3.1.2.1. Empirical models

1. Basing on several simple parameters, [Engorholm and Amy, 1983] formulated the next model. Concentration for the most common chlorination DBP, $CHCl_3$ is given by

$$[CHCl_3] = k_1 k_2 \left[\frac{[Cl_2]}{[TOC]}\right]_{t_0}^{\alpha} .[TOC]_{t_0}^{\beta} .t^{\theta} \qquad (\mathbf{3.4})$$

k_1 – related to the pH influence – a, β are precursor dependent parameters
k_2 and θ are functions of the temperature
These constants are experimentally assessed working with a given precursor (for instance, a synthetic solution of humic acids). The authors advocate calibrating in accordance with the chosen precursor and with seasonal variations.

2. The model developed by [Casey and Chua, 1997] proposes simultaneously equations for chlorine decay and THMs formation.
The applied standard chlorination dose, which is that recommended by World Health Organisation, was used throughout the study on the 12 Irish surface waters investigated. This standardisation was calculated to produce a RFC (Residual Free Chlorine) concentration of 0.5 mg/L after a 30-min contact time. It was found that the RFC decay rate could be approximately modelled as a first order reaction using the 2 h RFC concentration to quantify the reaction rate constant. Evolution of the RFC decay is then given by

$$C_t = C_0 e^{-kt} \qquad (\mathbf{3.5})$$

In the same time, it was found that the rate of total THM (TTHM) formation could be modelled as a hyperbolic growth function, defined by two parameters

$$TTMH_t = TTHM_{\max} \frac{t}{t_{50} + t} \qquad (\mathbf{3.6})$$

Obviously, according to the precedent equation, t_{5O} is defined as the time necessary for the RCT concentration to reach half of its maximal and final value, $TTHM_{max}$. Experimentally, the final state was reached 48 hours after the chlorination, this limit being set by the stabilisation of haloforms concentrations. The THM species formed in the test set of waters included chloroform ($CHCl_3$), bromodichloromethane ($CHBrCl_2$) and dibromochloromethane ($CHBr_2Cl$). Bromoform ($CHBr_3$) was not detected in any of the samples.
Assuming such a simple model, one should not be surprised to observe a relative large range for the parameters values adjusted to the experimental data. For the set of waters studied, the t_{50} values varied in the range 1.06-2.48 h, while the $TTHM_{max}$ values varied in the range 22-56 µg/L. No doubt under

these conditions that careful attention has to be paid to the calibration of the model.

- 3.1.2.2. Semi-empirical models

Contrary to the literature on empirical models to which a host of authors are contributing, semi-empirical modelling seems to have become more obsolete. Nevertheless, interesting results can still be found (see [McClellan et al., 2006]). So, a model was developed by [Kavanaugh et al., 1980] to represent the reactions of chlorine with NOM; the authors postulated the following total stoichiometric reaction

$$3HOCl + TOC \xrightarrow{k_n} THMs \qquad (\mathbf{3.7})$$

where k_n is a reaction rate constant

The general expression for the reaction rate is

$$\frac{d[THM]}{dt} = k_n [HOCl]^m [TOC] \qquad (\mathbf{3.8})$$

Let f be the amount of total chlorine (in mol) present in the THMs per mol of consumed chlorine

$$f = \frac{3[THMs]}{[HOCl]_0} \text{ substituting in (3.8)}$$

$$\frac{d[THMs]}{dt} = k_n [TOC] \left[[HOCl]_0 - \frac{3[THMs]}{f} \right]^m \qquad (\mathbf{3.9})$$

The study of several samples originating from various sources revealed that f is temperature-, and pH-dependent. f is correlated to the chlorination rate applied as well. This implies calibration for every water. According to Kavanaugh, this is due to the exaggerated simplicity of his model, which does not satisfactorily represent chemical complexity. Yet it provides an estimation of the potential long-term THMs formation.

- 3.1.2.3. Mechanistic models

1. [McClellan et al., 2006] proposed a mechanism where three classes of reactive functional groups within the NOM are hypothesised:

1. Sites that react with chlorine instantly relative to the time scale of interest (minutes to days). These reactions are treated as constants in the model.

2. Sites that react with chlorine (HOCl or OCl^-) where the first (rate-limiting) step is second-order (first-order in NOM and first-order in chlorine). These are called S_1 sites.

3. S_2 sites, where there is a rate-limiting initial step that is first-order in NOM, leading to an active form, S_2^-, that participates in a faster second-order reaction with HOCl.

The prototype for the S_2 reaction pathway is the classical haloform reaction of ketones with halogens, where the rate-limiting step (first-order in ketone) is a proton dissociation to form enolate. For the S_1 and S_2 pathways, a series of faster chlorine-consuming steps follow, producing halogenated and oxidized organic compounds, CO_2, and Cl^-. The amount of formation of each by-product is an initial amount (representing "instantaneous" formation) plus the

sum of specified fractions of the total site consumption through the S_1 and S_2 pathways. The rate of chlorine consumption is equal to the total rate of site consumption through each pathway multiplied by stoichiometric coefficients representing consumption in intermediate fast steps. The conceptual reaction mechanism is depicted in schematic form in figure **3.1**.

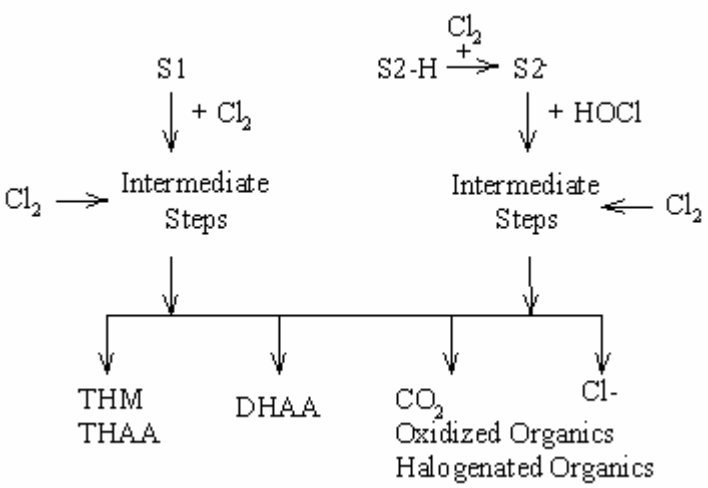

Figure 3.1 Conceptual reaction mechanism, adapted from [McClellan et al., 2006]

In this study, the experiments were conducted using three samples collected at different times (July and November) from the same source, filter effluent of the Lake Gaillard Water Treatment Plant, Connecticut. This plant treats an impounded surface water source. A data set from a different water source (filter effluent from the Robert E. McQaude Water Treatment Plant in Andover, Massachusetts) was also collected to evaluate the ease of adaptation of the model when fitted outside the original calibration domain. These experimental data sets thus enabled the authors to basically test the robustness of the model.

There are 21 parameters to be adjusted. This number has to be compared with the 28 and 25 values that must be determined with other models (those of [Amy et al., 1987] and [Clark, 1998] respectively, as cited in [McClellan et al., 2006]). 15 of the parameters are adjusted to data originating from bench scale experiments, the remaining 6 describing initial NOM site, chlorine, THM, and HAA concentrations are subsequently adapted to the water samples of the data set. Hence, the calibration procedure is not straightforward: two software packages were used for computations and data analysis in [McClellan et al., 2006]. The numerical optimisation routines namely converge on a solution with the proposed model only with very good initial parameter estimates (close to their optimum values). Hence, an initialisation code was developed by the authors.

The results were satisfactory: with a reduced number of parameter to be adjusted, the mechanistic model gave a superior fit to the data set compared to either the power function or second-order forms (those of [Amy et al., 1987] and [Clark, 1998] resp.), as measured by an adjusted coefficient of multiple determination, although all three models fitted the data well. When changing water, the model behaved correctly as well. Most important fact: only the 6 parameters for NOM and DBPs had to be re-evaluated. It seems that two of those parameters representing reactive site concentrations within

the NOM molecules are especially site specific. However, there are some reservations to express: (1) limited testing of the model was performed where the rate constant parameters were calibrated; (2) the waters to which the model was applied exhibited similar quality.

2. Basing on the previously developed model of [Adin et al., 1991] and on studies conducted at the Chemical Engineering Department of the National School of Chemistry, Rennes, [Bégoc, 2000] proposed a mechanistic model for THM formation. We first give schematic representation of Adin's model (figure **3.2**), then present the reaction pathway developed by Bégoc.
[Adin et al., 1991] postulated the following reaction pathway for THM formation

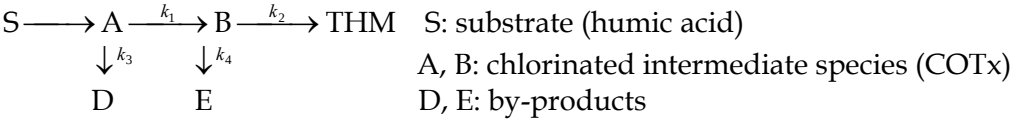

Figure 3.2 Schematic representation of Adin's reaction pathway

Inspired by the previous reaction pathway, Bégoc modelled THM formation with a multi-step reaction pathway leading from chlorine to THMs and HAAs.
It can schematically summarised in both figures **3.3** and **3.4**

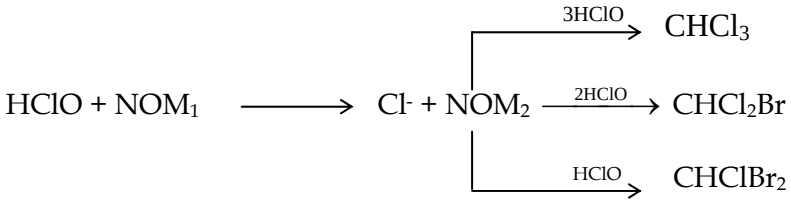

$NOM_1 = \alpha.NOM_i$, i.e. NOM_1 is a fraction of the initial NOM.
NOM_2, NOM_3 are different oxidised form of NOM

Figure 3.3 Schematic representation of Bégoc's reaction pathway, 1: 2 steps THMs formation

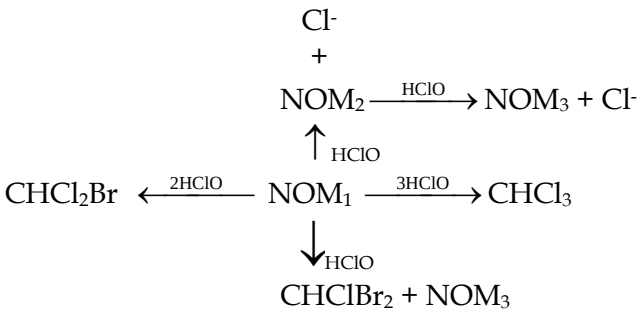

$NOM_1 = \alpha.NOM_i$, i.e. NOM_1 is a fraction of the initial NOM.
NOM_2, NOM_3 are different oxidised form of NOM

Figure 3.4 Schematic representation of Bégoc's reaction pathway, 2: 1 steps THMs formation+chlorine decay

Bégoc combined the two approaches mentioned in figures **3.3** and **3.4**:

i. THMs may be formed after two successive chlorination steps of NOM. The first reaction form chlorinated intermediate species of NOM (denoted NOM_2), which react further with chlorine to evolve into THMs and other by-products (i.e. HAAs) using several possible pathways (figure **3.3**).

ii. THMs can also be formed by direct chlorination of NOM, without intermediate form of NOM. These reactions can either involve one, two or three molecules of hypochlorite. Besides, the chlorine decay is modelled by two successive reactions transforming NOM_1 into NOM_2 (instantaneous chlorine demand), then NOM_2 into NOM_3, what corresponds to long-term decay (figure **3.4**).

The complete set of reactions involved in this model is given in section **4.3.1.** where it is implemented in a simulator.

3.1.3. Disinfection

The first models used to explain the survival of microorganisms in natural environment after addition of disinfectant were designed on systems that had no chlorine demand. Thus, chlorine concentration was presumed constant throughout the disinfection. The simplest and most famous disinfection model (**3.10**) was proposed by Chick and Watson (1908). Chick postulated that the death of microorganisms within a time interval is caused by a multiplicity of independent phenomena. For a given disinfectant concentration, all the other factors being fixed, the mortality remains stable in each time unit. The inactivation kinetics are then expressed as

$$\frac{dN}{dt} = -kC^n N \qquad (\mathbf{3.10})$$

where:
n: dilution coefficient
C: disinfectant concentration
N: microorganism concentration
k : apparent constant rate, sometimes called lethality coefficient

However, the precedent relation is solely valid for a constant disinfectant concentration, what is absolutely not the case when one considers a typical disinfection experiment (done with natural waters for example). The chlorine demand may affect significantly the efficiency of disinfection: qualitatively in converting free chlorine into halogenated organic or inorganic compounds; quantitatively diminishing the total residual chlorine. To cope with this problem, diverse empirical or semi-empirical approaches were proposed. One of them, developed by [Hom, 1972] under constant disinfection residual in a homogeneous batch system, provides a relationship between disinfectant concentration and contact time, via two empirical constants m and n (**3.11**). The Hom model successfully describes the disinfection of *Giardia* and *Cryptosporidium* and converts to the Chick-Watson model when m is equal to

1. Under typical disinfection conditions, disinfectant concentration decay is generally assumed to be first order (**3.12**, see Equation **3.5**).

$$\frac{dN}{dt} = -kmC^n N.t^{m-1} \quad (\mathbf{3.11})$$

$$C = C_0 e^{-k't} \quad (\mathbf{3.12})$$

where:
k': first order decay rate of disinfectant
C_0: initial disinfectant concentration
k, m, n: empirical constants for Hom model
t = contact time

Variations on these disinfection models are possible but are rarely used. The simple Chick-Watson model was the most appropriate model for comparing *Cryptosporidium* disinfection data from a number of research groups, because of the inherent variation in experimental data (unpublished data, International Cryptosporidium CT Workshop, Washington, DC, January 12–14, 1998 as cited by [LeChevallier et Au, 2004]).This lead to the formulation of the CT concept (see **1.2**, the introduction of this chapter and **Appendix B**) promoted by the USEPA and then used in correlation with the SWTR (Surface Water Treatment Rule)[6].

Though a significant effort has been invested to develop predictive models for DBPs in drinking water, the main benefit for modelling appears to be their usefulness to identify factors influencing DBPs formation and fate followed by chlorination of water. Some empirical models can also be applied for predicting DBPs, but mainly subject to conditions (i.e., within the specific range of independent variables) and for the specific case that served for model development (experimental water or site-specific distribution system). Semi-empirical models seem to behave better when implemented outside the calibration domain, but their adaptability remains somehow restricted.
Our research efforts must consequently focus on investigating the capacity of models developed with laboratory-scaled data to estimate real seasonal and spatial variations of DBPs. A better adaptation to on site conditions could be possible developing a quasi-mechanistic model with a restricted number of specific parameters.

[6] Effective December 31, 1990, the Surface Water Treatment Rule (SWTR) applies to all US systems that use surface water or groundwater under the direct influence of surface water. The Rule established drinking water treatment techniques in lieu of maximum contaminant levels for *Giardia lamblia*, viruses, heterotrophic plate count bacteria, *Legionella*, and turbidity.
The Rule requires **99.9** percent (3-log) removal and/or inactivation of ***Giardia*** cysts, and **99.99** percent (4-log) removal and/or inactivation of **viruses**. To meet these requirements, water systems must disinfect under strigent conditions, filter water until certain source water-quality and site-specific conditions are met, and be operated by qualified personal.

3.2. Ozonation

3.2.1 Preliminaries

As stated above (section **1.2**), ozone is a gas of limited solubility that must first be dissolved into water to be effective against microorganisms. Once dissolved, aqueous ozone engages in complex chemistry that includes auto-decomposition and reaction with various constituents of the water, in addition to reaction with microorganisms [Duguet et al., 2006].

Aqueous ozone may react with various species in two manners: direct reaction by molecular ozone; indirect reaction through radical species formed when ozone decomposes in water. Depending on treatment priorities, either pathway may be relevant. Indeed, if one is concerned with disinfection, only the direct, slow and selective reactions of molecular ozone with constituents of natural water should be taken into account. Now, if one wants to focus on DBPs formation, rapid radical reactions (particularly those involving hydroxyl radicals) with many types of dissolved species shall also be relevant and added to the previous reaction pathway for disinfection [Doré, 1989].

Besides, it has been shown that ozone contactors should be designed with the lowest possible backmixing so that the target inactivation efficiency can be achieved with the lowest possible formation of bromate [Tang et al., 2005]. This explains why, in practice, disinfection progresses throughout the works, being favoured by a slow flow approaching the ideal conditions reigning in a PFR (Plug Flow Reactor). So, the distinction between direct-slow-molecular and indirect-fast-radical pathways may also be linked with different hydraulic behaviours.

3.2.2. Ozone decomposition

- 3.2.2.1. Mechanisms

The mechanism of ozone reaction and decomposition has been the subject of numerous studies (e.g. [Langlais et al., 1991]). The two most widely accepted mechanisms for decomposition of ozone in water are shown in Table **3.2**.

Table 3.2 Mechanisms of ozone decomposition in water

	Hoigné, Staehelin and Bader				Tomiyasu, Fukutomi and Gordon			
Initiation	$O_3 + HO^- \xrightarrow{k_1} HO_2^\bullet + O_2^{-\bullet}$	$k_1 = 7.0\ 10^1\ M^{-1}s^{-1}$	(3.13)		$O_3 + HO^- \xrightarrow{k_{10}} HO_2^- + O_2$	$k_{10} = 40\ M^{-1}s^{-1}$	(3.22)
	$HO_2^\bullet \rightleftharpoons H^+ + O_2^{-\bullet}$	$k_2 = 10^{-4.8}$	(3.14)		$HO_2^- + O_3 \xrightarrow{k_{11}} HO_2^\bullet + O_3^{-\bullet}$	$k_{11} = 2.2\ 10^6\ M^{-1}s^{-1}$	(3.23)
					$HO_2^\bullet + HO^- \rightleftharpoons H_2O + O_2^{-\bullet}$	$k_{12} = 10^{-4.8}$	(3.24)
Propagation-Termination	$O_3 + O_2^{-\bullet} \xrightarrow{k_3} O_3^{-\bullet} + O_2$	$k_3 = 1.6\ 10^9\ M^{-1}s^{-1}$	(3.15)		$O_3 + O_2^{-\bullet} \xrightarrow{k_3} O_3^{-\bullet} + O_2$	$k_3 = 1.6\ 10^9\ M^{-1}s^{-1}$	(3.25)
	$H^+ + O_3^{-\bullet} \underset{k_{-4}}{\overset{k_4}{\rightleftharpoons}} HO_3^\bullet$	$k_4 = 5.2\ 10^{10}\ M^{-1}s^{-1}$ $k_{-4} = 2.3\ 10^2\ s^{-1}$	(3.16)		$H_2O + O_3^{-\bullet} \xrightarrow{k_{13}} HO^\bullet + O_2 + HO^-$	$k_{13} = 20\text{-}30\ M^{-1}s^{-1}$	(3.26)
	$HO_3^\bullet \xrightarrow{k_5} HO^\bullet + O_2$	$k_5 = 1.1\ 10^5\ s^{-1}$	(3.17)		$HO^\bullet + O_3^{-\bullet} \xrightarrow{k_{14}} O_2^{-\bullet} + HO_2^\bullet$	$k_{14} = 6\ 10^9\ M^{-1}s^{-1}$	(3.27)
	$HO^\bullet + O_3 \xrightarrow{k_6} HO_4^\bullet$	$k_6 = 2.0\ 10^9\ M^{-1}s^{-1}$	(3.18)		$HO^\bullet + O_3^{-\bullet} \xrightarrow{k_{15}} O_3 + HO^-$	$k_{15} = 2.5\ 10^9\ M^{-1}s^{-1}$	(3.28)
	$HO_4^\bullet \xrightarrow{k_7} HO_2^\bullet + O_2$	$k_7 = 2.8\ 10^4\ s^{-1}$	(3.19)		$HO^\bullet + O_3 \xrightarrow{k_{16}} HO_2^\bullet + O_2$	$k_{16} = 4.2\ 10^8\ M^{-1}s^{-1}$	(3.29)
	$HO_4^\bullet + HO_4^\bullet \longrightarrow H_2O_2 + 2\ O_3$		(3.20)				
	$HO_4^\bullet + HO_3^\bullet \longrightarrow H_2O_2 + O_3 + O_2$		(3.21)				

HSB (Hoigné, Staehelin and Bader) state that the initial step is an oxygen-atom transfer from ozone to a hydroxide ion, followed by a reverse one-electron transfer. In contrast, TFG (Tomiyasu, Fukutomi and Gordon) only state an oxygen-atom transfer. However, the fundamental reaction in both mechanisms is the initial step, where ozone reacts with HO^-.
Considering the choice of an ozone decay mechanism, one should keep in mind that the TFG model was developed working under extremely basic conditions (11 < pH < 13), whereas the HSB model is indicated for waters at near neutral or low pH levels. On the other hand, some species as $HO_3\bullet$ and $HO_4\bullet$ radicals appearing in the HSB model were never detected and still are hypothetical.
Since decomposition begins with a reaction involving HO^-, the stability of an ozone solution is thus highly dependent on pH and decreases as alkalinity rises [Roth and Sullivan, 1983]. At pH above 8 and in presence of radical scavengers, the initiation rate has been shown to be proportional to the concentrations of ozone and HO^- [Hoigné et al., 1985]. However, in acidic solutions the reaction with HO^- cannot be the only initiation step. Predicted reaction rates below pH 4 using a mechanism based only on reaction with HO^- are much lower than those determined experimentally. According to [Sehested et al., 1991], the ozone equilibrium reaction (Equation **3.30**) becomes significant and the initiation reaction is surface catalysed.

$$O_3 \xleftrightarrow{k_{30},k_{-30}} O + O_2 \qquad (\mathbf{3.30})$$

With $k_{30} = 10^{-7}\ s^{-1}$
$k_{-30} = 4.10^9\ M^{-1}s^{-1}$

Atomic O reacts further with H_2O

$$O + H_2O \leftrightarrow 2HO\cdot \qquad (\mathbf{3.31})$$

or more likely forms an excited O_3*, from recombination, that subsequently reacts with H_2O. The reaction rate for this step has been evaluated at k = 5 $M^{-1}s^{-1}$.

$$O_3 * + H_2O \leftrightarrow H_2O_2 + O_2 \qquad (\mathbf{3.32})$$

Formed species can then continue to react forming other radicals such as $O_2\bullet^-/HO_2\bullet$. The propagating products, $HO\bullet$ and $HO_2\bullet$, diffuse and react with O_3 in the bulk, continuing the chain reaction. Only low concentrations of the terminating species are present in the bulk, why the significant part of the termination reactions (**3.33-3.35**) also takes place at the surfaces [Eriksson, 2005].

$$HO\cdot + HO\cdot \xleftrightarrow{k_{33}} H_2O_2$$
$$HO\cdot + HO_2\cdot \xleftrightarrow{k_{34}} H_2O + O_2 \qquad (\mathbf{3.33}\text{ to }\mathbf{3.35})$$
$$HO_2\cdot + HO_2\cdot \xleftrightarrow{k_{35}} H_2O_2 + O_2$$

With $k_{33} = 6.10^9\ M^{-1}s^{-1}$
$k_{34} = 7.10^9\ M^{-1}s^{-1}$
$k_{35} = 8.10^5\ M^{-1}s^{-1}$

- 3.2.2.2. Factors influencing ozone decomposition

Contradictory to the behaviour in weakly alkaline solution, the depletion rate of ozone is reduced in strongly alkaline solutions. The half-life of ozone at room temperature is about 2 minutes in 1 M NaOH solution, compared to 40 minutes in 5 M and 83 hours in 20 M solutions [Eriksson, 2005]. Furthermore, stability of aqueous ozone is affected by many other factors. Temperature for instance, as in the case of chlorine, plays a central role since higher temperature of the solution gives faster ozone depletion. We reproduce in figure **3.5** experimental results obtained by Eriksson working in pure aqueous solutions and following ozone decay at various controlled temperatures.

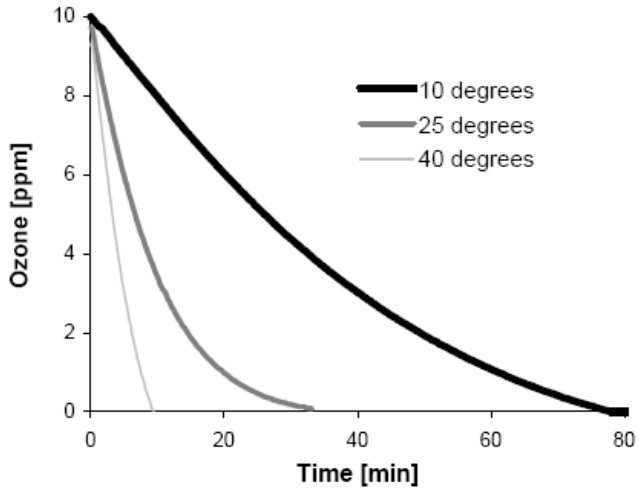

Figure 3.5 When the temperature is increased, so is the rate of depletion [Eriksson, 2005]

Many other factors highly influence ozone decay: pH, bromide concentration, alkalinity, NOM, ammonia… A good overview of these topics is given by [Zhang, 2006] and [Westerhoff, 2002]-see **3.2.4.2.**

- 3.2.2.3. Empirical models

In natural water, the reaction and decomposition of ozone are strongly dependent on water quality. Some species may induce the formation of a superoxide ion ($O_2^{\bullet -}$) from an ozone molecule, which then initiates the ozone chain reaction. These species are called *initiators*. Some other species may react with the hydroxyl radical ($HO\cdot$) and regenerate the superoxide anion ($O_2^{\bullet -}$ or $HO_2^{\bullet -}$), these species promote ozone decomposition, and are called *promoters*. There are also some species that are capable of consuming hydroxyl radical but do not generate new radicals. These species provide a stabilizing effect on the ozone molecule in the water, and are called *inhibitors*. Aqueous ozone chemistry is still the subject of research. Some researchers have tried to develop kinetic-based mechanistic models to predict ozone reactions ([Yurteri and Gurol, 1988]; [Chelkowska et al., 1992]; [Westerhoff et al., 1997]), but the precise description of ozone reactions remains difficult at the present time because of the complexity of ozone reactions and limited information on kinetic constants.

This lead to the development of empirical relations comparable to those found for chlorine decay. Thus, many expressions for long-term ozone decay rate in aqueous solutions can be found in the literature. We refer interested readers to [Savary, 2002] for a short review of the most common empirical laws for long-term ozone decay. For our part, we shall concentrate on the models proposing pseudo first-order kinetics

$$\frac{d[O_3]}{dt} = -w[O_3] \qquad (\mathbf{3.36})$$

Indeed, a host of authors has postulated, used and verified such dependence since bygone days. However, a clear definition setting standardized guidelines for the application of (**3.36**) was only given in 1994 by [Hoigné and Bader, 1994]. The authors suggested a simple method to characterise the raw-water quality by analysing the instantaneous demand (see **3.3.3.**) and the second half-life of ozone. As for chlorine, ozone is actually consumed in two steps when added to natural water: first rapidly, then more slowly. The amount of ozone consumed during the first stage can be represented by the instantaneous ozone demand, which corresponds to the difference between the administered dose and the remaining ozone after a few seconds. The rapid reaction step is followed by a moderate or slower ozone decay stage. Hoigné introduced a convenient parameter called the second half-life, defined as the ozone decomposition rate in the timeframe where the residual concentration decreases from 50 to 25% of its initial value.

In the following, we solely review two studies, where equation (**3.36**) has been implemented. Purpose was then to assess the sensibility of the aggregated constant w to operating conditions. Thus, [Yurteri and Gurol, 1988] proposed the next relation

$$\log(w) = -3.98 + 0.66.pH + 0.61.\log(TOC) - 0.42.\log\frac{TAC}{10} \qquad (\mathbf{3.37})$$

with the following requirements

- synthetic waters
- magnetically agitated discontinuous reactor
- T = 20 ± 1 °C
- 6.8 < pH < 9
- 0.3 < TOC < 5 g.m^{-3}
- 10 < TAC < 500 g $CaCO_3$.m^{-3}

Working with a potable water from the distribution network, [Wang, 1995] found w to be of the following form

$$\log(w) = -4 + 0.29.pH + 1.19.\log(TOC) - 0.41.\log(TAC) \qquad (\mathbf{3.38})$$

under the subsequent conditions

- T = 15 °C
- 7.5 < pH < 8.1
- 2 < TOC < 6 g.m^{-3}
- 84 < TAC < 150 g $CaCO_3$.m^{-3}

- 3.2.2.4. Role of NOM

The previous relations (**3.37**) and (**3.38**) stand for complex phenomena involving plethoric species, of which most of the reactivities remain unknown. Hence, their use is still limited, not to say difficult. Researchers, in order to separate and distinguish the causes of such intricate phenomena, have split NOM in different fractions, accounting for different effects (initiation, promotion, scavenging of radical species).

[von Gunten, 2003a] proposes thus a reaction pathway involving different NOM species: NOM_1, NOM_2, NOM_3, NOM_4. The below mechanism (**3.39** to **3.46**) illustrates how NOM can affect the ozone stability: it can either (i) directly react with ozone (**3.39** and **3.40**), or (ii) indirectly affect its stability through scavenging of hydroxyl radicals (**3.41** to **3.44**). Since inhibitors consist, in natural waters, of a fraction of the NOM and carbonate/bicarbonate [von Gunten, 2003a], the reactions (**3.45**) and (**3.46**) were added.

$$O_3 + NOM_1 \rightarrow NOM_{1,ox} \quad (\mathbf{3.39})$$

$$O_3 + NOM_2 \rightarrow NOM_2^{+}\cdot + O_3^{-}\cdot \quad (\mathbf{3.40})$$

The two previous reactions are generally attributed to double bonds, activated aromatic systems, amines and sulfides.

$$HO\cdot + NOM_3 \rightarrow \begin{cases} NOM_3\cdot + H_2O \\ NOM_3\cdot + HO^- \end{cases} \quad (\mathbf{3.41})$$

$$NOM_3\cdot + O_2 \rightarrow NOM_3^{+} + O_2^{-}\cdot \quad (\mathbf{3.42})$$

The two first scavenging reactions (**3.41**) and (**3.42**) constitute the part of the reaction sequence called propagation, given that they induce the formation of a superoxide radical, which, in turn, can react quickly with ozone to form a hydroxyl radical.

$$HO\cdot + NOM_4 \rightarrow NOM_4\cdot + H_2O \quad (\mathbf{3.43})$$

$$NOM_4\cdot + O_2 \rightarrow no\ O_2^{-}\bullet\ formation \quad (\mathbf{3.44})$$

$$HO\cdot + CO_3^{2-} \rightarrow CO_3^{-}\cdot + HO^- \quad (\mathbf{3.45})$$

$$HO\cdot + HCO_3^{-} \rightarrow CO_3^{-}\cdot + H_2O \quad (\mathbf{3.46})$$

While the rate constants for the reactions of all inorganic species (including carbonates) are known, it is difficult to assess the stability of ozone in natural waters due to the unknown effect of NOM. In particular, it is impossible to estimate the fraction of the NOM, which promotes or inhibits ozone decay [von Gunten, 2003a]. There have been various attempts to deduct both the kinetics of the direct ozone-NOM reaction and the promoting and inhibiting NOM fractions from spectroscopic and structural investigation of the NOM. The rate constant for direct reaction of ozone with NOM showed the best correlation with the UV absorbance or the specific absorbance (SUVA) at 254 nm. It is more difficult to estimate the fraction of promotion and inhibition of NOM [von Gunten, 2003a].

Basing on the following reaction pathway (**3.47** to **3.50**) developed in [Hoigné and Bader, 1994], [Park et al., 2001] analysed the results of their study, which investigated four river waters at different TOC rate (ranging from 0.7 to 4.9 $mg.L^{-1}$). The reaction pathway was particularly intended to enlighten the role of NOM in the instantaneous ozone demand variations with ozone dose (on instantaneous ozone demand, see next section **3.2.3.**).

$$O_3 + NOM_d \rightarrow products \quad (\mathbf{3.47})$$

$$O_3 + NOM_i \rightarrow HO\cdot + products \quad (\mathbf{3.48})$$

$$HO\cdot + NOM_p \rightarrow O_2^{-}\cdot + products \quad (\mathbf{3.49})$$

$$HO\cdot + NOM_s \rightarrow products \quad (\mathbf{3.50})$$

Here, NOM_d is the constituent of NOM likely to consume ozone by direct reactions; NOM_i, NOM_p, NOM_s are respectively constituents that may respectively act as initiators, promoters, inhibitors of the HO• chain reaction. According to the previous reaction pathway, NOM may be engaged either in direct or in chain reactions. Regarding ozone consumption, these two types of reaction act diversely: whereas direct reactions only consume ozone, chain reactions produce additional radical species (hydroxyl and superoxide), which then react very quickly to decompose ozone. Thus, a competition is taking place for ozone decay between NOM and radical species subsequently formed that results in an equilibrium.

Although being formulated differently, the previous reaction pathways ([von Gunten, 2003a] and [Hoigné and Bader, 1994]) are quite similar, the first one letting appear intermediate species (radicals) engaged in intermediate reactions. Given that the radicals are extremely reactive species, such distinction between pathways does not significantly change kinetics. The following equivalences can thus be established:

$NOM_1 \equiv NOM_d$ $\quad$ $NOM_2 \equiv NOM_i$

$NOM_3 \equiv NOM_p$ $\quad$ $NOM_4 \equiv NOM_s$

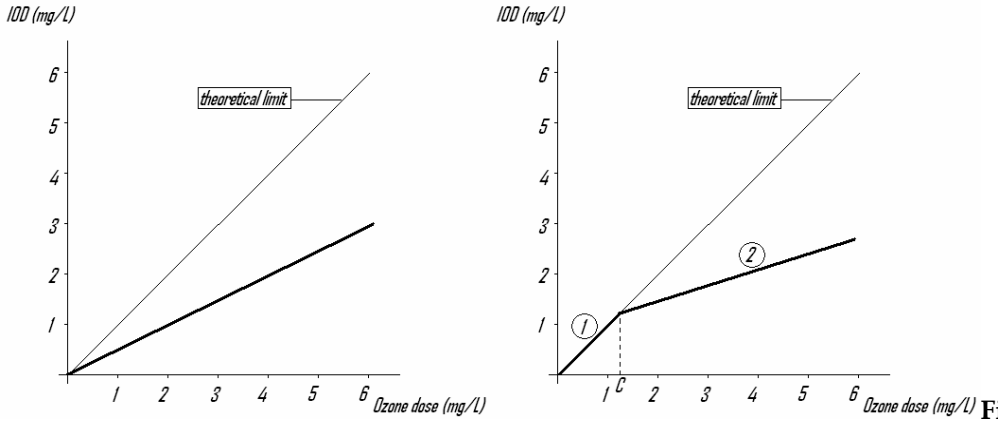

Figures 3.6 and 3.7 Instantaneous ozone demand vs. ozone dose. 3.3: in absence of NOM_d; 3.4: in presence of NOM_d.

Figures **3.6** and **3.7** schematically present the evolution of instantaneous ozone demand as a function of ozone dose for two NOM compositions. In

absence of NOM_d, the equilibrium between radicals and the NOM species involved in the HO• chain reaction is reached independently of the ozone dose (figure **3.6**). In presence of NOM_d, the previous equilibrium is more intricate since it involves more species. Basically, two domains can thus be observed (**3.7**): in ①, the ozone consumption is essentially due to direct reactions; for higher ozone doses, as in ②, both types of reactions occur successively. We then have graphically $[NOM_d]_{initial} = C$.
Note that we took here a simplistic example, where direct reactions are supposed to be much faster than chain reactions. This is not the general case, where the curve are smoother, eventually stagnating for very high ozone doses (and where $[NOM_d]_{initial} \leq C$).

[Savary, 2002] distinguishes three fractions in NOM: initiators and promoters (no difference is made between them), scavengers and final NOM not reacting anymore. A reaction for ozone consumption by NOM has also been proposed (**3.55**), of which reaction rate was calibrated to an empirical correlation such as those presented above (**3.2.2.3.**).

$$NOM_{1,a} + O_3 \rightarrow NOM_2 + HO\cdot \quad (\mathbf{3.51})$$

$$NOM_{1,b} + O_3 \rightarrow NOM_2 + HO\cdot \quad (\mathbf{3.52})$$

$$NOM_2 + HO\cdot \rightarrow NOM_f \quad (\mathbf{3.53})$$

pH dependence was observed and lead to the separation of the initiators in two different classes. Hence a pKa was defined for NOM

$$NOM_{1,a} \leftrightarrow NOM_{1,b} + H^+ \quad (\mathbf{3.54})$$

$$NOM + O_3 \rightarrow products \quad (\mathbf{3.55})$$

The effects of the inhibition fraction were found to be negligible when compared to those of carbonate/bicarbonate. Hence, the model consisted essentially of (**3.51**, **3.52 3.54** and **3.55**). Another model of reactions engaging NOM can be found in [Kim, 2004]. It has to be noted that pH dependence was also implemented in this model, though in a different manner.

3.2.3. Instantaneous ozone demand

Instantaneous ozone demand often cannot be taken in account when modelling, because of its difficult measurement. Nevertheless, many authors remarked that this demand could be possibly linearly linked to the UV absorbance, although this remains paradoxical. Such linear ozone consumption would namely suggest the chromophoric groups or classes responsible for UV absorbance to have a uniform reactivity towards ozone (this would eliminate possible "privileged" classes of organic compounds to be considered during decolorisation of ozonated waters) [Buffle, 2005].

In her PhD, [Muñoz Ramirez, 1997] determined apparent kinetics for instantaneous ozone demand, applying a method based on the competition for accessing ozone between NOM and a compound, of which kinetics were already known. Assuming many reactions in parallel, the average reaction speed is given by:

$$r = \sum_i k_{0,i}\left[S_{0,i}\right]\cdot\left[O_3\right] \qquad (3.56)$$

Studying waters from Neuilly sur Marne and Choisy-le-Roi (in the Parisian surroundings), she showed the parameter $\sum_i k_{0,i}\left[S_{0,i}\right]$ could reasonably be correlated to 254nm UV absorbance, except when mineral species such as NO_2^-, Fe^{2+}, Mn^{2+} were present and notably participated to instantaneous ozone demand:

$$\sum_i k_{0,i}\left[S_{0,i}\right] = 11\cdot UV_{254} - 0.44 \qquad (3.57)$$

Nevertheless, this correlation remains weak and relatively difficult to exploit. Furthermore, instantaneous reactions involving ozone and inorganic species have as well to be taken into account in the set of reactions.

More recently, in his PhD thesis, [Buffle, 2005] focused on instantaneous ozone demand characterisation, grounding on an original experiment that allows to start measuring ozone decomposition in water (potable or wastewater) only 350 ms after ozone addition. Without getting in the details of a full explanation, the measurements could be 100 times faster with the continuous quench-flow system developed than with a discontinuous reactor system. The measurement system was employed to evaluate ozone decomposition and hydroxyl radical generation in surface waters and wastewater.
Though the relation between UV absorbance and ozone concentration is not the main topic of this work, it is several times mentioned as a linear relation. We shall therefore present here some results obtained by Buffle, even if the UV measurements were done at 285 nm.

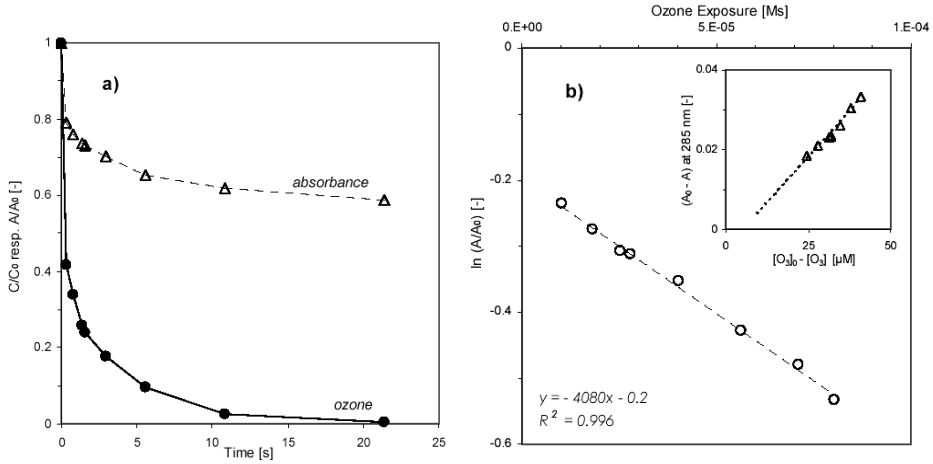

Figures 3.8 (a) and (b) Absorbance (285 nm) and dissolved ozone concentration profiles for a wastewater from Zürich at pH 8 after ozone addition (2.1 mg.L^{-1} representing 44 µM). (a) linear time scale; (b ozone exposure $\int_{u=0}^{u=t} O_3 du$ semi-log scale.

The empirical correlation obtained by Buffle is reported on figure **3.8 (b)**:

$$\ln\left(\frac{A(t)}{A_0}\right) = -4080\cdot\int_{u=0}^{u=t} O_3 du - 0.2 \qquad (3.58)$$

Obviously, this relation cannot simply be extended to any water. It deeply depends on specific characteristics varying from site to site, from water to water. In fact, the absorbance drop varies considerably according to the type of water: it can represent only 10-20% for potable waters, and over 90% for wastewaters. Clearly, a modelling becomes quite tricky under these conditions!
Buffle tackled the problem introducing a kinetic model based on distributions of NOM moieties. His results showed indeed that the radical chain reaction did not appear to control ozone decomposition in wastewater. He therefore hypothesised ozone decomposition to be controlled by direct reactions between ozone and some highly reactive moieties of the dissolved organic matter. Using a fitted distribution, changes in ozone dose could be well predicted by the model, thereby supporting the above hypothesis.
Although seducing, this approach remains case dependent and cannot be extrapolated without a preliminary calibration procedure, which is fairly complicated because of the long calibration and the experimental equipment it requires.

3.2.4 Bromate formation

- 3.2.4.1. Generalities

Bromide ions occur in natural waters in highly variable quantities, ranging from 10 to 1000 $\mu g.L^{-1}$. Originally due to natural processes (e.g. salt water intrusion, geological specificities…), their presence is increased by anthropogenic activities such as potassium mining, coal mining etc. Generally, waters containing less than 20 $\mu g.L^{-1}$ bromide are unproblematic regarding bromine-derived by-products. The situation tends to be trickier for levels in the range 50-100 $\mu g.L^{-1}$ and becomes a serious problem above 100 $\mu g.L^{-1}$ [von Gunten, 2003b].
Indeed, as soon as ozone is being dispersed in natural water containing bromides, bromate may be formed. There are two main pathways[7] to oxidise bromide

- Direct molecular oxidation through ozone
- Indirect radical reaction involving species preliminary formed during ozone degradation (mainly through HO• and CO_3^-•)

Figure **3.9** represents the reaction pathway leading to bromate from bromide

[7] Some authors distinguish three pathways conducting to bromate: direct, direct-indirect and indirect-direct ozonations [Song et al., 1997].

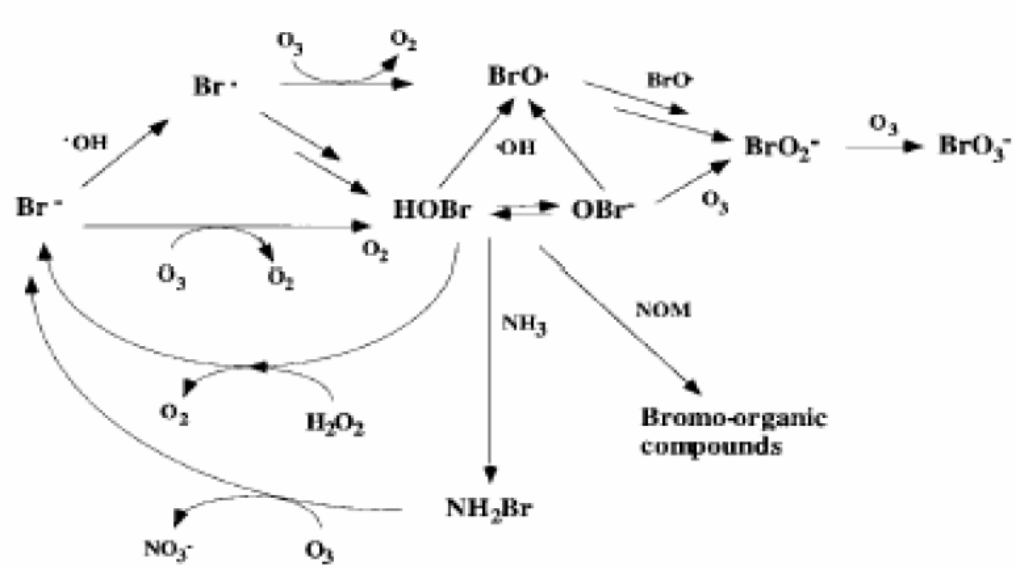

Figure 3.9 Bromate formation pathways [von Gunten and Pinkernell, 2000]

Important Remark:

The quantities of ozone engaged in bromate formation are negligible compared to overall ozone decay in natural waters. Therefore, the reactions presented in the below picture do not have significant influence upon ozone profile. Thus, in our case, seeking to simulate an ozonation process knowing (i) some inlet concentrations - excepting ozone - (ii) and residual ozone, one should act as follows:

1. assess initial ozone concentration simulating ozone decay. According to the previous explanations, this step solely necessitates one of the models presented in **3.2.2.**
2. determine bromate fate, performing the simulation calculations with a more exhaustive model.

The first step corresponds to a BVP (Boundary Value Problem, see **5.1.**), whereas the second is an IVP (Initial Value Problem).

- 3.2.4.2. Factors influencing bromate formation

Given the undetermined character of NOM, many species found in water can reveal to be initiators, promoters, or inhibitors of ozone decomposition and bromate formation. Hence, many factors may act upon bromate formation. We only list here the main parameters.

Temperature

Reaction rate constants, equilibrium constants, Henry's law coefficients… all these parameters are temperature-dependent. Under those circumstances, trying to find out what are the consequences to an increase or a drop in temperature becomes complex. However, the main effect of temperature concerns hydroxyl radicals concentration: since the concentration of hydroxyl radicals increases with temperature, bromate formation will be accelerated at

higher temperatures, though some authors agree that temperature has a relatively small effect on bromate formation relative to pH and ammonia concentration [von Gunten and Pinkernell, 2000].

pH

Hydroxyde ions are initiators of the chain reaction for ozone decomposition. An increase in pH therefore promotes ozone decomposition and influences the oxidation reactions of ozone with other species [Krasner et al., 1995]. It was notably reported that dissolved ozone at pH levels below 7, does not react with water and is present as molecular O_3. As the pH is elevated, however, spontaneous decomposition of ozone occurs to finally produce a variety of very reactive free radials, such as the hydroxyl radical (HO•) [Zhang, 2006].

pH has great influence on the bromate formation as well. Decreasing pH can thus change the bromate formation in two ways

i. Shift of HOBr/OBr^- equilibrium to HOBr to prevent further oxidation by ozone
ii. Decrease of the rate of HO• radical formation from ozone decomposition, which drops the oxidation rate of HOBr. This explains why bromate formation is often controlled by pH depression

Bromide

Since bromate is an oxidised form of bromide, one could expect an increase in bromide concentration to be reflected on bromate concentration. This was indeed observed in numerous studies. Moreover, high bromide concentrations favour molecular ozone decomposition mechanism, what in turn prolongs the second half-time of ozone (**3.2.2.3.**).

Alkalinity

Carbonate and bicarbonate ions can scavenge the hydroxyl radicals formed during ozone decomposition. As a result, alkaline species may reduce the decomposition rate of the dissolved ozone and inhibit the hydroxyl radical pathway of bromate formation. However, above pH 8.5, the effect of alkalinity becomes pH dependent because carbonate ions scavenge HO• radicals with a rate constant much larger than that of bicarbonate ion [Hoigné, 1994].

Finally, an increase in alkalinity would favour bromate formation only under high pH conditions as

i. The equilibrium HCO_3^-/ CO_3^{2-} is shifted (pKa = 10.3), advantaging CO_3^{2-} ions that are more reactive than HCO_3^- towards HO• radicals
ii. Both HO• radicals and BrO^- ions concentrations increase with pH (pKa(HOBr/OBr^-) = 8.86). The carbonates and bicarbonates may react first with HO• to form the radical species CO_3^{-}•, which in turn would react with BrO^-, leading to bromate formation [von Gunten and Hoigné, 1993]

Natural organic matter (NOM)
As stated above (**3.2.2.4.**), the stability of ozone largely depends on the type and content of NOM. Generally, the presence of the NOM in water will lower the stability of ozone through direct reaction with molecular ozone and consumption of HO• radicals. The presence of NOM inhibits the formation of bromate especially at the initial period of ozonation (see **3.2.2.4.** and particularly figures **3.6** and **3.7**).

Ammonia
Though limited reactivity with ozone, ammonia (NH_3), in the presence of bromide ions, can mask the hypobromate ions formed during ozonation and thereby delay the formation of bromate, bromoform and further bromo-organic compounds [Langlais et al., 1991]. As a result, the formation of bromate can be inhibited in ammonia-containing water. Addition of ammonia may then be used as a bromate control method. However, bromate removal by ammonia addition is not efficient for waters that have a low pH and/or already contain high ammonia levels [Westerhoff, 2002].

Table **3.3** gives an overview of the consequences of a change in the over-listed parameters upon disinfection efficiency, decomposition rate of ozone and bromate formation.

Table 3.3 Summary of the effects of water parameters, adapted from [Westerhoff, 2002]

Parameter increasing	Disinfection efficiency	Ozone decomposition rate	Bromate formation rate
Temperature	+	+	+
pH	-	+	+
Bromide	-	+	+
Alkalinity	+	-	+*for high pH*, -*else*
NOM	-	+	-
Ammonia	unchanged	unchanged	-

- 3.2.4.3. Empirical models

[Song et al., 1996]
The authors developed an empirical model based on a set of experimental points obtained in a closed reactor. Data was collected according to a design of experiments built to cover a wide range of conditions. The evolution of bromate concentration is evaluated according to

$$[BrO_3^-] = 10^{-6.11}[Br^-]_0^{0.88}[DOC]^{-1.18}[N-NH_3]^{-0.18}[O_3]^{1.42}\, pH^{5.11}[Alk]^{0.18}\, t^{0.27} \quad (\mathbf{3.59})$$

under the subsequent conditions
- 6.5 < pH < 8.5
- 100 < [Br-] < 1000 µg.L^{-1}
- 1 < [$CaCO_3$ alk.] < 216 mg.L^{-1}

- 1.5 < [COD] < 6.0 mg.L^{-1}
- 0.005 < [N-NH_3] < 0.70 mg.L^{-1}
- 1.5 < [O_3] < 6.0 mg.L^{-1}
- 1 < t < 30 min.

Since its formulation, this model has been validated by different researchers and is being nowadays widely used as prediction tool [Savary, 2002].

[Ozekin and Amy, 1997]
Following empirical models were developed from a compilation of data available in the literature. Waters containing ammonia where treated separately. The correlations (**3.60**) and (**3.61**) are valid for a temperature of 20 °C only.

Model without ammoniac (**3.60**)

$$\log[BrO_3^-] = -3.361 + 0.006.t + 0.249.pH + 1.575.\log[O_3] + 1.136.\log[Br^-] - 1.267.\log[COD]$$

Model with ammoniac (**3.61**)

$$\log[BrO_3^-] = -3.561 + 0.006.t + 0.253.pH + 1.598.\log[O_3] + 1.137.\log.[Br^-] - 1.186.\log.[COD] - 0.086.\log.[NH_3]$$

under following conditions
- 6.5 < pH < 8.5
- 69 < [Br-] < 440 µg.L^{-1}
- 1.9 < [COD] < 8.4 mg.L^{-1}
- 0 < [N-NH_3] < 3 mg.L^{-1}
- 1.05 < [O_3] < 10 mg.L^{-1}
- 1 < t < 60 min.

The following equation can be used afterwards to account for the temperature effect on bromate formation

$$[BrO_3^-]_T = [BrO_3^-]_{20°C}.1.035^{T-20} \qquad (\mathbf{3.62})$$

- 3.2.4.4. Mechanistic models

Although relative consensus on the reaction pathway leading to bromate formation [von Gunten, 2003b], various differences may be found when comparing mechanistic models. We shall present in this section three examples originating from (i) [Westerhoff et al., 1998], (ii) [Savary, 2002] and (iii) [Kim et al., 2004].

[Westerhoff et al., 1998]
Purpose of this study was to discuss the use of numerical models that link ozone consumption reactions with bromide oxidation reactions. Hence, three models were developed and compared; we shall present here only the more complete, which includes the HSB decay model coupled with a reaction pathway for bromide oxidation.

Table 3.4 Ozone decomposition mechanism used by Westerhoff et al. (HSB+3.23 (TFG))

Equation no.	Reaction	k or pK_a
2	$O_3 + OH^- \rightarrow HO_2^- + O_2$	70 $M^{-1} s^{-1}$
3	$HO_2 \leftrightarrow H^+ O_2^-$	4.8
4	$O_3 + O_2^- \rightarrow O_3^- + O_2$	1.6×10^9 $M^{-1} s^{-1}$
5	$HO_3 \leftrightarrow H^+ O_3^-$	8.2
6	$HO_3 \rightarrow HO + O_2$	1.1×10^5 s^{-1}
7	$HO + O_3 \rightarrow HO_4$	2.0×10^9 $M^{-1} s^{-1}$
8	$HO_4 \rightarrow HO_2 + O_2$	2.8×10^4 s^{-1}
9	$HO_4 + HO_4 \rightarrow H_2O_2 + 2O_3$	5.0×10^9 $M^{-1} s^{-1}$
10	$HO_4 + HO_3 \rightarrow H_2O_2 + O_2 + O_3$	5.0×10^9 $M^{-1} s^{-1}$
11	$H_2O_2 \leftrightarrow HO_2^- + H^+$	11.6
12	$O_3 + HO_2^- \rightarrow HO + O_2 + O_2$	2.2×10^6 $M^{-1} s^{-1}$

Table **3.4** gives the ozone decay mechanism implemented. In reality, it also comprises a reaction from the TFG model (equation **12** from the table, see **3.2.2.**). All the reactions were found in literature; therefore, no calibration was necessary. The predictions of the reaction model were compared to observed ozone residuals for experimental baseline conditions (Initially, pH = 7.5, O_3 dose = 62.5 µM, NOM-free water, [Br^-] = 5 µM). It appeared that the model over evaluated ozone concentration for reaction times exceeding one hour (after one an half hour, a discrepancy from about 40% was reported).

Table **3.5** presents the reactions of bromide oxidation. Reactions **45** and **46** were added herein to assess the importance of indirect oxidation pathway. Addition of 0.7 to 2.0 mM of t-butanol, depending on the ozone dosage, conducts namely to a predicted scavenging of hydroxyl radicals exceeding 90%. The batch ozonation experiments (pH = 6.5 to 8.5, O_3 dosages = 30 to 125 mM, NOM-free water, [Br^-] = 1 to 5 mM) allowed that way to delineate the qualitative significance of the radical pathway: radical chain reactions accounted for approximately 40 to 65% of the bromate formation. This evaluation was repeated numerically introducing fictive compounds into the reaction pathway: radical reactions were found to be responsible for 70% of the bromate formation. Both results are not surprising ([von Gunten, 2003b], [Laplanche et al., 1998]).

The first simulation runs done with literature values for the reaction rate constants did not give satisfaction. The authors decided therefore to adjust a key parameter to fit calculated profiles to experimental data: it was k_{13}, reaction rate constant of the 13th reaction. Values found in the literature range from 90 to 270 $M^{-1}s^{-1}$; the final value of 50 $M^{-1}s^{-1}$ was selected. Lowering the k_{13} value resulted in a better simulation of observed bromide concentrations and only lead to a slight under prediction of bromate concentrations. The results could however be ameliorated: only an error of 15% concerning bromate; underestimation of 100% for bromine, overestimation of 100% for bromide.

Table 3.5 Reaction pathway leading to bromate ions through oxidation of bromide

Equation no.	Reaction	k or pK_a	Reference
13	$Br^- + O_3 \rightarrow BrO^- + O_2$	50 $M^{-1} s^{-1}$	fitted parameter
14	$BrO^- + O_3 \rightarrow Br^- + 2O_2$	300 $M^{-1} s^{-1}$	Haag and Hoigne, 1983
15	$BrO^- + O_3 \rightarrow BrO_2^- + O_2$	100 $M^{-1} s^{-1}$	Haag and Hoigne, 1983
16	$HOBr \leftrightarrow H^+ + BrO^-$	9.0	von Gunten and Hoigne, 1994
17	$BrO_2^- + O_3 \rightarrow BrO_3^- + O_2$	1×10^5 $M^{-1} s^{-1}$	Haag and Hoigne, 1983
18	$Br^- + HO \rightarrow BrOH^-$	1.1×10^{10} $M^{-1} s^{-1}$	Zehavi and Rabini, 1972
19	$BrOH^- \rightarrow Br^- + HO$	3.3×10^7 s^{-1}	Zehavi and Rabini, 1972
20	$BrOH^- \rightarrow Br + OH^-$	4.2×10^6 s^{-1}	Zehavi and Rabini, 1972
21	$Br + Br^- \rightarrow Br_2^-$	2×10^9 $M^{-1} s^{-1}$	Zehavi and Rabini, 1972
22	$Br + O_3 \rightarrow BrO + O_2$	1×10^{10} $M^{-1} s^{-1}$	Taube, 1942
23	$Br_2^- + Br_2^- \rightarrow Br_3^- + Br^-$	2×10^9 $M^{-1} s^{-1}$	Sutton *et al.*, 1965
24	$Br_3^- \leftrightarrow Br_2 + Br^-$	1.23	Sutton *et al.*, 1965
25	$Br_2 + H_2O \rightarrow HOBr - Br^- + H^+$	8.24 $M^{-1} s^{-1}$	Sutton *et al.*, 1965
26	$BrO^- + Br_2^- \rightarrow BrO - 2Br^-$	8×10^7 $M^{-1} s^{-1}$	Buxton and Dainton, 1968
27	$BrO^- + HO \rightarrow BrO + OH^-$	4.5×10^9 $M^{-1} s^{-1}$	Buxton and Dainton, 1968
28	$HOBr + H_2O_2 \rightarrow Br^- + H_2O$	7×10^4 $M^{-1} s^{-1}$	von Gunten *et al.*, 1996
29	$BrO^- + H_2O_2 \rightarrow Br^- - H_2O_2$	2×10^5 $M^{-1} s^{-1}$	von Gunten *et al.*, 1996
30	$BrO^- + Br \rightarrow BrO + Br^-$	4.1×10^9 $M^{-1} s^{-1}$	Klanning and Wolff, 1985
31	$BrO + BrO + H_2O \rightarrow BrO^- + BrO_2^- + 2H^+$	4.9×10^9 $M^{-1} s^{-1}$	Buxton and Dainton, 1968
32	$BrO_2^- + HO \rightarrow BrO_2 + OH^-$	2×10^9 $M^{-1} s^{-1}$	Buxton and Dainton, 1968
33	$BrO_2 - BrO_2 \rightarrow Br_2O_4$	1.4×10^9 $M^{-1} s^{-1}$	Buxton and Dainton, 1968
34	$Br_2O_4 \rightarrow BrO_2 + BrO_2$	7×10^9 $M^{-1} s^{-1}$	Buxton and Dainton, 1968
35	$Br_2O_4 + OH^- \rightarrow BrO_3^- + BrO_2^- + H^+$	7×10^8 $M^{-1} s^{-1}$	Buxton and Dainton, 1968
36	$HCO_3^- \leftrightarrow CO_3^{2-} + H^+$	10.25	
37	$CO_2 + H_2O \leftrightarrow HCO_3^- + H^+$	6.37	
38	$CO_3^{2-} + HO \rightarrow CO_3^- + OH^-$	3.7×10^8 $M^{-1} s^{-1}$	Buxton *et al.*, 1988
39	$HCO_3^- + HO \rightarrow HCO_3 + OH^-$	8×10^6 $M^{-1} s^{-1}$	Buxton *et al.*, 1988
40	$ROC + HO \rightarrow$ Products + ROC	2×10^8 $M^{-1} s^{-1}$	Westerhoff *et al.*, 1997b
41	$HCO_3 \leftrightarrow CO_3^- + H^+$	9.6	Chen *et al.*, 1973
42	$CO_3^- + BrO^- \rightarrow BrO + CO_3^{2-}$	4.3×10^7 $M^{-1} s^{-1}$	Klanning and Wolff, 1985
43	$HOBr + HO \rightarrow BrO - H_2O$	2×10^9 $M^{-1} s^{-1}$	Buxton and Dainton, 1968
44	$HOBr + O_2^- \rightarrow Br \cdot OH^- + O_2$	9.5×10^8 $M^{-1} s^{-1}$	Schwarz and Bielski, 1986
45	t-butanol + $O_3 \rightarrow$ Products	6×10^5 $M^{-1} s^{-1}$	Buxton *et al.*, 1988
46	t-butanol + $O_3 \rightarrow$ Products	3×10^3 $M^{-1} s^{-1}$	Buxton *et al.*, 1988

Further, the authors decided to study waters containing NOM (DOC = 3 $mg.L^{-1}$ of isolated NOM material). In parallel, they incorporated reactions involving NOM in the pathway. Reactions between NOM and hydroxyl or BrO• radicals and hypobromite/hypobromous acid were thus taken into account with the following equations

$$HO\cdot + \text{NOM} \xrightarrow{k_{HO\bullet}} \text{product 1} \qquad (\mathbf{3.63})$$

$$OBr^- + NOM \xrightarrow{k_{Br,2}} Br^- + \text{product 2} \qquad (\mathbf{3.64})$$

$$HOBr + NOM \xrightarrow{k_{Br,2}} Br^- + \text{product 3} \qquad (\mathbf{3.65})$$

$$BrO\cdot + NOM \xrightarrow{k_3} HOBr + \text{products} \qquad (\mathbf{3.66})$$

where $k_{HO\bullet} = 3.96.10^8\ M^{-1}s^{-1}$
$k_{Br,2} = 5\ M^{-1}s^{-1}$
$k_3 = 5.10^3\ M^{-1}s^{-1}$

The authors considered here NOM solely as scavenger species, thus excluding its potential to form radicals (see **3.2.2.4.**). Despite this complex reaction pathway, the results of the simulation runs were not fully

satisfactory; Westerhoff et al. concluded on the difficulty for researchers to integrate the intricate effects of NOM into a precise prediction model for bromate formation.

[Savary, 2002]
Designed to predict by-products formation (with emphasis on bromate) during ozonation processes, this model contains an ozone decay mechanism accompanied by a bromate formation reactions set. Only the latter shall be presented in this section.
As [Westerhoff et al., 1998] previously, Savary decided to minimise the amount of reactions between radical species. Although potential high reactivity, a reaction that involves two species with very low concentrations can actually not account significantly in the overall chemical mechanisms. Additionally, some activation energies of the reactions involved in the pathway could not be found in literature; they were therefore guessed according to following table **3.6**.

Table 3.6 Assumptions made concerning values missing in the literature

Reaction type	Activation energy
Radical reaction involving mineral species	7.5 kJ.mol^{-1}
Radical reaction involving organic species	15 kJ.mol^{-1}
Molecular reaction	42 kJ.mol^{-1}
Reaction between radical species	*Not considered*

We give in the two next pages the reactions considered by Savary in her Ph.D. thesis, with their reaction rate constants calculated for a temperature of 25 °C. The reader is referred to section **3.2.2.4.**, where a presentation of the reactions involving NOM is given.

First numerical tests made by introducing fictive tracer (see Westerhoff et al. above) revealed possible simplification of the model we present in the following. Indeed, it appeared that such species as Br_2O_4, $Br_2^{-}\bullet$, $BrO_2\bullet$ were not likely to form under normal process conditions.
At 25°C,

$$2BrO_2\cdot \rightarrow Br_2O_4 \qquad k_d = 1.4.10^9\ M^{-1}s^{-1} \qquad (\mathbf{3.67})$$

$$Br_2O_4 \rightarrow 2BrO_2\cdot \qquad k_i = 7.10^7\ s^{-1} \qquad (\mathbf{3.68})$$

Here, given the reaction rate constants, one might think Br_2O_4 should be formed. However, reaction (**3.67**) involves two radical species; the ratio $\frac{k_d}{k_i}$ is not large enough in this case to compensate the weakness of radical concentrations.
The subsequent mechanism presented in table **3.7** also includes reactions accounting for the oxidation of pesticides (designated under "**P**"). These are quite general and applicable to other pesticides (they were here applied on *atrazine* degradation) under the requirement of being calibrated. More generally, the modelling of oxidation for other micropollutants or species leading to micropollutants remains simple. Considering pathogens such as

oocysts of the protozoan parasite *Cryptosporidium parvum*, which have shown strong resistance to free chlorine and monochloramine, the authors, as [Kim et al., 2004], often chose the CT approach using inactivation curves. The latter have been characterized by the presence of an initial lag phase during which little inactivation occurs followed by a phase of pseudo first-order decrease in viability. As a result, the CT required to achieve a certain level of *Cryptosporidium parvum oocyst* inactivation has been found to be independent of the dissolved ozone concentration [Driedger et al., 2001].

Future task will hence consists, in order to reduce the number of chemical reactions, in assessing the relative importance of each single way part of the global reaction pathway. Having evaluated the "liveliness", the "vivacity" of each branch, we will then be able to cut down those inactive.

Table 3.7 Reaction pathway proposed by Savary (T = 25°C)

$Br^- + O_3$	→	BrO^-	k=160	$M^{-1}.s^{-1}$
$BrO^- + O_3$	→	Br^-	k=330	$M^{-1}.s^{-1}$
$BrO^- + O_3$	→	BrO_2^-	k=100	$M^{-1}.s^{-1}$
$BrO_2^- + O_3$	→	BrO_3^-	k>1.0e6	$M^{-1}.s^{-1}$
$Br^- + HO^\bullet$	→	$BrOH^{-\bullet}$	K=1.0e10	$M^{-1}.s^{-1}$
$BrOH^{-\bullet}$	→	Br-+HO•	k=3.3e7	s^{-1}
$BrOH^{-\bullet}$	→	$Br^\bullet + HO^-$	k=4.2e6	s^{-1}
$Br^- + Br^\bullet$	→	$Br_2^{-\bullet}$	k=1.0e10	$M^{-1}.s^{-1}$
$2Br_2^{-\bullet} + H_2O$	→	$3Br^- + BrOH$	k=2.0e9	$M^{-1}.s^{-1}$
$Br_2^{-\bullet} + BrO^-$	→	$2Br^- + BrO^\bullet$	k=8e7	$M^{-1}.s^{-1}$
$BrO^- + HO^\bullet$	→	$BrO^\bullet + HO^-$	k=4.5e9	$M^{-1}.s^{-1}$
$BrOH + HO^\bullet$	→	$BrO^\bullet + H_2O$	k=2e9	$M^{-1}.s^{-1}$
$2BrO^\bullet + H_2O$	→	$BrO^- + BrO_2^-$	k=4.9e9	$M^{-1}.s^{-1}$
$BrO_2^- + HO^\bullet$	→	$BrO_2^{\bullet} + HO^-$	k=2e9	$M^{-1}.s^{-1}$
$2BrO_2^{\bullet}$	→	Br_2O_4	k=1.4e9	$M^{-1}.s^{-1}$
Br_2O_4	→	$2BrO_2^{\bullet}$	k=7e7	s^{-1}
$BrO_2^{\bullet} + HO^\bullet$	→	$BrO_3^- + H^+$	k=2e9	$M^{-1}.s^{-1}$
$Br^\bullet + OBr^-$	→	$BrO^\bullet + Br^-$	k=4.1e9	$M^{-1}.s^{-1}$
$Br_2^{-\bullet}$	→	$Br^- + Br^\bullet$	k=5e4	s^{-1}
$BrO^\bullet + BrO_2^-$	→	$BrO^- + BrO_2^{\bullet}$	k=3.4e8	$M^{-1}.s^{-1}$
$BrO_2^- + Br_2^{-\bullet}$	→	$Br^- + BrO^\bullet + BrO^-$	k=8e7	$M^{-1}.s^{-1}$
$P + O_3$	→	P_{ox}	k=13	$M^{-1}.s^{-1}$
$P + HO^\bullet$	→	P_{ox}	k=2.4e9	$M^{-1}.s^{-1}$
$O_3 + HO_2^-$	→	$O_3^{-\bullet} + HO_2^\bullet$	k=1.5e6	$M^{-1}.s^{-1}$
$O_3^{-\bullet} + H_2O$	→	$HO^\bullet + O_2 + HO^-$	k=15	s^{-1}
$HO_2^- + HO^\bullet$	→	$HO_2^\bullet + H_2O$	k=7.5e9	$M^{-1}.s^{-1}$
$H_2O_2 + HO^\bullet$	→	$HO_2^\bullet + H_2O$	k=7e7	$M^{-1}.s^{-1}$
$O_3 + O_2^{-\bullet}$	→	$O_3^- + O_2$	k=1,6e9	$M^{-1}.s^{-1}$
$O_3 + HO^\bullet$	→	$HO_2^\bullet + O_2$	k=5e8	$M^{-1}.s^{-1}$
$CO_3^{-\bullet} + BrO^-$	→	$CO_3^{2-} + BrO^\bullet$	k=4.3e7	$M^{-1}.s^{-1}$
$CO_3^{2-} + HO^\bullet$	→	$CO_3^{-\bullet} + HO^-$	k=3.9e8	$M^{-1}.s^{-1}$
$HCO_3^- + HO^\bullet$	→	$HCO_3^{\bullet} + HO^-$	k=8.5e6	$M^{-1}.s^{-1}$
$CO_3^{-\bullet} + BrO_2^-$	→	$CO_3^{2-} + BrO_2^\bullet$	k=1.1e8	$M^{-1}.s^{-1}$
$CO_3^{-\bullet} + O_3$	→	H_2CO_3	k=1e9	$M^{-1}.s^{-1}$
$CO_3^{-\bullet} + HO_2^-$	→	$CO_3^{2-} + HO_2^\bullet$	k=5.6e7	$M^{-1}.s^{-1}$
$CO_3^{-\bullet} + H_2O_2$	→	$HCO_3^- + HO_2^\bullet$	k=800000	$M^{-1}.s^{-1}$
$HCO_3^- + O_2^{-\bullet}$	→	$CO_3^{-\bullet} + HO_2^-$	k=2e6	$M^{-1}.s^{-1}$
$HCO_3^{\bullet} + BrO^-$	→	$HCO_3^- + BrO^\bullet$	k=4.3e7	$M^{-1}.s^{-1}$
$COT_1a + O_3$	→	$COT_2 + HO^\bullet$		
$O_3 + COT_1b$	→	$COT_2 + HO^\bullet$	*See next tables*	
$COT_2 + HO^\bullet$	→	COT_S		
$COT + HO^\bullet$	→	*products (no radicals)*		

Table 3.8 Reactions involving pH, adapted from [Savary, 2002]

$Br^{\bullet} - HO^-$	→	$BrOH^{-\bullet}$	k=1.3e10	$M^{-1}.s^{-1}$
O_3+HO^-	→	$HO_2^-+O_2$	k=70	$M^{-1}.s^{-1}$
$Br_2O_4+HO^-$	→	$BrO_2^-+BrO_3^-$	k=7e8	$M^{-1}.s^{-1}$

Table 3.9 Acid/base equilibria, adapted from [Savary, 2002]

BrO^-+H^+	→	BrOH	pKa=8.86
HOBr	→	BrO^-+H^+	
$HO_2^{\bullet}$	→	$O_2^{-\bullet}+H^+$	pka=4.8
$O_2^{-\bullet}+H^+$	→	$HO_2^{\bullet}$	
H_2O_2	→	$HO_2^-+H^+$	pka=11.6
$HO_2^-+H^+$	→	H_2O_2	
HCO_3^-	→	$CO_3^{2-}+H^+$	pka=10.3
$CO_3^{2-}+H^+$	→	HCO_3^-	
$H_2CO_3^{\bullet}$	→	$HCO_3^-+H^+$	pka=6.3
$HCO_3^-+H^+$	→	H_2CO_3	
HCO_3	→	$CO_3^{-\bullet}+H^+$	pka=9.6
$CO_3^{-\bullet}+H^+$	→	$HCO_3^{\bullet}$	
COT_1a	→	COT_1b+H^+	*See table 2.10*
COT_1b+H^+	→	COT_1a	

Table 3.10 Constant values for the initiating fraction of NOM

Sample date	k_{acid}	k_{basic}	pKa
1999, Oct. 28	0.5	500	9.7
1999, Dec. 13	0.5	400	8.9
2000, March 6	0.5	500	10.1
2000, April 3	0.5	494	8.3

[Kim et al., 2004]
This model was developed to simultaneously assess *Cryptosporidium parvum oocyst* inactivation and bromate formation during ozonation of synthetic solutions in batch and flow-through reactors.
For the initiation stage of ozone decomposition, two reactions are proposed in the following reaction pathway. Both reactions have been used in various modelling studies (due to a lack of clear experimental evidence to select one over the other) and, in fact, [Kim et al., 2004] report good predictions on

ozone decomposition with both reactions. The authors finally chose R1 after having compared the simulated ratios $\frac{[HO\cdot]}{[O_3]}$ for R1 and R1′.

no.	reaction	constant	ref	no.	reaction	constant	ref
			Ozone Decomposition				
R1	$O_3 + OH^- \rightarrow HO_2^\bullet + O_2^{\bullet-}$	$k_1 = 38\ M^{-1}\ s^{-1}$	*21, 22*	R8	$HO^\bullet + O_3 \rightarrow HO_2^\bullet + O_2$	$k_8 = 2.6 \times 10^8\ M^{-1}\ s^{-1}$	*24[c], 44[c]*
R1′	$O_3 + OH^- \rightarrow HO_2^- + O_2$	$k_1 = 70\ M^{-1}\ s^{-1}$	*21, 22*	R8′	$HO^\bullet + O_3 \rightarrow HO_4^\bullet$	$k_{8'} = 2.0 \times 10^9\ M^{-1}\ s^{-1}$	*24[e]*
R2	$H_2O_2 \leftrightarrow HO_2^- + H^+$	$pK_a = 11.6$	*60*	R9	$HO^\bullet + H_2O_2 \rightarrow HO_2^\bullet + H_2O$	$k_9 = 2.7 \times 10^7\ M^{-1}\ s^{-1}$	*45*
R3	$O_3 + HO_2^- \rightarrow HO^\bullet + O_2^{\bullet-} + O_2$	$k_3 = 2.8 \times 10^6\ M^{-1}\ s^{-1}$	*21[a]*	R10	$HO^\bullet + HO_2^- \rightarrow O_2^{\bullet-} + H_2O$	$k_{10} = 7.5 \times 10^9\ M^{-1}\ s^{-1}$	*45*
R4	$HO_2^\bullet \leftrightarrow O_2^{\bullet-} + H^+$	$pK_a = 4.8$	*25*	R11	$HO^\bullet + HO^\bullet \rightarrow H_2O_2$	$k_{11} = 5.5 \times 10^9\ M^{-1}\ s^{-1}$	*24*
R5	$O_3 + O_2^{\bullet-} \rightarrow O_3^{\bullet-} + O_2$	$k_5 = 1.6 \times 10^9\ M^{-1}\ s^{-1}$	*25[b], 43[c]*	R12	$HO\cdot + O_2^{\bullet-} \rightarrow OH^- + O_2$	$k_{12} = 1 \times 10^{10}\ M^{-1}\ s^{-1}$	*24*
R6a	$O_3^{\bullet-} + H^+ \rightarrow HO_3^\bullet$	$k_{6a} = 5.2 \times 10^{10}\ M^{-1}\ s^{-1}$	*25*	R13	$HO^\bullet + HO_3^\bullet \rightarrow H_2O_2 + O_2$	$k_{13} = 5 \times 10^9\ M^{-1}\ s^{-1}$	*24*
R6b	$HO_3^\bullet \rightarrow O_3^{\bullet-} + H^+$	$k_{6b} = 3.3 \times 10^2\ s^{-1}$	*25*	R14	$O_2^{\bullet-} + HO_3^\bullet \rightarrow OH^- + 2O_2$	$k_{14} = 1 \times 10^{10}\ M^{-1}\ s^{-1}$	*24*
R7	$HO_3^\bullet \rightarrow HO^\bullet + O_2$	$k_7 = 1.1 \times 10^5\ s^{-1}$	*25[d]*	R15	$HO_3^\bullet + HO_3^\bullet \rightarrow H_2O_2 + 2O_2$	$k_{15} = 5 \times 10^9\ M^{-1}\ s^{-1}$	*24*
			Bromate Formation				
R20	$Br^- + O_3 \rightarrow O_2 + OBr^-$	$k_{20} = 160\ M^{-1}\ s^{-1}$	*46*	R31b	$HOBr + H^+ + Br^- \rightarrow Br_2 + H_2O$	$k_{31b} = 1.6 \times 10^{10}\ M^{-2} s^{-1}$	*53*
R21	$OBr^- + O_3 \rightarrow 2O_2 + Br^-$	$k_{21} = 330\ M^{-1}\ s^{-1}$	*46*	R32	$HOBr \leftrightarrow BrO^- + H^+$	$pK_a = 8.8$	*46*
R22	$OBr^- + O_3 \rightarrow BrO_2^- + O_2$	$k_{22} = 100\ M^{-1}\ s^{-1}$	*46*	R33	$OBr^- + Br^\bullet \rightarrow BrO^\bullet + Br^-$	$k_{33} = 4.1 \times 10^9\ M^{-1}\ s^{-1}$	*49*
R23	$BrO_2^- + O_3 \rightarrow BrO_3^- + O_2$	$k_{23} = 5.7 \times 10^4\ M^{-1}\ s^{-1}$	*46, 47[f]*	R34	$OBr^- + {}^\bullet OH \rightarrow BrO^\bullet + OH^-$	$k_{34} = 4.2 \times 10^9\ M^{-1}\ s^{-1}$	*54*
R24a	$Br^- + {}^\bullet OH \rightarrow BrOH^{\bullet-}$	$k_{24a} = 1.1 \times 10^{10}\ M^{-1}\ s^{-1}$	*48*	R35	$HOBr + {}^\bullet OH \rightarrow BrO^\bullet + H_2O$	$k_{35} = 2.0 \times 10^9\ M^{-1}\ s^{-1}$	*49*
R24b	$BrOH^{\bullet-} \rightarrow Br^- + {}^\bullet OH$	$k_{24b} = 3.3 \times 10^7\ s^{-1}$	*48*	R36	$HOBr + O_2^{\bullet-} \rightarrow O_2 + Br^\bullet + OH^-$	$k_{36} = 3.5 \times 10^9\ M^{-1}\ s^{-1}$	*55*
R25a	$BrOH^{\bullet-} \rightarrow Br^\bullet + OH^-$	$k_{25a} = 4.2 \times 10^6\ s^{-1}$	*48*	R37	$HOBr + HO_2^- \rightarrow Br^- + O_2 + H_2O$	$k_{37} = 7.6 \times 10^8\ M^{-1}\ s^{-1}$	*56*
R25b	$Br^\bullet + OH^- \rightarrow BrOH^{\bullet-}$	$k_{25b} = 1.3 \times 10^{10}\ M^{-1}\ s^{-1}$	*49*	R38	$O_3 + Br^\bullet \rightarrow O_2 + BrO^\bullet$	$k_{38} = 1.5 \times 10^8\ M^{-1}\ s^{-1}$	*19*
R26	$BrOH^{\bullet-} + H^+ \rightarrow Br^\bullet + H_2O$	$k_{26} = 4.4 \times 10^{10}\ M^{-1}\ s^{-1}$	*48*	R39	$2BrO^\bullet + H_2O \rightarrow OBr^- + BrO_2^- + 2H^+$	$k_{39} = 5 \times 10^9\ M^{-1}\ s^{-1}$	*54*
R27	$BrOH^{\bullet-} + Br^- \rightarrow Br_2^{\bullet-} + OH^-$	$k_{27} = 2 \times 10^8\ M^{-1}\ s^{-1}$	*50*	R40	$BrO_2^- + BrO^\bullet \rightarrow OBr^- + BrO_2^\bullet$	$k_{40} = 4.0 \times 10^8\ M^{-1}\ s^{-1}$	*57*
R28a	$Br^\bullet + Br^- \rightarrow Br_2^{\bullet-}$	$k_{28a} = 1 \times 10^{10}\ M^{-1}\ s^{-1}$	*48*	R41	$BrO_2^- + {}^\bullet OH \rightarrow BrO_2^\bullet + OH^-$	$k_{41} = 2.0 \times 10^9\ M^{-1}\ s^{-1}$	*58*
R28b	$Br_2^{\bullet-} \rightarrow Br^\bullet + Br^-$	$k_{28b} = 1 \times 10^5\ s^{-1}$	*48*	R42	$BrO_2^- + Br_2^{\bullet-} \rightarrow OBr^- + BrO^\bullet + Br^-$	$k_{42} = 8 \times 10^7\ M^{-1}\ s^{-1}$	*54*
R29	$Br_2^{\bullet-} + Br_2^{\bullet-} \rightarrow Br_3^- + Br^-$	$k_{29} = 2 \times 10^9\ M^{-1}\ s^{-1}$	*51*	R43	$BrO_2^\bullet + {}^\bullet OH \rightarrow BrO_3^- + H^+$	$k_{43} = 2 \times 10^9\ M^{-1}\ s^{-1}$	*59*
R30a	$Br_3^- \rightarrow Br_2 + Br^-$	$k_{30a} = 8.3 \times 10^8\ s^{-1}$	*52*	R44a	$BrO_2^\bullet + BrO_2^\bullet \rightarrow Br_2O_4$	$k_{44a} = 6.0 \times 10^9\ M^{-1}\ s^{-1}$	*59*
R30b	$Br_2 + Br^- \rightarrow Br_3^-$	$k_{30b} = 10^{10}\ M^{-1}\ s^{-1}$	*52*	R44b	$Br_2O_4 \rightarrow BrO_2^\bullet + BrO_2^\bullet$	$k_{44b} = 3.1 \times 10^5\ s^{-1}$	*59*
R31a	$Br_2 + H_2O \rightarrow HOBr + H^+ + Br^-$	$k_{31a} = 97\ s^{-1}$	*53*	R45	$Br_2O_4 + OH^- \rightarrow BrO_3^- + BrO_2^- + H^+$	$k_{45} = 7 \times 10^8\ M^{-1}\ s^{-1}$	*54*
			Carbonate and Phosphate				
R50	$H_2CO_3{}^* \leftrightarrow H^+ + HCO_3^-$	$pK_{a,1} = 6.38$	*60*	R58	$CO_3^{\bullet-} + O_2^{\bullet-} \rightarrow CO_3^{2-} + O_2$	$k_{58} = 6.5 \times 10^8\ M^{-1}\ s^{-1}$	*64[c], 65[b]*
R51	$HCO_3^- \leftrightarrow H^+ + CO_3^{2-}$	$pK_{a,2} = 10.38$	*60*	R59	$CO_3^{\bullet-} + HO_2^- \rightarrow CO_3^{2-} + HO_2^\bullet$	$k_{59} = 5.6 \times 10^7\ M^{-1}\ s^{-1}$	*64*
R52	$HO^\bullet + HCO_3^- \rightarrow HCO_3^\bullet + OH^-$	$k_{52} = 8.5 \times 10^6\ M^{-1}\ s^{-1}$	*61*	R60	$CO_3^{\bullet-} + H_2O_2 \rightarrow HCO_3^- + HO_2^\bullet$	$k_{60} = 8 \times 10^5\ M^{-1}\ s^{-1}$	*64*
R53	$HO^\bullet + CO_3^{2-} \rightarrow CO_3^{\bullet-} + OH^-$	$k_{53} = 3.9 \times 10^8\ M^{-1}\ s^{-1}$	*58*	R61	$H_3PO_4 \leftrightarrow H_2PO_4^- + H^+$	$pK_a = 2.3$	*60*
R54	$HCO_3^\bullet \leftrightarrow H^+ + CO_3^{\bullet-}$	$pK_a < 0$	*62*	R62	$H_2PO_4^- \leftrightarrow HPO_4^{2-} + H^+$	$pK_a = 7.2$	*60*
R55	$OBr^- + CO_3^{\bullet-} \rightarrow BrO^\bullet + CO_3^{2-}$	$k_{55} = 4.3 \times 10^7\ M^{-1}\ s^{-1}$	*54*	R63	$HPO_4^{2-} \leftrightarrow PO_4^{3-} + H^+$	$pK_a = 12.3$	*60*
R56	$BrO_2^- + CO_3^{\bullet-} \rightarrow BrO_2^\bullet + CO_3^{2-}$	$k_{56} = 1.1 \times 10^8\ M^{-1}\ s^{-1}$	*54*	R64	$O_3^{\bullet-} + H_2PO_4^- \rightarrow HO_3^\bullet + HPO_4^{2-}$	$k_{64} = 2.1 \times 10^8\ M^{-1}\ s^{-1}$	*25*
R57	$CO_3^{\bullet-} + O_3^{\bullet-} \rightarrow CO_3^{2-} + O_3$	$k_{57} = 6 \times 10^7\ M^{-1}\ s^{-1}$	*63*	R65	$HO_3^\bullet + HPO_4^{2-} \rightarrow O_3^{\bullet-} + H_2PO_4^-$	$k_{65} = 2.0 \times 10^7\ M^{-1}\ s^{-1}$	*25*
			Water				
R90	$H_2O \leftrightarrow H^+ + OH^-$	$pK_w = 14.17$	*60*				

4. Hydrodynamics

Currently available simulators for drinking waters do not propose accurate modelling possibilities for the hydrodynamics of oxidation tanks. Certainly justified when simulating a whole treatment works, is this situation still acceptable when focusing on a single step, oxidation? Corollarily, how precise, how refined, should be a systemic model with regards to the final results in terms of chemical predictions?
Purpose of this report is not to answer those questions yet, but rather to evaluate how pertinent they are. Hence, we shall present first the methods used to define systemic models, then, taking a simple numerical example done with $SimO_3$, we will compare results obtained with two models of a same oxidation reactor.
Explanations on systemic models can be found in ***Appendix C****.*

4.1. Preliminaries

In most simulators, in fact all of those presented in this review except $SimO_3$ ([Gimbel and Rietveld, 2002], [Savary, 2002]) the hydrodynamics are modelled by series of CSTRs (including recirculation loops etc…), set up to reproduce as accurately as possible the characteristics of the installation (issued from the RTD – Residence Time Distribution).
Albeit simplifying the process modelling, the exclusive use of CSTRs does not exactly reproduce the physical aspects of hydrodynamics, what could affect the kinetic trends. [Dumeau de Traversay, 2000] actually chooses to eliminate a modelling that would include only series of CSTRs arguing $t_{a,CSTR} = 0$ not to have a physical validity ($t_{a,CSTR}$ is the appearance time, where 0.1% of the tracer mass has transferred). This purely hydrodynamic ground surely has some incidence on the kinetics, since it is well known - [Dumeau de Traversay, 2000], [Mälzer und Nahrstedt, 2002] – that PFRs have better reaction advancement than CSTRs.
It may be possible that a modelling of the PFRs through CSTRs cascades would lead to an extension in calculation times, but it should not be so significant since the numerical methods for solving BVPs already work with temporal meshes[8], be it multiple shooting or relaxation methods (see **5.2**). Besides, relaxation methods may be more affected than shooting methods, given that mesh selection strategies for collocation are a little bit less effective than adaptative stepsize control for IVPs.

[8] and hence subdivide the reactors yet

4.2. Calibration

As chemical models, which necessitate to be calibrated to on-site specificities (mostly related to water quality), the hydraulic modelling has to be adapted. There are basically three ways to handle this, depending on the precision desired/required: fitting to experimental chemical data, to experimental tracer studies, to numerical CFD (Computational Fluid Dynamics).
To adjust ones' systemic scheme in order to fit the chemical simulation results to experimental data could surprise. It is nevertheless a frequently employed calibration method: working with OTTER, the ozonation steps (e.g. pre-ozonation, inter-ozonation…) are required to be calibrated adjusting the number of CSTRs and the ozone bubble size [WRc OTTER User Documentation]. In doing so, the user will find values for these two parameters that minimise the prediction error for the decomposition of a specific species, say *Escherichia Coli*. This remains however a coarse approach and should be avoided.
Consequently, we shall solely present in the following the two other calibration methods, based on purely hydraulic comparisons.

4.2.1. Definitions and properties of RTD curves

A complete explanation on tracer studies can be found in [Dumeau de Traversay, 2000] or elsewhere in the literature or on the web. We shall therefore only say few words on RTD, recalling basic definitions or properties.
The RTD function E is the function defined such as $E(t)dt$ is equal to the fraction of fluid exiting the reactor that has spent a time between (t) and $(t + dt)$ in the reactor. As it can be graphically seen on figure **4.1**, this fraction corresponds to the (orange) band under the E curve. Clearly, the normalisation condition implies $\int_0^\infty E(t)dt = 1$. The quantity $\int_{t_1}^\infty E(t)dt$ represents the fraction of fluid having spent a time larger than t_1 in the reactor.

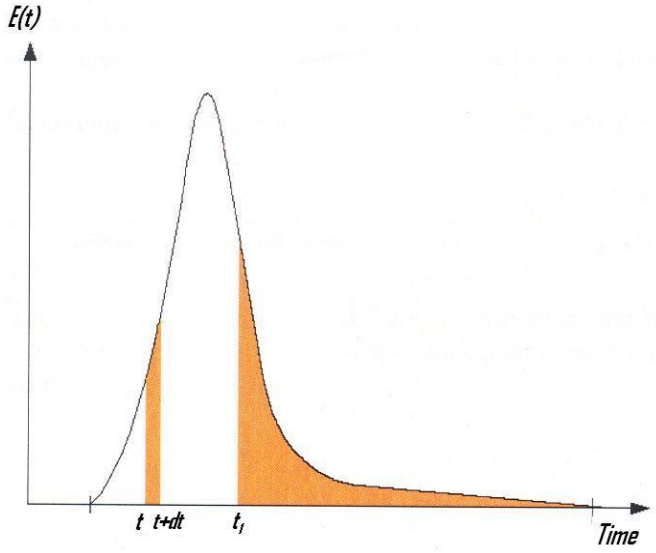

Figure 4.1 Example of a RTD E-curve

The experimental RTD curves are obtained through tracer studies. Roughly speaking, the method consists in injecting the tracer so as to get a Dirac peak or a Heavyside step profile for the tracer inlet concentration, following then the tracer outlet concentration. Injection represents thus a key parameter for this technique as it has to be performed in a manner that do not perturbs nor alters the flow conditions. Various measurements or calculations (see table **4.1**) can then be done to characterise the hydrodynamic behaviour of a tank

Table 4.1 Main parameters associated to RTD

Formula	Name – description
t_x	Time by which x% of the tracer's mass has transferred
t_{90}/t_{10}	Dispersion indice of Morill
$t_m = \int_0^\infty tE(t)dt$	Mean residence time
$\sigma^2 = \int_0^\infty (t-t_m)^2 E(t)dt$	Variance (related to dispersion)

The adjustment is done afterwards considering quantitative parameters such as those presented in the table above as well as qualitative information (e.g. intensity and peak positions on the measured curves). In the next section, to illustrate calibration procedures using RTD fitting and CFD calculations, we give the example of a typical ozonation contact chamber and its systemic modelling.

4.2.2. Example: ozonation contact chamber

- First step: calibration through RTD

An usual systemic configuration for contact tanks is the PFR-jCSTRs combination, where a PFR is followed by a cascade of CSTRs composed of j identical reactors. The parameters to be determined, to be calibrated, are in this case: (i) t_{PFR} and t_{CSTR}, mean residence times in the PFR and in each of the CSTRs respectively; (ii) the unspecified number *j*.

To get a better idea on how these parameters interact and on their relative influence over the RTD, we propose some testing. Simple numerical experiences can namely be performed to assess the sensitivity of the response (actually the E curve) to each of the over mentioned parameters. This is easily done with Matlab™, fixing two of the parameters and letting the third vary.

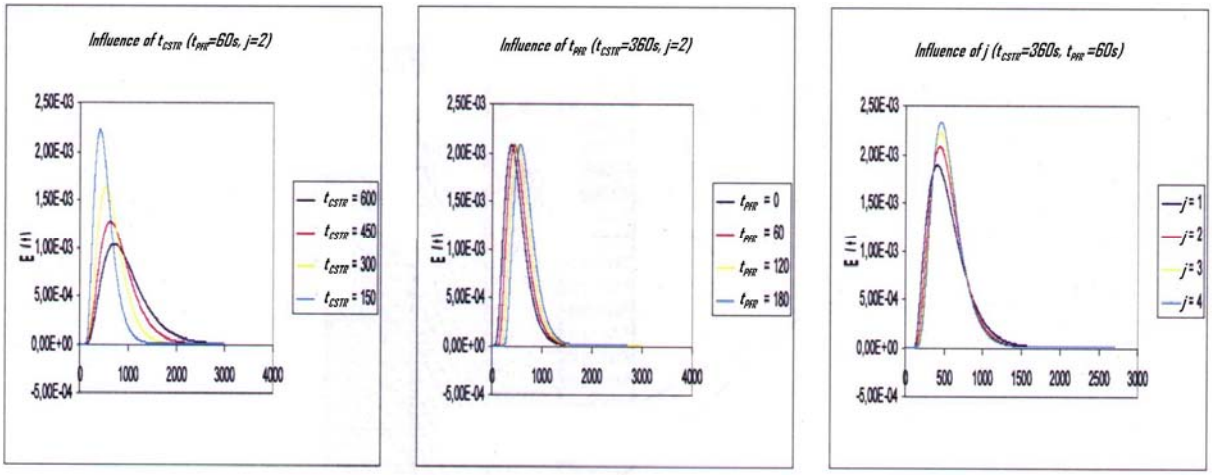

Figures 4.2 (a), (b) and (c) Comparison of the influence of each parameter: (a) influence of t_{CSTR}; (b) influence of t_{PFR}; (c) influence of j

This does not constitute and could not replace any sensitivity analysis. Nevertheless, it is interesting at first sight, to coarsely assess some main dependences. It can that way be easily seen on figures **4.2 (a)**, **(b)** and **(c)** that

- an increase of the residence time in each of the CSTRs (t_{CSTR}) causes a drop in the maximal value of the fonction and its temporal widening
- an increase of the residence time in the PFR (t_{PFR}) causes a delay in the peak apparition
- an increase of the number of CSTRs (j) causes enhancement of the peak without any temporal widening

Even if t_{CSTR} seems to be the most prevalent parameter, a more detailed study reveals without difficulty different couples (t_{CSTR}, j) that give the same RTD (figure **4.3**).

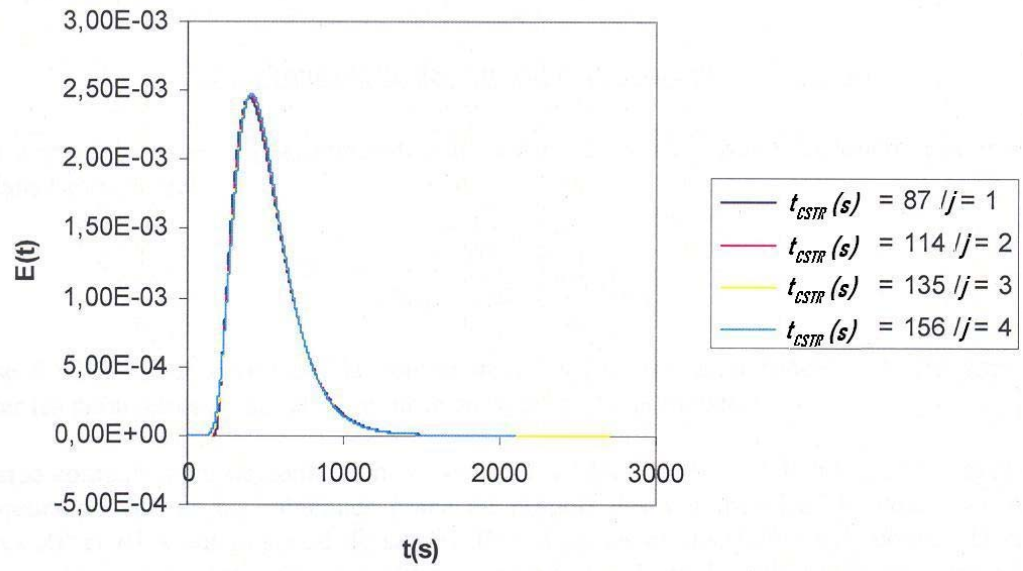

Figure 4.3 RTD for different systemic models. "Clearly", the graphs overlap each other.

- Second step: calibration through CFD

Given that such an adjustment method cannot guarantee uniqueness of the calibration and that different systemic models could represent the same hydrodynamic conditions, the degree of freedom has to be reduced introducing additional information. This can be achieved through the use of CFD: with a better insight of the hydraulic behaviours, we shall determine additional relations allowing us to fix the parameters.

The CFD simulation results were obtained with the Fluent commercial code that resolves the flow equations using finite volume approximation. Then, simply by examining the velocity fields in steady state conditions (figure **4.4**), which graphically summarize the hydrodynamic behaviour of the reactor, we can express a relation between t_{CSTR} and t_{PFR}. The systemic model is subsequently obtained without difficulties.

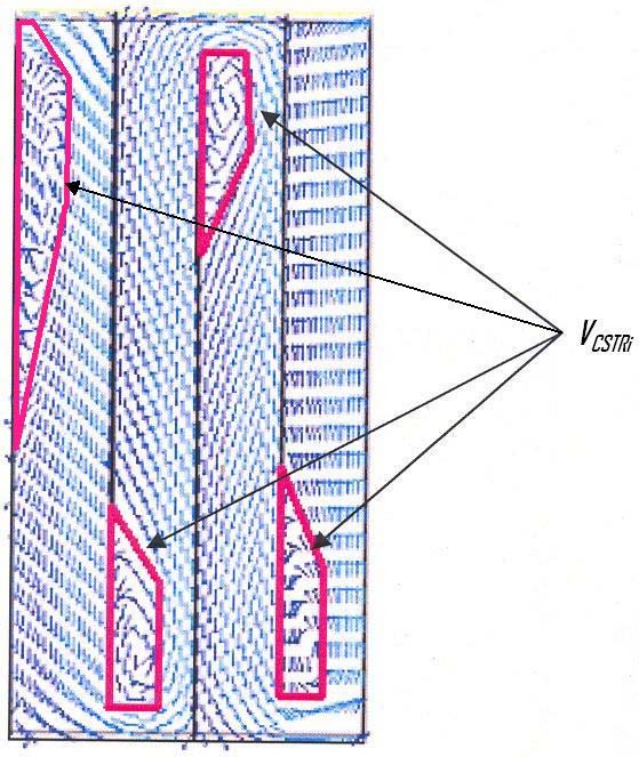

The ratio $\frac{\sum_i V_{CSTR,i}}{V_{total}}$ can be evaluated graphically measuring the surfaces marked with (red) surroundings.

Additionally, this determination could be accompanied by the analysis of the turbulent kinetic energy distribution [Dumeau de Traversay et al., 2001] in order to better locate the back-mixing zones and to estimate the direct flow and recycling flow volumes with respect to the incoming flow rate. In such a simple case, we preferred to skip this step of the calibration.

Figure 4.4 Velocity Field determined by CFD.

4.3. Second example: two models simulated with $SimO_3$

As the previous section suggests, the procedures of setting up a systemic model can be more or less refined. This point, stressed out in the introduction of this section shall now be illustrated by a concrete example done with our presently available simulator $SimO_3$.
Even if systemic models presented below were calibrated referring to hydrodynamic behaviours, their evaluation shall be done regarding their accuracy for chemical previsions. Indeed, the calibration procedures shall be balanced with the refinement of chemical pathways and (to a smaller extent) to the ability of numerical methods to converge to an acceptable solution. This can only be done examining the final results, the concentration profiles. Here the question is: Which repercussions may have the choice of a procedure?

4.3.1. Chemical model

The concepts governing the chemical reaction model used have already been presented in section **3.1.2.3.** We shall now give all the reactions involved in it

Equations of ammoniated species in water

$NH_3 + HClO \rightarrow NH_2Cl + H^+$ (**4.1**)
$NH_2Cl + HClO \rightarrow NHCl_2 + H_2O$ (**4.2**)
$NHCl_2 + HClO \rightarrow NCl_3 + H_2O$ (**4.3**)
$NCl_3 + H_2O \rightarrow NHCl_2 + HClO$ (**4.4**)
$NHCl_2 + 3H_2O \rightarrow NOH + 2Cl^- + 2H_3O^+$ (**4.5**)
$NOH + NH_2Cl \rightarrow N_2 + Cl- + H_3O^+$ (**4.6**)
$NOH + NHCl_2 + H2O \rightarrow N_2 + HOCl + H_3O^+ + Cl^-$ (**4.7**)
$NOH + 2\ HClO + 3\ H_2O \rightarrow NO_3^- + 2\ Cl^- + 3\ H_3O^+$ (**4.8**)

Acido-basic equilibria

$NH_4^+ + H_2O \leftrightarrow NH_3 + H_3O^+$ (**4.9**)
$HClO + H_2O \leftrightarrow ClO^- + H_3O^+$ (**4.10**)
$HBrO + H_2O \leftrightarrow BrO^- + H_3O^+$ (**4.11**)

Reactions involving NOM

Chorine decay

$NOM_1 + HClO \rightarrow NOM_2 + Cl^-$ (**4.12**)
$NOM_2 + HClO \rightarrow NOM_3 + Cl^-$ (**4.13**)

One step THMs formation

$NOM_1 + 3HClO \rightarrow CHCl_3$ (**4.14**)
$NOM_1 + 2\ HClO + HBrO \rightarrow CHCl_2Br$ (**4.15**)
$NOM_1 + HClO + 2\ HBrO \rightarrow CHClBr_2$ (**4.16**)

Two steps THMs formation

$NOM_2 + 3HClO \rightarrow CHCl_3$ (**4.17**)
$NOM_2 + 2\ HClO + HBrO \rightarrow CHCl_2Br$ (**4.18**)
$NOM_2 + HClO + 2\ HBrO \rightarrow CHClBr_2$ (**4.19**)

Inactivation of *Giardia*

$N\_life + HClO \rightarrow N\_killed\ (TCC.mL^{-1})$ (**4.20**)

$N\_life + ClO^- \rightarrow N\_killed\ (TCC.mL^{-1})$ (**4.21**)

$Giardia\_life + HClO \rightarrow Giardia\_killed\ (USEPA)$ (**4.22**)

$Giardia\_life + ClO^- \rightarrow Giardia\_killed\ (USEPA)$ (**4.23**)

Bromide oxidation

$HClO + Br^- \rightarrow HBrO + Cl^-$ (**4.24**)

4.3.2. Systemic models

We defined three different systemic representations of the same oxidation tank, or, at least, of similar tanks. Clearly, the differences between them are so important that their numerical RTD would not coincide. The idea is here to estimate the incidence of an important simplification in modelling on the kinetics calculations. First, a reference systemic model was designed; then a simplified reactor deriving from it was built. A third model originating from the second using only PFRs is also presented.

The reference reactor was chosen because it exhibits certain characteristics:
-simultaneous presence of CSTRs and PFRs
-presence of various branches for water flow
-a branch without recirculation (1)
-a branch (2) with recirculation loop (3)

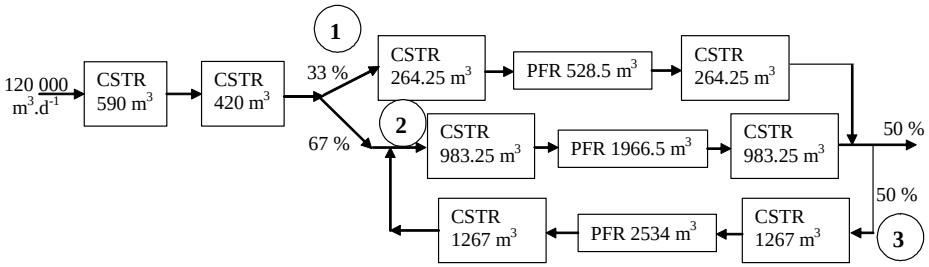

Figure 4.5 Systemic model (A) of reference reactor

The previous model has been simplified, leading to the definition of an alternative model, where branches (1) and (2) were considered as a single branch. Fewer components (ideal reactors) were used to describe the hydrodynamics.

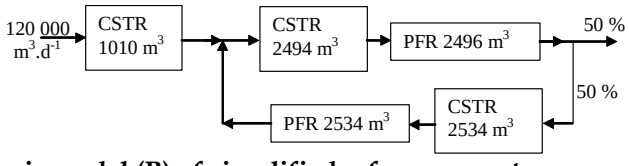

Figure 4.6 Systemic model (B) of simplified reference reactor

Finally, a third systemic model was designed to study the influence of the reactor type upon disinfection (reactor C = reactor B only composed of PFRs). Indeed, as stated in **3.2.1.** for ozonation, flow conditions have great impact on kinetics: a slow flow without back mixing is generally desired to reach good levels of disinfection with low DBPs formation rates.

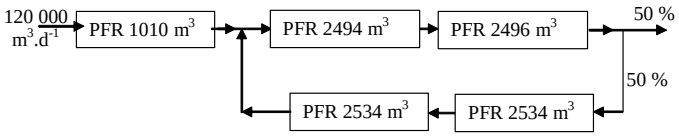

Figure 4.7 Systemic model (C)

4.3.3. Results and discussion

For each systemic model, a simulation was run under same conditions. Initial conditions for the simulation runs are gathered in table **4.2**.

Table 4.2 Initial values used for the simulations

Species	Initial value (concentration, number)
Cl_2	3 $mg.L^{-1}$
active TOC (reacting stoichiometrically with chlorine)	0.129 $mg.L^{-1}$
$N\_NH_4^+$	0.26 $mg.L^{-1}$
Br^-	35 $\mu g.L^{-1}$
N_life	800 $TCC.mL^{-1}$
Giardia_life	0.1 (arbitrary)

Since reactor A is taken as reference, results were expressed as relative deviations. They are summarised in figure **4.8.** The criteria chosen for comparison are: chlorine, TTHMs, inactivation of TCC, inactivation of *Giardia lamblia*.

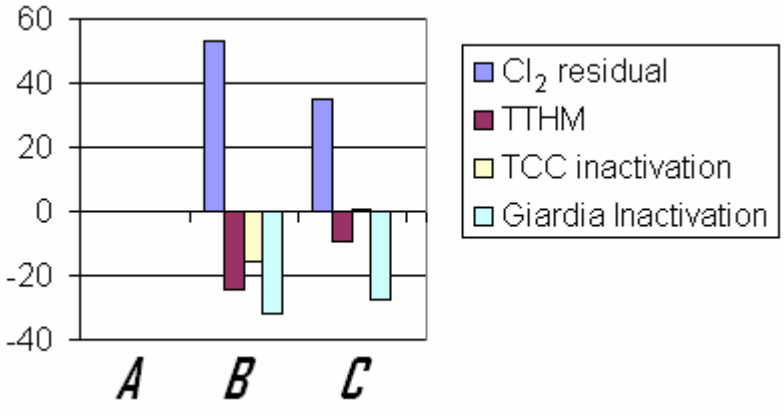

Figure 4.8 Relative deviations (%) to reactor A

Results showed that a simplification in systemic modelling resulted in an over prediction for chlorine residual and under predictions for other species or criteria considered.

Reactor B: In this case, chlorine decay was highly under predicted compared to reactor A. The absence of branch (1), where no recirculation occurs seems to have great impact on the results. Actually, the species travelling in such a branch can be quite different from those present in branches with recirculation loops: roughly speaking, one could expect to encounter "older" species in the latter. In the case of a mechanism with intermediates species (as NOM_2, contributing to chlorine decay), this seriously affects kinetics; first

chlorine decay, then other species of which formation or inactivation depend on chlorine concentration.

Reactor C: as expected, comparing to reactor B, the exclusive use of PFRs gave better results in terms of inactivation of both TCC and *Giardia*. The TTHMs formed were however formed at higher rates. This can be linked to the higher chlorine consumption.

4.4. Towards a typology of oxidation tanks

In introduction to this work, we specified the very general requirements of the simulator we propose to build up. Amidst them, adaptability plays a key role. Adaptability to on-site conditions means both (i) adaptability to chemical characteristics (i.e. water quality) and (ii) to hydrodynamic specificities (e.g. reactor geometry, equipment…).
This has much to do with calibration and, consequently, with efficiency in predicting concentration profiles. A thorough calibration is not conceivable on site; we thus decided to opt for a restricted procedure, giving the user the possibility to choose between different configurations (chemical, hydraulic). In doing so, one would dispose of two types of lists: a list of reaction pathways coming into play according to water quality; and a list of typical reactors representing all the hydrodynamic conditions encountered on site.
Following the prescribing of a calibration procedure (precedent sections), our task shall be then to establish such classification. Based on various (e.g. technical, physical, geometrical…) considerations, this typology will have to be drawn up carefully. Again, the simplicity of use and editing will have to be balanced with the accuracy of the simulator's prediction; the length of the list will have to be balanced with its ability to describe satisfactorily all possible configurations.
Though begun, this part will remain in progress for a while, given that it will really develop only after the establishing of calibration procedures.

4.5. Modelling of oxidation tanks

In this section, we shall give the equations to be solved when modeling oxidation tanks. Both chemical and physical phenomena will be taken into account, shortly presenting the equations related to chemical kinetics, transfer and mass balances. Eventually, the specificity of our approach will be enlightened with respects to modelling equations.

4.5.1. Chemical kinetics

Reaction rate

For specified chemical species, the rate of a reaction is defined as the derivative of concentration with respect to time. Reaction rates can thus either be positive or negative: a positive rate means the concentration is increasing with time, e.g. for a product; a negative rate means the concentration is falling with time, e.g. for a reagent. Defining an overall reaction rate, one should avoid such discrepancies considering one or another species engaged in a reaction. Therefore, the overall rate of a reaction includes the stoichiometric coefficients ν (positive for products, negative for reagents) in its definition. Given the following example, say

$$\left|\nu_{R_1}\right| R_1 + \left|\nu_{R_2}\right| R_2 \rightarrow \left|\nu_P\right| P \qquad (\mathbf{4.25})$$

The reaction rate becomes actually independent of the species considered when the reaction rate definition is defined as in (**4.26**)

$$r = \frac{1}{\nu_{R_1}} \cdot \frac{d[R_1]}{dt} = \frac{1}{\nu_{R_2}} \cdot \frac{d[R_2]}{dt} = \frac{1}{\nu_P} \cdot \frac{d[P]}{dt} \qquad (\mathbf{4.26})$$

Rate laws

In simple cases such as those considered herein, reactions are often found to have explicit rate laws of the form

$$r = k.[R_1]^{\alpha_1}.[R_2]^{\alpha_2} \qquad (\mathbf{4.27})$$

For an elementary process, the coefficients in (**4.27**) are substituted by the stoichiometric coefficients, i.e. $\alpha_1 = \nu_{R_1}$ and $\alpha_2 = \nu_{R_2}$. Moreover, temperature dependence is generally expressed by the Arrhenius law

$$k = k_0.\exp\left(\frac{-E_A}{RT}\right) \qquad (\mathbf{4.28})$$

where E_A: Energy of activation of the considered reaction (kJ.mol^{-1})
R: Universal gas constant (kJ.K^{-1}.mol^{-1})
T: Temperature (K)

More information on chemical kinetics is available on the internet portal of the University of Cambridge (see bibliography for further details).

4.5.2. Transfer

Without getting in details of theories for mass transfer occurring at liquid-gaseous interfaces (one could refer to [Kraume, 2004] for such information), we shall say few words on most commonly used models.
The most usual approach consists in applying the film model, which considers a stagnant layer of thickness δ between the interface and the bulk of the reacting phase, where mass transfer occurs, according to a stationary process (Whitman, 1923). More complex descriptions have been developed by Higbie (1935) and later by Danckwerts (1951) assuming that, at the interface, small stagnant elements of liquid are constantly replaced leading to a non-stationary diffusional mass transfer process. After contact time, these elements are withdrawn from the interface, mixed within the liquid bulk and replaced by fresh elements (surface renewal). While Higbie considers an equal renewal rate for each element, Danckwerts suggests an equal probability s for each element to be replaced at any instant of time, independent of its age. In the following, we will opt for the film model to describe mass transfer.
Since ozone is sparingly soluble in water, the gas phase resistance is usually considered negligible and the concentration gradient on liquid phase film controls the ozone mass transfer rate in the bulk fluid [Langlais et al., 1991]. Thus, the interfacial transfer of ozone between gas and the water can be modelled as

$$\frac{dN}{dt} = k_L \cdot a\left(C^* - C\right) \cdot dV \qquad (\mathbf{4.29})$$

where $\frac{dN}{dt}$: molar flow rate at the interface (mol.s^{-1})
k_L : liquid phase mass transfer coefficient (m.s^{-1})
a : volumetric interfacial area (m^{-1})
C : steady-state liquid phase ozone concentration (mol.m^{-3})
C^* : steady-state saturated liquid phase ozone concentration (mol.m^{-3})
dV : elementary volume considered (m^3)

■ The liquid phase mass transfer coefficient of ozone $\boldsymbol{k_L}$ can be determined by batch-scale experiments or estimated using some empirical equations proposed by Higbie (1935), Van Hughmark (1967), and Calderbank (1959). The Higbie model has been widely used to simulate mass transfer in ozonation system (**4.30**)

$$k_L = 2\sqrt{\frac{D_{O_3} V_{gas}}{\pi \cdot d_b}} \qquad (\mathbf{4.30})$$

with D_{O3} : molecular diffusivity of ozone in water

V_{gas} : gas slip velocity; $V_{gas} = |U_g - U_l|$, where U_g and U_l are respectively gas and liquid velocities

Even though relation (**4.30**) has been developed for single bubbles, its application in estimations for mass transfer coefficient k_L has been justified for bubble column design ([Hallensleben, 1980] as cited by [Bin and Roustan, 2000]).

■ The value of parameter ***a*** can be evaluated using equation (**4.31**) under the assumption that ozone is dispersed in the gaseous phase in form of identical spherical bubbles

$$a = r_g \cdot \frac{6}{d_b} \qquad (4.31)$$

with r_g : local gas phase fraction
d_b : bubble diameter

Usually, the underlying assumption of (**4.31**) cannot be satisfied, so the specific interfacial area ***a*** is not very accurately determined. Large differences may thus often be observed when comparing correlations developed for bubble columns and those suggested for single bubbles [Bin and Roustan, 2000]. To tackle such discrepancies, some authors suggested correlations to directly evaluate the product $k_L a$, which do not involve the representative bubble diameter and/or bubble rise velocity.

■ Dealing with concrete cases, one often prefer to use an evaluation of $k_L a$ instead of proceeding in a two-step manner. This type of correlations are developed on particular types of reactors (here, a bubble column) and require knowledge of the column diameter, gas superficial velocity, some fluid parameters. [Hikita et al., 1981] proposed the following relation

$$\frac{k_L a V_{SG}}{g} = 14.9 f \left(\frac{V_{SG}\mu_L}{\sigma}\right)^{1.76} \left(\frac{\rho_L \sigma^3}{g\mu_L^4}\right)^{0.25} \left(\frac{\mu_G}{\mu_L}\right)^{0.24} \left(\frac{\mu_L}{\rho_L D_{O_3}}\right)^{-0.6} \qquad (4.32)$$

where V_{SG} : superficial gas velocity
g : gravitational constant
μ : absolute dynamical viscosity (indexes L and G refer to liquid and gas)
σ : interfacial tension
ρ : volumic mass

The coefficient f varies with according to medium specifications:

$f = 1$ for a non-electrolytical medium
$f = 10^{0.07}$ if $I < 1.0$ g(ions).L^{-1}
$f = 1.1*10^{0.02}$ if $I > 1.0$ g(ions).L^{-1}

■ The liquid equilibrium concentration, C^*, can be estimated using the modified Henry's law (**4.33**)

$$C^* = \frac{C_{gas}}{H_C} \quad (4.33)$$

where C_{gas} : concentration in the bulk gas
H_C : modified Henry's constant

■ Empirical relations for modified Henry's constant have been developed by various researchers. We simply report here two of them.

i. [Perry et al., 1973] proposed a set of two equations for H_C. These are quite often used when modeling ozone transfer ([Zhang, 2006], [Kim et al., 2002]).

$$\log(H_C) = \begin{cases} 3.25 - \frac{840}{T} & \text{for } 278\text{ K} \le T \le 288\text{ K} \\ 6.20 - \frac{1687}{T} & \text{for } 288\text{ K} < T \le 303\text{ K} \end{cases} \quad (4.34)\ (4.35)$$

ii. Other authors use instead the following relation, available in [Langlais et al., 1991]

$$\ln(H_C) = 22.3 - \frac{4030}{T} \quad (4.36)$$

4.5.3. Mass balances

The mass that enters a system must (conservation of mass principle) either leave the system or accumulate within the system, i.e.

$$\text{IN} = \text{OUT} + \text{ACC} \quad (4.37)$$

where IN denotes what enters the system, OUT denotes what leaves the system and ACC denotes accumulation within the system (which may be negative or positive). Mass balances are often developed for total mass crossing the boundaries of a system, but they can also focus on one element (e.g. carbon) or chemical compound (e.g. water) as in our case. When mass balances are written for specific compounds, a production term (PROD) is introduced such that (**4.37**) becomes

$$\text{IN} + \text{PROD} = \text{OUT} + \text{ACC} \quad (4.38)$$

The production term here describes chemical reaction rates (see **4.5.1.**). It can either be positive or negative, depending on the type of species (i.e. product or reagent).

Mass balances can either be integral or differential. Basically, an integral mass balance is a black box approach considering the overall behaviour of a system, whereas a differential mass balances focuses on mechanisms within the system. Both kinds of balances have to be solved when modeling hydrodynamics with systemic schemes, referring to two types of reactors:

CSTRs or PFRs. Thus, we shall illustrate in the following mass balances with these two examples.

CSTRs

Main property of CSTRs is the chemical homogeneity (i.e. the constant concentrations) of the compounds throughout the reactor. Thus, a CSTR can be considered exactly as a black box, in which aggregated phenomena occur. An integral mass balance is therefore particularly adapted. Figure **4.9** depicts a CSTR with its parameters.

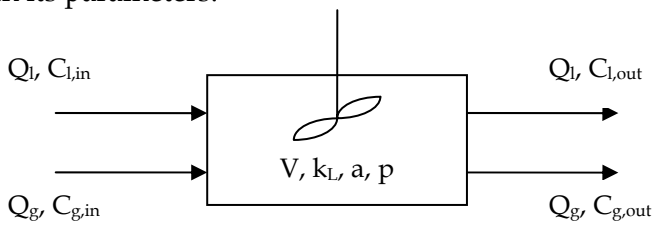

Legend: Respectively,
Q and C stand for flow and concentration
The indexes g and l for gaseous and liquid phases
in and out for inlet and outlet
p: pressure within the reactor

Figure 4.9 Schematic representation of a CSTR with its parameters

Since mass balances are performed on specific elements involved in more than one reaction, we should precise the definitions for chemical kinetics given above. Let us consider a chemical species termed A. We shall define two ensembles

1. $\mathcal{C}^A$ ensemble of rea**C**tions in which A is involved (either as reagent or as product)

2. $\mathcal{G}$ ensemble of rea**G**ents of $\mathcal{C}^A$

Moreover, the subsequent parameters must also be introduced

- ν_A stoichiometric coefficients of A in $\mathcal{C}^A$
- r stands for the elements of $\mathcal{G}$
- α_r are the exponents associated to r in the rate laws of $\mathcal{C}^A$

With the previous notations, the reaction rate relative to A can be expressed as follows (**4.39**)

$$r^A = \sum_{\mathcal{C}^A} \nu_A \prod_{\mathcal{G}} [r]^{\alpha_r} \qquad \textbf{(4.39)}$$

Note: The concentrations $[r]$ *are the concentrations found within the reactor, i.e. equal to outlet concentrations (chemical homogeneity of CSTRs).*

The mass balances for the reactor follow:

For the liquid phase

$$Q_l\left(C_{l,in}^A - C_{l,out}^A\right) + Vk_L a \cdot \left(\frac{p}{H^A} fC_{g,out}^A - C_{l,out}^A\right) + Vr^A = 0 \qquad (\mathbf{4.40})$$

For the gaseous phase

$$Q_g\left(C_{g,in}^A - C_{g,out}^A\right) - Vk_L a \cdot \left(\frac{p}{H^A} fC_{g,out}^A - C_{l,out}^A\right) = 0 \qquad (\mathbf{4.41})$$

where f is a correction factor to convert molar fractions into concentrations
p is the gas pressure
H^A is Henry's constant for the compound A (different from the previous H_C)

PFRs (monophasic)

Here, the mass balance is performed on an elementary volume and written under the simple form of an ODE (**4.42 a and b**) (Ordinary differential Equation, see **Appendix D**).

$$\begin{cases} \dfrac{dC_{l,out}^A}{dt} = r^A & \text{for } 0 < t \le V/Q \\ C_{l,out}^A = C_{l,in}^A & \text{for } t = 0 \end{cases} \qquad (\mathbf{4.42\ a\ and\ b})$$

As mentioned earlier, these equations will have to be solved as BVPs (unlike equations (**4.42 a and b**)). In the equations presented above, this means either $C_{l,out}^A$ or $C_{l,in}^A$ may be known. An incompletely known initial state reveals itself to be difficult to solve. However, some methods for BVPs exist and are presented in the next chapter.

5. Applied mathematics

The reader not familiar with the concept of ODE (Ordinary Differential Equation), and with its usual numerical resolution methods, should have a quick look at the explanations given in ***appendices D*** *and* ***E****.*

5.1. What is a Boundary Value Problem?

When ODEs are required to satisfy boundary conditions at more than one value of the independent variable, the resulting problem is called a *two-point boundary value problem TPBVP or BVP*. As the terminology indicates, the most common case by far is where boundary conditions are supposed to be satisfied at two points – usually the starting and ending values of the integration. However, the term "two-point boundary value problem" is also used loosely to include more complicated cases, e.g., where some conditions are specified at endpoints, other at interior points.
Unlike IVPs (Initial Value Problems), for which we are able to start an acceptable solution at its beginning taking the initial values and just marching it along by numerical integration to its end (see Euler's Method, **Appendix E**), the boundary conditions at the starting point do not determine a unique solution to start with.
Consequently, guaranteeing solution existence and uniqueness for BVPs is considerably more difficult than it is for IVPs. As illustration, consider the following example (taken from [Ascher et al., 1995])
Given a scalar, second-order linear BVP, say

$$\begin{cases} u''+u=0 \\ 0<x<b \end{cases} \qquad \textbf{(5.1a)}$$

satisfying the boundary conditions

$$\begin{cases} u(0)=0 \\ u(b)=\beta \end{cases} \qquad \textbf{(5.1b)}$$

The general solution to (**5.1a**), which vanishes at $x = 0$ is $u(x) = c.\sin(x)$, where c is an arbitrary constant. Thus, if $b = n.\pi$, then Equation (1a, b) has no solution when $\beta \neq 0$ and an infinite number of solutions when $\beta = 0$ (one for each value of c). Note that if, on the other hand, we now replace the condition on $u(b)$ by the initial condition

$$u'(0)=s \qquad \textbf{(5.2)}$$

Then the theorem on existence and uniqueness of solutions for IVPs guarantees that for any given scalar s, there exists an unique solution for all $x \geq 0$. Of course, that solution is

$$u(x)=s.\sin(x) \qquad \textbf{(5.3)}$$

The failure in this example to have existence or uniqueness of a solution for certain distinct values of b is typical of linear BVPs and illustrate the fact that existence and uniqueness of a BVP solution is not straightforward: it may either have a finite number of solution, or infinitely many, or none. This explains why BVP solvers require users to provide a *good* guess for the solution desired. For nonlinear problems, the situation can be much more complex. For example, it is possible that no solutions exist for all b sufficiently large.

We shall now present two families of numerical methods designed to solve BVPs: shooting methods and relaxation (also called collocation, or finite difference) methods.

5.2. How do we solve it?

5.2.1. Shooting methods

In shooting methods, we choose values for all the dependant variables at one boundary. These values must be consistent with any boundary conditions for *that* boundary, but otherwise are arranged to depend on arbitrary free parameters of which values we initially "randomly" guess. We then integrate the ODEs by initial value methods, arriving at the other boundary. In general, we find discrepancies from the desired boundary values there. Now we have a multidimensional root finding problem: find the adjustment of the free parameters at the starting point that zeroes the discrepancies at the other boundary point. If we liken integrating the differential equations to following the trajectory of a shot from gun to target, then picking the initial conditions corresponds to aiming (figure **5.1**). The shooting method provides a systematic approach to taking a set of "ranging" shots that allow us to improve our "aim" systematically.

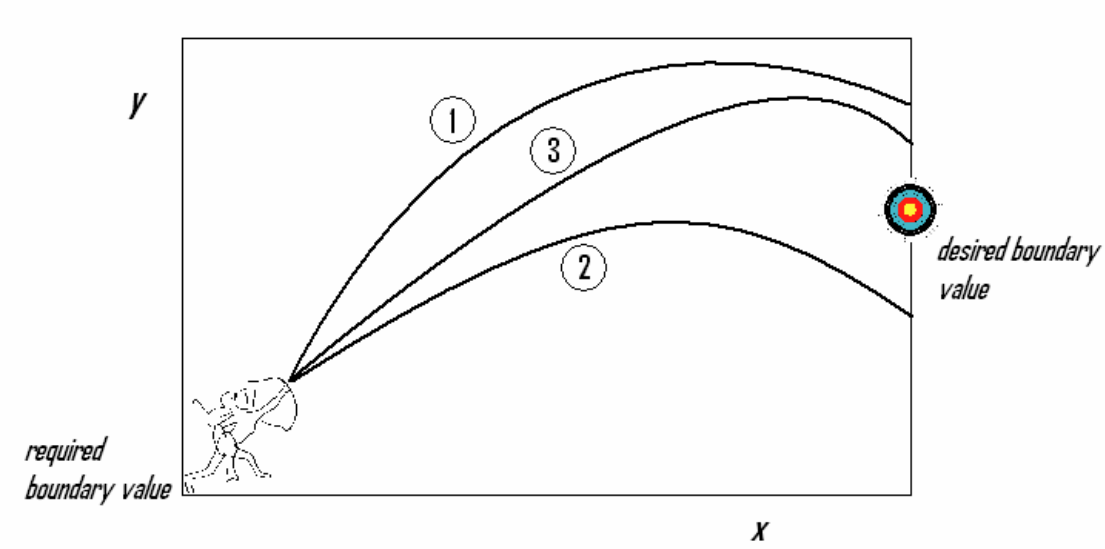

Figure 5.1 Shooting method (schematic). Trial integrations that satisfy the boundary condition at one endpoint are "launched." The discrepancies from the desired boundary condition at the other endpoint serve to adjust the starting conditions, until boundary conditions at both endpoints are ultimately satisfied, adapted from [William et al., 1993].

As another variant of the shooting method, we can guess unknown free parameters at both ends of the domain, integrate the equations to a common midpoint, and seek to adjust the guessed parameters so that the solution joins "smoothly" at the fitting point. In all shooting methods, trial solutions satisfy the differential equations "exactly" (or as exactly as we care to perform our numerical integration), but the trial solutions come to satisfy the required boundary conditions only after the iterations are finished.

Even if the above presented strategy for shooting is a simple concept easy to implement, it highly suffers from its instability[9]. This major drawback already

[9] An excellent presentation is given by [Diehl, 2006], where the notion of stability for IVPs and BVPs is clearly exposed.

arises in the linear case. Due to roundoff error accumulation, the IVPs integrated in the process could be unstable, even the BVP is well conditioned. A rough (but often approximately achievable) bound of this error is of the order [Ascher et al., 1995]

$$\varepsilon_M e^{L(b-a)} \qquad (\mathbf{5.4})$$

Where $L = \max_x \|A(x)\|$ and ε_M is the machine precision. In an attempt to decrease this bound, it is natural to restrict the size of domains over which IVPs are integrated. Thus, the interval of integration [a, b] is subdivided by a mesh

$$a = x_1 < x_2 < \cdots < x_{N-1} < x_N = b$$

And then, as in shooting, initial value integrations are performed on each subinterval $[x_i, x_{i+1}]$, $1 \le i \le N$ (see figure **5.2**). The resulting solution segments are patched up to form a continuous solution over the entire interval [a, b]. This leads to the method of *multiple shooting*.

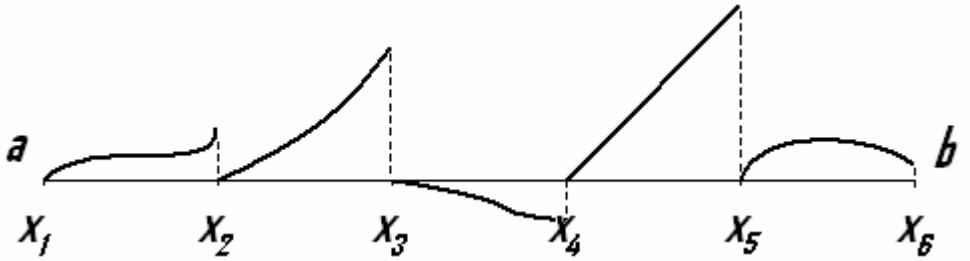

Figure 5.2 Multiple shooting (schematic). The integration interval [a, b] has been split in subdomains where single shooting is applied. Additional constraints are introduces at the mesh points.

Though working with much more larger systems compared to those of single shooting, the computational costs are not as prohibitive one could suppose. Indeed, some intrinsic properties of the problem formulation can easily be exploited (e.g. the banded structure of the Jacobian, the possibility of "condensing" etc… [Ascher et al., 1995], [Diehl, 2006]).

5.2.2. Relaxation methods

Relaxation methods use a different approach. The differential equations are replaced by finite-difference equations on a mesh of points that spans the range of the integration. A trial solution consists of values for the dependent variables at each mesh point, *not* satisfying the desired finite-difference equations, nor necessarily even satisfying the required boundary conditions (see figure **5.3**).

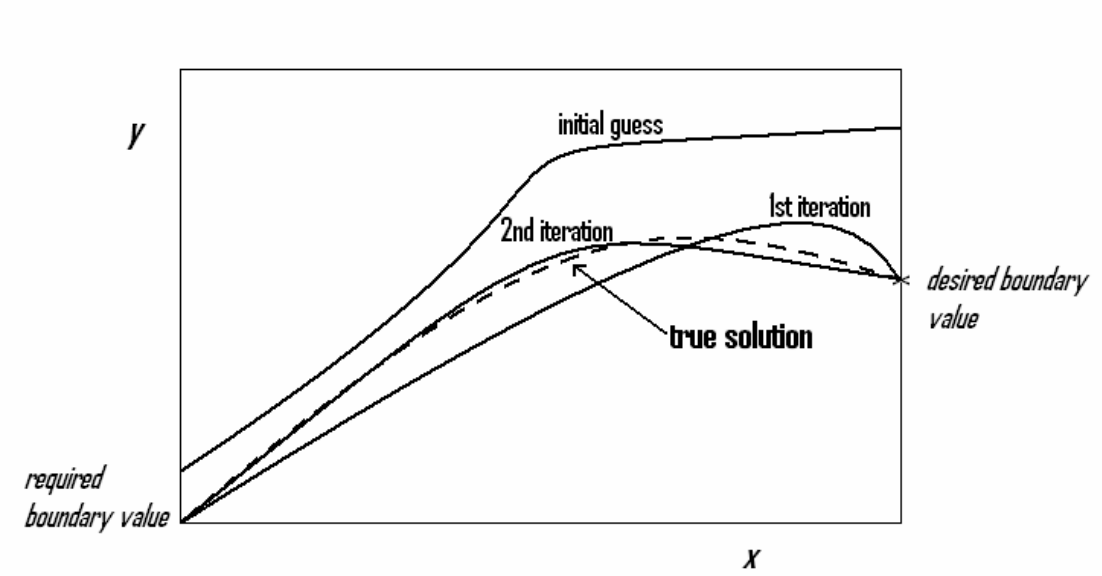

Figure 5.3 Relaxation method (schematic). An initial solution is guessed that approximately satisfies the differential equation and boundary conditions. An iterative process adjusts the function to bring it into close agreement with the true solution, adapted from [William et al., 1993].

The iteration, now called *relaxation*, consists in adjusting all the values on the mesh so as to bring them into successively closer agreement with the finite-difference equations and, simultaneously, with the boundary conditions. For example, if the problem involves three coupled equations and a mesh of one hundred points, we must guess and improve three hundred variables representing the solution.
Relaxation methods then determine the solution by starting with a guess and improving it, iteratively. As the iterations progress to the solution, the result is said to *relax* to the true solution. Given that the approximated solution is made up of the union of all the polynomial interpolation functions for each subinterval of the mesh, collocation methods principally differ in:
-The choice of the collocation points (different schemes exist: Lobatto – used with Matlab's bvp4c, Gauss…)
-The choice of the polynomial basis (e.g. B-splines, Hermite-splines, Runge-Kutta-basis, …) [Diehl, 2006].

5.2.3. Elements of comparison

Trying to compare numerical methods is often a difficult task, as mentioned by [Ascher et al., 1995]. Much more is involved than just an evaluation of arithmetic operations needed in each method when one seeks to preliminary compare them. However, some general considerations can be given and set in regards of the specific constraints of our problem.

- When the IVPs are very unstable, shooting should be avoided. Unstable IVPs can namely cause a shooting code to fail because the integration "blows up" before reaching the end of the interval. More often, though, the IVP solver reaches the end, but is unable to compute an accurate result there and, in turn, the nonlinear equation solver is unable to find accurate initial values. A variety of techniques are employed to improve shooting, but when the IVPs are very

unstable, shooting is just not a natural approach to solving BVPs [Shampine et al., 2000].

- Relaxation works better than shooting when the boundary conditions are especially delicate or subtle, or when they involve complicated algebraic relations that cannot easily be solved in closed form.
- Relaxation works best when the solution is smooth and not highly oscillatory. Such oscillations would require many gridpoints for an accurate representation. Moreover, the number and position of required points may not be known *a priori*. Shooting methods are then preferred in such cases, because their variable stepsize integrations adjust naturally to a solution's particularities [William et al., 1993].
- Good initial guesses are the secret of efficient relaxation methods. Often one has to solve a problem many times, each time with a slightly different value of some parameter. In that case, the previous solution is usually a good initial guess when the parameter is changed, and relaxation will work well.

Relaxation methods are often preferred when the ODEs have extraneous solutions which, while not appearing in the final solution satisfying all boundary conditions, may wreak havoc on the initial values integrations required by shooting. The typical case is that of trying to maintain a dying exponential in the presence of growing exponentials [William et al., 1993]. This explains why most efforts to solve practical stiff BVPs reported to date have used finite difference methods. Many methods exist which are supported by a fairly thorough analysis, or by a good practical experience, or by both [Ascher et al., 1995].

Table 5.1 First elements of comparison for the choice of the numerical method. The topics of main relevance in our problem correspond to the greyed cells.

Topic\Num. method	Relaxation	Shooting
Unstable IVPs	**X**	
Subtle BCs	**X**	
Oscillatory solution		**X**
Stiff problem	**X**	
Poor guesses		**X**

Table **5.1** summarises the first conclusions that can be drawn from the literature. We shall now see how pertinent the criteria are in regards of our problem

- The IVPs, representing the chemical mass balances, to be solved are not particularly unstable
- The boundary conditions are straightforward
- The solutions do not behave oscillatory (smooth concentration profiles)
- The problem is extremely stiff[10]: the chemical rate constants range from 10^{20} $M^{-1}.s^{-1}$ to 10 $M^{-1}.s^{-1}$ (M=mol.L^{-1})
- Initial guesses are not obvious

[10] On stiffness for ODEs or BVPs, see **Appendix F**

Concerning the last point, it seems that a combined approach with artificial intelligence methods (as ANNs – Artificial Neural Networks) could help to provide sufficiently good guesses. Hence, even if guesses have to be made over the entire integration interval, a way could be found to solve the equations with relaxation methods.
The most challenging part of the numerical analysis for our problem consists certainly in the stiffness of the equations. Although shooting methods can be effective in the treatment of such BVPs, relaxation is often preferred. This is also reflected in the amount of papers where finite-difference techniques are employed to solve stiff BVPs. However, this crucial point should not be decided so far: many practical stiff BVPs were handled with the shooting approach [Leineweber et al., 1997], [England et al., 2002].

To gain experience on BVP solving, we have decided to first perform some testing with Matlab™'s built-in subroutine bvp4c. Quite easy to implement, this relaxation method allows us to have a first glance at the concrete problem we will solve.

5.3. First numerical tests

5.3.1. Bvp4c

We give first some specific explanations about the subroutine used with Matlab to solve BVPs. A more exhaustive presentation can be found in [Shampine et al., 2000] or [Ketzscher and Shampine, 2003].

bvp4c implements a collocation method for the solution of BVPs of the form

$$\begin{cases} y' = f(x, y, p) \\ a \le x \le b \end{cases} \tag{5.5}$$

subject to general nonlinear, two-point boundary conditions

$$g(y(a), y(b), p) = 0 \tag{5.6}$$

Here p is a vector of unknown parameters. For simplicity it is suppressed in the expressions that follow. The approximate solution S(x) is a continuous function that is a cubic polynomial on each subinterval $[x_n, x_{n+1}]$ of a mesh $a=x_0 < x_1 <\ldots< x_N = b$. It satisfies the boundary conditions

$$g(S(a), S(b)) = 0 \tag{5.7}$$

and the differential equations (collocates) at both ends and the midpoint of each subinterval

$$\begin{gathered} S'(x_n) = f(x_n, S(x_n)) \\ S'\left(\frac{x_n + x_{n+1}}{2}\right) = f\left(\frac{x_n + x_{n+1}}{2}, S\left(\frac{x_n + x_{n+1}}{2}\right)\right) \\ S'(x_{n+1}) = f(x_{n+1}, S(x_{n+1})) \end{gathered} \tag{5.8 to 5.10}$$

These conditions result in a system of nonlinear algebraic equations for the coefficients defining *S(x)*. In contrast to shooting, the solution *y(x)* is approximated over the whole interval [a; b] and the boundary conditions are taken into account at all times. The nonlinear algebraic equations are solved iteratively by linearization, so this approach relies upon the linear equation solvers of Matlab™ rather than its IVP codes. The basic method of bvp4c, which we call Simpson's method, is well-known and is found in a number of codes.

As already said in the previous section, BVP codes require users to supply a guess for the solution desired. In doing so, the user also guesses also an initial mesh that should reveal the behaviour of the desired solution. The codes then adapt the mesh so as to obtain an accurate numerical solution with a modest number of mesh points. Coming up with a sufficiently good guess is often the hardest part of solving a BVP. bvp4c takes an unusual approach to the control of error that helps it deal with poor guesses. The continuity of *S(x)* on [a, b] and collocation at the ends of each subinterval constrain *S(x)* to have a continuous derivative on [a, b]. For such an approximation, the residual *r(x)* in the ODEs is defined by

$$r(x) = S'(x) - f(x, S(x)) \tag{5.11}$$

Put differently, this says that S(x) is the exact solution of the perturbed ODEs

$$S'(x) = f(x, S(x)) + r(x) \qquad (\mathbf{5.12})$$

Similarly, the residual in the boundary conditions is *g(S(a), S(b))*.
The task of bvp4c is hence to control the sizes of these residuals. If the residuals are uniformly small, *S(x)* is a good solution in the sense that it is the exact solution of a problem close to the one supplied to the solver. Shooting codes can also be described as controlling the sizes of these residuals: at each step, an IVP code controls the local error, which is equivalent to controlling the size of the residual of an appropriate continuous extension of the formula used, and the nonlinear equation solver is used to find initial values for which the residual in the boundary conditions is small.
Residual control has important virtues: residuals are well-defined no matter how bad the approximate solution, and residuals can be evaluated anywhere simply by evaluating *f(x, S(x))* or *g(S(a), S(b))*. bvp4c is based on algorithms that are plausible even when the initial mesh is very poor, yet furnish the correct results as the step size tends to zero, exploiting some very interesting properties of the Simpson method [Shampine et al., 2000].

5.3.2. Simulation results

We present here some of the first results trying to solve BVPs of relevance with bvp4c. These problems were chosen because of their chemical application: they correspond actually to the ozonation decomposition mechanisms found in [Savary, 2002] and [Westerhoff et al., 1998] (see **3.2.4.4.**).

Unfortunately, due to a computer crash, we are unable to present here the results of the simulations run under Matlab.

Conclusion

Trying to answer the questions formulated in introduction of this report, some responses were found while other questions appeared. We shall summarise here the first findings that can be drawn from our study, the next actions to be taken and their related objectives, the questions raised by our approach.

1. Preliminary contacts to build up a common TECHN'EAU modelling platform were taken with the teams of WRc and TU Delft.
2. Solving our kind of numerical problem, one should give preference to relaxation over shooting methods. The next step is hence to refine the results already obtained with bvp4c. Nevertheless, the possibility of multiple shooting is not evinced. Moreover, variational methods, not cited here, (Galerkin, Finite-Elements methods) are also widely used to solve comparable problems. Could we take advantage of them if we fail in our first attempts?
3. It is doubtful if the systemic schemes should include PFRs, given that all possible numerical methods base on discretisation. The theoretical loss (even if a CSTR cascade models a PFR adequately) would surely be compensated by the gain in simplicity.
4. Hydrodynamic calibration methods are not difficult to implement, under the assumption that a CFD study has been made. We now have to choose an ad-hoc calibration procedure, the typology of oxidation tanks being a step further… although establishing such classification can influence over calibration procedure (trough the limitation of the reactors present on the list for example).
5. Chemical phenomena as instantaneous ozone demand and NOM implication are only partially understood and will be probably modelled via semi-empirical (as in the model developed in [Savary, 2002] for $SimO_3$), empirical-statistical tools or artificial intelligence-based methods. These tools could also be used to provide initial guesses for the solver.
6. Inspired by the previous studies listed in this report (but not only), chemical pathways will have to be selected. This task does not represent a major challenge for ozonation given the existing literature; it seems however more difficult in the case of chlorination. We shall hence rather opt for a semi-mechanistic model for chlorination.
7. Last point: sensitivity, i.e. how hydrodynamics, kinetics and (in lesser part) numerical methods interact. Answering the corollary question: how refined should be the reaction pathway? How accurate should be hydraulic modelling? cannot be overlooked and will be our major concern developing the simulator.

Bibliography

Articles and books

- **Adin A., Katzhendler J., Alkaslassy D.** and **Rav-Acha C**., THM formation in chlorinated drinking water: a kinetic model, *Water Research*, Vol. 25, No. 7, pp. 797-805, 1991.
- **Amy G. L., Chadik P. A.** and **Chowdhury Z. K**, Developing Models for Predicting Trihalomethane Formation Potential and Kinetics, *Journal A.W.W.A.*, Vol. 79, No. 7, pp. 89-97, 1987.
- **Ascher U. M.**, **Mattheij R. M. M.** and **Russel R. D.**, Numerical Solution of Boundary Value Problems for Ordinary Differential Equations, SIAM Classics in Applied Mathematics, Philadelphia, 1995.
- **Bégoc C.**, Proposition d'un modèle mécanistique pour la formation des THM, Master's degree thesis, ENSC-R, Laboratoire de Chimie des Nuisances et Génie de l'Environnement, 2000.
- **Bin A. K.** and **Roustan M.,** Mass transfer in ozone reactors, *Proceedings of the international specialised symposium on IOA 2000, Fundamental and engineering concepts for ozone reactor design*, Toulouse, March 1-3, pp. 99-131, 2000.
- **Boccelli D. L., Tryby M. E., Uber J. G.** and **Summers R. S.**, A reactive species model for chlorine decay and THM formation under rechlorination conditions, *Water Research,* Vol. 37, pp. 2654-2666, 2003.
- **Buffle M.-O.**, Mechanistic Investigation of the Initial Phase of Ozone Decomposition in Drinking Water and Wastewater, Ph. D thesis, Swiss Federal Institute of Technology Zürich, pp. 49-84, 2005.
- **Butt G.** and **Head R.**, Development of a prototype treatment works management based on real-time process simulation, *Water Science and Technology: Water supply*, Vol. 2, No. 1, pp. 81-86, 2002.
- **Casey T. J.** and **Chua K. H.,** Aspects of THM formation in drinking waters, *Aqua - Journal of Water Supply: Research and Technology*, Vol. 46, No. 1, pp. 31-39, 1997.
- **Chelkowska K., Grasso D., Fabian I.** and **Gordon G.**, Numerical simulation of aqueous ozone decomposition, *Ozone Science and Engineering*, Vol. 23, pp. 259-284, 1992.
- **Clark R. M**., Predicting Chlorine Residuals and Formation of TTHMs in Drinking Water, *Journal of Environmental Engineering, ASCE*, Vol. 124, No. 12, pp. 1203-1210, 1998.
- **Doré M.**, Chimie des oxydants et traitement des eaux, Tec et Doc Lavoisier, Paris, 1989.
- **Driedger A.M., Rennecker J.L**. and **Mariñas B.J.**, Inactivation of Cryptosporidium parvum oocysts with ozone and monochloramine at low temperature, *Water research*, Vol. 35, No. 1, pp. 41-48, 2001.
- **Dudley J.** and **Dillon G.**, Water treatment simulators: state-of-the-art review, Techneau internal note, 2005.
- **Duguet J. P. et al.,** Réglementation et traitement des eaux destinées à la consommation humaine, Association Scientifique et Technique pour l'Eau et l'Environnement. (A.S.T.E.E.). Paris, 2006.

- **Dumeau de Traversay C.**, De la mécanique des fluides numérique à l'approche systémique: application aux réacteurs d'oxydation en potabilisation, PhD thesis ENSC-R, Laboratoire de Chimie des Nuisances et Génie de l'Environnement, 2000.
- **Dumeau de Traversay C.**, **Luck F.**, **Wolbert D.** and **Laplanche A.**, Hydrodynamics of ozonation tanks: definition of systemic models from CFD, Vivendi internal note, 2001.
- **England R.**, **Lamour R.** and **Lopez-Estrada J.**, Multiple shooting using a dichotomically stable integrator for solving differential-algebraic equations, *Applied numerical mathematics*, Vol. 42, Issues 1-3, pp. 117-131, 2002.
- **Engorholm B. A.** and **Amy G. L.**, A predictive model for chloroform formation from humic acid, *Journal A.W.W.A.*, Vol. 75, No. 8, pp. 418-423, 1983.
- **Gang D. C., Clevenger T. E.** and **Banerji S. K.**, Modeling chlorine decay in surface water, *Journal of Environmental Informatics,* Vol. 1, No. 1, pp. 21-27, 2003.
- **Gimbel R.** and **Rietveld L.C.**, Concept study to buid up a co-operation with the TU-Delft in the field of drinking water treatment plant modelling (METREX and Stimela), Gerard-Mercator-Universität Duisburg / TU Delft, Internal note, January 2002.
- **Hallensleben J.,** Simultaner Stoffaustausch von CO_2 und Sauerstoff an Einzelnblasen und in Blasenschwärmen, Ph. D. thesis, Universität Hannover, 1980.
- **Harrington G. W.**, **Chowdury Z. K.** and **Owen D. M.**, Developing a computer model to simulate DBP formation during water treatment, *Journal A.W.W.A.*, Vol. 84, No. 11, pp. 78-87, 1992.
- **Head R.**, **Shepherd D.**, **Butt G.** and **Buck G.**, OTTER mathematical process simulation of potable water treatment, *Water Science and Technology: Water supply*, Vol. 2, No. 1, pp. 95-101, 2002.
- **Hikita H., Asai S., Tanigawa K., Segawa K.** and **Kitao M**., The volumetric liquid-phase mass transfer coefficient in bubble columns, *Chemical Engineering Journal*, Vol. 22, No. 1, pp. 61-69, 1981.
- **Hoigné J.** and **Bader H.,** Characterization of water quality criteria for ozonation processes. Part II: Lifetime of added ozone, *Ozone Science and Engineering,* Vol. 16, No. 2, pp. 121-134, 1994.
- **Hoigné J.**, **Bader H.** and **Haag W**., Rate constants of reactions of ozone with organic and inorganic compounds in water-III. Inorganic compounds and radicals, *Water Research*, Vol. 19, No. 8, pp. 993-1004, 1985.
- **Hoigné J.**, Characterization of water-quality criteria for ozonation processes.1: Minimal set of analytical data, *Ozone Science and Engineering*, Vol. 16, No. 2, pp. 113-120, 1994.
- **Hom L. W.,** Kinetics of chlorine disinfection in an ecosystem, *Journal of the Sanitary Engineering Division*, Vol. 98, No. 1, pp. 183-194, 1972.
- **Jadas-Hécart A., Morer A. E., Stitout M., Bouillot P.** and **Legube B.**, Modélisation de la demande en chlore d'une eau traitée, *Water Research*, Vol. 26, pp. 1073-1084, 1992.
- **Kavanaugh M. C., Trussell A. R., Cromer J.** and **Trussell R. R.**, An empirical kinetic model of trihalomethane formation: applications to meet

the proposed THM standards, *Journal A.W.W.A.*, Vol. 72, No. 10, pp. 578-582, 1980.
- **Kim J.-H.,** Integrated optimization of cryptosporidium inactivation and bromate formation control in ozone contactor, Ph. D. thesis, University of Illinois, 2002.
- **Kim J. H., Tomiak R. B.** and **Mariñas B. J.**, Inactivation of Cryptosporidium oocysts in a pilot-scale ozone bubble-diffuser contactor. I: Model development. *Journal of Environmental Engineering-Asce*, Vol. 128, No. 6, pp. 514-521, 2002.
- **Kim J.-H., von Gunten U.** and **Mariñas B. J.**, Simultaneous predicion of *Cryptosporidium parvum Oocyst* inactivation and bromate formation during ozonation of synthetic waters, *Environ. Sci. Technol.*, Vol. 38, No. 7, pp. 2232-2241, 2004.
- **Krasner S. W., Gramith J. T., Coffey B. M.** and **Yates R.S.**, Impact of water quality and operational parameters on the formation and control of bromate during ozonation, *Water Supply*, Vol. 13, No. 1, pp. 145-156, 1995.
- **Langlais B., Reckhow D. A.** and **Brink D.R.,** Ozone in Water Treatment: Application and Engineering, LEWIS, 1991.
- **Laplanche A., Lemasle M., Wolbert D., Galey C.** and **Cavard J.**, Contribution of molecular and radical mechanisms in bromate formation during ozonation processes, *International Regional Conference I.O.A. Poitiers, September 23-25*, 29-1-29-10, 1998.
- **Leineweber D.**, **Bock H. G.**, **Schlöder J. P.**, **Gallitzendörfer J. V.**, **Schäfer A.**, **Jansohn P.**, A Boundary value problem approach to the optimisation of chemical processes described by DAE models, Technical report preprint 97-14, IWR, Universität Heidelberg, 1997.
- **Lu W.**, **Kiéné L.** and **Lévi Y.,** Chlorine demand of biofilms in water distribution systems, *Water Research,* Vol. 33, No. 3, pp. 827–835, 1999.
- **Mälzer H.-J.** und **Nahrstedt A.**, Modellierung mehrstufiger Trinkwasseraufbereitungsanlagen mittels eines expertensystem-basierten Simulationsmodells (METREX) am Beispiel von Oberflächenwasser, Abschlussbericht, I.W.W., 2002.
- **Muñoz Ramirez G.**, Approche cinétique de la demande immédiate en ozone, PhD thesis ENSC-R, Laboratoire de Chimie des Nuisances et Génie de l'Environnement, 1997.
- **Noack R.** and **Doerr W.**, Reaction of chlorine dioxide and mixtures there of with humic acids: in interim report, *Water Chlorination: environmental impact and health effects*, Vol. 2, pp. 49-58, 1977.
- **Ozekin K.** and **Amy G.,** Threshold levels of bromate formation in drinking water, *Ozone Science and Engineering*, Vol. 19, No. 4, pp. 323-337, 1997.
- **Park H.-S., Hwang T.-M., Kang J. W., Choi H.** and **Oh H.-J.,** Characterization of raw water for the ozone application measuring ozone consumption rate, *Water Research*, Vol. 35, No. 11, pp. 2607-2614, 2001.
- **Perry R. H., Green D. W.** and **Maloney J.O.**, Chemical Engineers handbook. New York, McGraw-Hill Professional, 1973.
- **Qualls R. G.** and **Johnson J. D.**, Kinetics of short-term consumption of chlorine by fulvic acid, *Environ. Sci. Technol.*, Vol. 17, pp. 692–698, 1983.
- **Rietveld L.C.**, Improving operation of drinking water treatment through modelling, Ph.D. thesis, T.U. Delft, 2005.

- **Rietveld L.C., van Schagen K.M.** and **van Dijk J.C.**, Information technology for linking research to education and training in drinking water treatment, Proceedings of the 2004 Water Institute of Southern Africa (WISA) Biennal Conference, May 2nd-6th, Cape Town, South Africa.
- **Roccaro P.**, **Mancini G.** and **Vagliasindi F. G. A.**, Water intended for human consumption – Part I: Compliance with European water quality standards, *Desalination*, Vol. 176, No. 1, pp. 1-11, 2005.
- **Roth J. A**. and **Sullivan D. E.** Kinetics of Ozone Decomposition in Water, Ozone: Science & Engineering, Vol. 20, No. 2, 137-140, 1983.
- **Sadiq R.** and **Rodriguez M.J.,** Disinfection by-products (DBPs) in drinking water and the predictive models for their occurrence: a review, *Science of the total environment*, Vol. 321, No.1-3, pp. 21-46, 2004.
- **Savary B.**, Influence des caractéristiques d'une eau naturelle sur la formation des ions bromates au cours de l'ozonation: Observations-Prévisions-Simulations dans un réacteur diphasique du type colonne à bulles, PhD thesis ENSC-R, Laboratoire de Chimie des Nuisances et Génie de l'Environnement, 2002.
- **Sehested K.**, **Corfitzen H., Holcman J., Fischer C. H**. and **Hart E. J**., The primary reaction in the decomposition of ozone in acidic aqueous solutions, *Environ. Sci. Technol*., Vol. 25, No. 9, pp. 1589-1596, 1991.
- **Song R., Minear R., Westerhoff R.** and **Amy G.,** Bromate formation and control during water ozonation, *Environmental Technology*, Vol. 17, No. 8, pp. 861-868, 1996.
- **Song R., Westerhoff R., Minear R.** and **Amy G.**, Bromate minimization during ozonation, *Journal A.W.W.A.,* Vol. 89, No. 6, pp. 69-78, 1997.
- **Tang G., Adu -Sarkodie K., Kim D., Kim J.-H, Teefy S., Shukairy H.** and **Mariñas B. J.**, Modeling *Cryptosporidium parvum Oocyst* inactivation and bromate formation in a full-scale ozone contactor, *Environ. Sci. Technol*., Vol. 39, No. 23, pp. 9343-9350, 2005.
- **USEPA**, Guidance manual for compliance with the filtration and disinfection requirements for public water systems using surface water sources. EPA 68-01-6989, U.S. Environmental Protection Agency, Washington, D.C, 1991.
- **van der Helm A.W.C.** and **Rietveld L.C.**, Modelling of drinking water treatment processes within the Stimela environment, *Water Science and Technology: Water supply*, Vol. 2, No. 1, pp. 87-93, 2002.
- **Vieira P., Coelho S. T.** and **Loureiro D.**, Accounting for the influence of initial chlorine concentration, TOC, iron and temperature when modelling chlorine decay in water supply, *Journal of water supply: Research and Technology-AQUA,* Vol. 53, No. 7, pp. 453-467, 2004.
- **von Gunten U.** and **Hoigné J,** Bromate formation during ozonation of bromide containing waters, *11th Ozone world congress proceedings, San Francisco*, Vol. 1, S-9-42, S-9-45, 1993.
- **von Gunten U.**, Ozonation of drinking water: Part I. Oxidation kinetics and product formation-Review, *Water Research*, Vol. 37, No. 7, pp. 1443-1467, 2003a.
- **von Gunten U.,** Ozonation of drinking water: Part II. Disinfection, and by-product formation in presence of bromide, iodide or chlorine, *Water Research*, Vol. 37, No. 7, pp. 1469-1487, 2003b.

- **von Gunten U., Pinkernell U.**, Ozonation of bromide-containing drinking waters: a delicate balance between disinfection and bromate formation. *Water Science and Technology*, Vol. 41, No. 7, pp. 53-59, 2000.
- **Wang R.** Y., Etude de l'hydrodynamique et du transfert de l'ozone dans une colonne à bulles en ascension libre, Ph.D. thesis, Université de Toulouse, 1995.
- **Westerhoff P.**, Kinetic-based models for bromate formation in natural waters, EPA report, 2002.
- **Westerhoff P., Song R., Amy G.** and **Minear R.,** Application of ozone decomposition models, *Ozone Science and Engineering*, Vol. 19, No. 1, pp. 55-74, 1997.
- **Westerhoff P.**, **Song R.**, **Amy G.** and **Minear R.**, Numerical kinetic models for bromide oxidation to bromine and bromate, *Water Research*, Vol. 32, No. 5, pp. 1687-1699, 1998.
- **William H.P.**, **Saul A.** and **Brian P.**, Numerical recipes in C: the art of scientific computing (2nd Ed.), Cambridge University Press, Cambridge, 1993.
- **Yurteri C.** and **Gurol M. D.**, Ozone consumption in natural waters: effects of background organic matter, pH and carbonate species. *Ozone Science & Engineering*, Vol. 10, No. 3, pp. 277-290, 1988.
- **Zhang J.,** An integrated design approach for improving drinking water ozone disinfection treatment based on computational fluid dynamics, Ph. D. thesis, University of Waterloo, Ontario, 2006.

Others (presentations and courses)

- **Adams J. Q.** and **Clark R. M.**, Controlling Disinfection By-Products and Microbial Contaminants in Drinking Water, Chapter 14: Control of microbial contaminants and Disinfection By-Products (DBPs): Cost and Performance, USEPA, 1991. Available at http://www.epa.gov/ORD/NRMRL/pubs/600r01110/600r01110chap14.pdf
- **Diehl M.**, Solution of boundary value problems, short course „nonlinear parameter estimation and optimum experimental design", Universität Heidelberg, June 2006. Available at http://www.iwr.uni-heidelberg.de/groups/agbock/TEACHING/SKRIPTE/PEXTALKS/pex4.pdf
- **Dudley J.**, State of the art in water treatment modelling programms, Presentation at the TU Delft, 2006. Available online at http://www.citg.tudelft.nl/live/binaries/5e94158e-81d6-41ef-929c-dce11cd4aa8d/doc/Dudley.pdf
- **Eriksson M.,** Ozone chemistry in aqueous solution-Ozone decomposition and stabilisation, Licentiate thesis, Department of Chemistry, Royal Institute of Technology, Stockholm, Sweden, 2005. Available at http://urn.kb.se/resolve?urn=urn:nbn:se:kth:diva-303
- **Ketzscher R.** and **Shampine L.F.**, S. A. Forth, Use of automatic differentiation in Matlab's boundary value solver bvp4c, Proceedings of the

20th Numerical Analysis Conference, University of Dundee, 2003. Available at http://www.dcmt.cranfield.ac.uk/esd/amor/filestore/rk_dundee03.pdf
- **Kim J.-H,** Integrated optimization of Cryptosporidium inactivation and bromate formation control in ozonation contactors, Presentation at the Gwangju Institute of Technology, May 27, 2004. Available at http://env1.kjist.ac.kr/~wr21/file/workshop/p3.pdf
- **Kraume M.,** Verfahrenstechnik I und II, Skripte zur Vorlesung, Technische Universität Berlin, 2004.
- **LeChevallier M. W.** and **Au K.-K.**, Water Treatment and Pathogen Control: Process Efficiency in Achieving Safe Drinking Water. Published by IWA Publishing, London, 2004. Chapter four available at http://www.who.int/water_sanitation_health/dwq/en/watreatpath4.pdf
- **McClellan J. N., Reckhow D. A., Tobiason J. E.** and **Edzwald J. K.,** A comprehensive kinetic model for chlorine decay and chlorination by-product formation, Department of Civil and Environmental Engineering, University of Massachusetts/Amherst, 2006. Available at http://www.ecs.umass.edu/cee/reckhow/publ/84/acschapter.html
- **Shampine L. F.**, **Kierzenka J.** and **Reichelt M. W.**, Solving boundary value problems for ordinary differential equations in Matlab with bvp4c, Matlab tutorial, 2000. Available at http://www.mathworks.com/bvp_tutorial
- WRc OTTER Version 2.0 User Documentation.

Internet resources

- City of Longmont: www.ci.longmont.co.us/water_waste/lab/treated.htm
- United States EPA Ground and Drinking Water Homepage: http://www.epa.gov/safewater/index.html
- Wikipedia Article on water purification: http://en.wikipedia.org/wiki/Water_purification
- Washington State Department of Health, Division of Environmental Health, Office of Drinking Water: http://ww2.doh.wa.gov/ehp/dw/RULES/lab_regula.htm
- The European Directive on the quality of water intended for human consumption (98/83/EC): http://europa.eu.int/eur-lex/pri/en/oj/dat/1998/l_330/l_33019981205en00320054.pdf
- Lectures notes on chemical kinetics from the Chemistry Teaching at the University of Cambridge. Available at: http://www-teach.ch.cam.ac.uk/teach/IA/Kinetics_05_full.pdf
- A very didactic web site about Euler's method: http://www.ugrad.math.ubc.ca/coursedoc/math100/notes/mordifeqs/euler.html
- Explanations about mathematics can be found at: http://mathworld.wolfram.com
- The most comprehensive software catalogue on the web (sic): http://www.mpassociates.gr
- Stimela homepage: http://www.stimela.nl

- WEST's Homepage: http://www.hemmis.com/products/west/default_west.htm
- About BioWin: http://www.envirosim.com/products/bw32/bw32intro.php
- About Watpro: http://www.hydromantis.com/software08.html

Appendix A

European legal frame for water disinfection

We reproduce here some extracts of the European council directive 98/83/EC of 3 November 1998 on the quality of water intended for human consumption.
The Directive 98/83/EC is intended to protect human health by laying down healthiness and purity requirements, which must be met by drinking water within the Community. It applies to all water intended for human consumption apart from natural mineral waters and waters which are medicinal products.
Member States shall ensure that such drinking water:

- does not contain any concentration of micro-organisms, parasites or any other substance which constitutes a potential human health risk;
- meets the minimum requirements (microbiological and chemical parameters and those relating to radioactivity) laid down by the directive.
- They will take any other action needed in order to guarantee the healthiness and purity of water intended for human consumption.

Compared to the previous European drinking water directive of 1980 the number of parameters has been reduced, allowing member to add parameters such as magnesium, total hardness, phenols, zinc, phosphate, calcium and chlorite.
We reproduce in the following pages the first annex of the directive 98/83/EC regarding the parameters and the parametric values to meet.

PART A

Microbiological parameters

Parameter	Parametric value (number/100 ml)
Escherichia coli (E. coli)	0
Enterococci	0

The following applies to water offered for sale in bottles or containers:

Parameter	Parametric value
Escherichia coli (E. coli)	0/250 ml
Enterococci	0/250 ml
Pseudomonas aeruginosa	0/250 ml
Colony count 22 °C	100/ml
Colony count 37 °C	20/ml

PART B

Chemical parameters

Parameter	Parametric value	Unit	Notes
Acrylamide	0,10	µg/l	Note 1
Antimony	5,0	µg/l	
Arsenic	10	µg/l	
Benzene	1,0	µg/l	
Benzo(a)pyrene	0,010	µg/l	
Boron	1,0	mg/l	
Bromate	10	µg/l	Note 2
Cadmium	5,0	µg/l	
Chromium	50	µg/l	
Copper	2,0	mg/l	Note 3
Cyanide	50	µg/l	
1,2-dichloroethane	3,0	µg/l	
Epichlorohydrin	0,10	µg/l	Note 1
Fluoride	1,5	mg/l	
Lead	10	µg/l	Notes 3 and 4
Mercury	1,0	µg/l	
Nickel	20	µg/l	Note 3
Nitrate	50	mg/l	Note 5
Nitrite	0,50	mg/l	Note 5
Pesticides	0,10	µg/l	Notes 6 and 7
Pesticides — Total	0,50	µg/l	Notes 6 and 8
Polycyclic aromatic hydrocarbons	0,10	µg/l	Sum of concentrations of specified compounds; Note 9
Selenium	10	µg/l	
Tetrachloroethene and Trichloroethene	10	µg/l	Sum of concentrations of specified parameters
Trihalomethanes — Total	100	µg/l	Sum of concentrations of specified compounds; Note 10
Vinyl chloride	0,50	µg/l	Note 1

Note 1: The parametric value refers to the residual monomer concentration in the water as calculated according to specifications of the maximum release from the corresponding polymer in contact with the water.

Note 2: Where possible, without compromising disinfection, Member States should strive for a lower value.

For the water referred to in Article 6(1)(a), (b) and (d), the value must be met, at the latest, 10 calendar years after the entry into force of the Directive. The parametric value for bromate from five years after the entry into force of this Directive until 10 years after its entry into force is 25 µg/l.

Note 3: The value applies to a sample of water intended for human consumption obtained by an adequate sampling method [1] at the tap and taken so as to be representative of a weekly average value ingested by consumers. Where appropriate the sampling and monitoring methods must be applied in a harmonised fashion to be drawn up in accordance with Article 7(4). Member States must take account of the occurrence of peak levels that may cause adverse effects on human health.

Note 4: For water referred to in Article 6(1)(a), (b) and (d), the value must be met, at the latest, 15 calendar years after the entry into force of this Directive. The parametric value for lead from five years after the entry into force of this Directive until 15 years after its entry into force is 25 µg/l.

Member States must ensure that all appropriate measures are taken to reduce the concentration of lead in water intended for human consumption as much as possible during the period needed to achieve compliance with the parametric value.

When implementing the measures to achieve compliance with that value Member States must progressively give priority where lead concentrations in water intended for human consumption are highest.

Note 5: Member States must ensure that the condition that [nitrate]/50 + [nitrite]/3 ≤ 1, the square brackets signifying the concentrations in mg/l for nitrate (NO_3) and nitrite (NO_2), is complied with and that the value of 0,10 mg/l for nitrites is complied with ex water treatment works.

Note 6: 'Pesticides' means:

— organic insecticides,

— organic herbicides,

— organic fungicides,

— organic nematocides,

— organic acaricides,

— organic algicides,

— organic rodenticides

— organic slimicides,

— related products (*inter alia*, growth regulators)

and their relevant metabolites, degradation and reaction products.

Only those pesticides which are likely to be present in a given supply need be monitored.

Note 7: The parametric value applies to each individual pesticide. In the case of aldrin, dieldrin, heptachlor and heptachlor epoxide the parametric value is 0,030 µg/l.

Note 8: 'Pesticides — Total' means the sum of all individual pesticides detected and quantified in the monitoring procedure.

Note 9: The specified compounds are:

— benzo(b)fluoranthene,

— benzo(k)fluoranthene,

— benzo(ghi)perylene,

— indeno(1,2,3-cd)pyrene.

Note 10: Where possible, without compromising disinfection, Member States should strive for a lower value.

The specified compounds are: chloroform, bromoform, dibromochloromethane, bromodichloromethane.

For the water referred to in Article 6(1)(a), (b) and (d), the value must be met, at the latest, 10 calendar years after the entry into force of this Directive. The parametric value for total THMs from five years after the entry into force of this Directive until 10 years after its entry into force is 150 µg/l.

Member States must ensure that all appropriate measures are taken to reduce the concentration of THMs in water intended for human consumption as much as possible during the period needed to achieve compliance with the parametric value.

When implementing the measures to achieve this value, Member States must progressively give priority to those areas where THM concentrations in water intended for human consumption are highest.

PART C

Indicator parameters

Parameter	Parametric value	Unit	Notes
Aluminium	200	µg/l	
Ammonium	0,50	mg/l	
Chloride	250	mg/l	Note 1
Clostridium perfringens (including spores)	0	number/100 ml	Note 2
Colour	Acceptable to consumers and no abnormal change		
Conductivity	2 500	µS cm^{-1} at 20 °C	Note 1
Hydrogen ion concentration	≥ 6,5 and ≤ 9,5	pH units	Notes 1 and 3
Iron	200	µg/l	
Manganese	50	µg/l	
Odour	Acceptable to consumers and no abnormal change		
Oxidisability	5,0	mg/l O_2	Note 4
Sulphate	250	mg/l	Note 1
Sodium	200	mg/l	
Taste	Acceptable to consumers and no abnormal change		
Colony count 22°	No abnormal change		
Coliform bacteria	0	number/100 ml	Note 5
Total organic carbon (TOC)	No abnormal change		Note 6
Turbidity	Acceptable to consumers and no abnormal change		Note 7

RADIOACTIVITY

Parameter	Parametric value	Unit	Notes
Tritium	100	Bq/l	Notes 8 and 10
Total indicative dose	0,10	mSv/year	Notes 9 and 10

Note 1: The water should not be aggressive.

Note 2: This parameter need not be measured unless the water originates from or is influenced by surface water. In the event of non-compliance with this parametric value, the Member State concerned must investigate the supply to ensure that there is no potential danger to human health arising from the presence of pathogenic micro-organisms, e.g. cryptosporidium. Member States must include the results of all such investigations in the reports they must submit under Article 13(2).

Note 3: For still water put into bottles or containers, the minimum value may be reduced to 4,5 pH units.

For water put into bottles or containers which is naturally rich in or artificially enriched with carbon dioxide, the minimum value may be lower.

Note 4: This parameter need not be measured if the parameter TOC is analysed.

Note 5: For water put into bottles or containers the unit is number/250 ml.

Note 6: This parameter need not be measured for supplies of less than 10 000 m^3 a day.

Note 7: In the case of surface water treatment, Member States should strive for a parametric value not exceeding 1,0 NTU (nephelometric turbidity units) in the water ex treatment works.

Note 8: Monitoring frequencies to be set later in Annex II.

Note 9: Excluding tritium, potassium -40, radon and radon decay products; monitoring frequencies, monitoring methods and the most relevant locations for monitoring points to be set later in Annex II.

Note 10:

1. The proposals required by Note 8 on monitoring frequencies, and Note 9 on monitoring frequencies, monitoring methods and the most relevant locations for monitoring points in Annex II shall be adopted in accordance with the procedure laid down in Article 12. When elaborating these proposals the Commission shall take into account *inter alia* the relevant provisions under existing legislation or appropriate monitoring programmes including monitoring results as derived from them. The Commission shall submit these proposals at the latest within 18 months following the date referred to in Article 18 of the Directive.

2. A Member State is not required to monitor drinking water for tritium or radioactivity to establish total indicative dose where it is satisfied that, on the basis of other monitoring carried out, the levels of tritium of the calculated total indicative dose are well below the parametric value. In that case, it shall communicate the grounds for its decision to the Commission, including the results of this other monitoring carried out.

Appendix B

The CT concept

In order to compare the biocidal effectiveness of disinfectants, the USEPA defined and imposed in 1991 the CT concept as measurement for disinfection. Major considerations are the disinfectant concentration and the time needed to attain inactivation of a certain microbial population exposed under specific conditions.
The CT concept originates from the disinfection model of Chick and Watson (1908), presented in section **3.1.3.** We recall here equation **2.10**

$$\frac{dN}{dt} = -kC^n N \qquad (\mathbf{B.1})$$

n: dilution coefficient
C: disinfectant concentration
N: microorganism concentration
k: apparent constant rate, sometimes called lethality coefficient

Assuming constant disinfectant concentration, one obtains

$$\ln\left(\frac{N}{N_0}\right) = -kC^n \cdot t \qquad (\mathbf{B.2})$$

For a dilution coefficient n = 1, the inactivation is then directly linked to the product Ct. This lead to the introduction of the CT concept in potable water treatment.

C is defined as average ozone residual concentration at the outlet of the contact chamber evaluated by direct measurement through contactor sampling ports or estimated from table **B.1**. T is the residence time which is usually prescribed as t_{10}, the residence time of the earliest ten percent of microorganisms to travel from the contactor inlet to outlet, as determined from a tracer RTD (Residence Time Distribution) ([USEPA, 1991], [Zhang, 2006]). The USEPA employs this conservative t_{10} value to ensure a minimum exposure time for ninety percent of the water and microorganisms entering a disinfection contactor to disinfectants.

Table B.1 C concentration values used in the CT calculation

Type of chamber	C value for the CT calculation
First dissolution	*Not applicable for* Cryptosporidium*, but certain inactivation credit can be granted for* Giardia *and viruses, provided that the ozone residual at the outlet of the first contact chamber met minimum concentration levels*
Reactive	C_{out}
Co-current dissolution	$\max(C_{out}, \frac{C_{in} + C_{out}}{2})$
Counter-current dissolution	$\frac{C_{out}}{2}$
Turbine diffuser	C_{out}

CT values have been developed for inactivation of various microorganisms for the major disinfectants. Examples of these values are shown in table **B.2** [Adams and Clark, 2001].
It is evident from table **B.2** that ozone shows the highest disinfection efficiency, inactivating 99% of most types of microorganisms at very low CT values. Chloramine shows the lowest efficiency. For these data, the dilution coefficient *n* has been shown to vary between 0.7 and 1.3; therefore, a value of *n* = 1 was chosen for the referenced analysis. Preformed chloramine was used because it is conservative with respect to CT values.

Table B.2 Summary of CT value ranges for inactivation of various microorganisms by disinfectants (mg.L^{-1}.min^{-1}), adapted from [Adams and Clark, 2001]

Microorganism	Free chlorine 6 < pH < 7	Preformed chloramine 8 < pH < 9	Chlorine dioxide 6 < pH < 7	Ozone 6 < pH < 7
E. coli	0.34 - 0.05	95 - 180	0.4 - 0.75	0.02
Polio virus – 1	1.1 – 2.5	768 – 3740	0.2 – 6.7	0.1 – 0.2
Rotavirus	0.01 – 0.05	3806 – 6476	0.2 – 2.1	0.006 – 0.06
Phage f_2	0.08 – 0.18	ND	ND	ND
G. lamblia cysts	47 – 150	2200[a]	26[a]	0.5 – 0.6
G. muris cysts	30 – 630	1400	7.2 – 18.5	1.8 – 2.0
Cryptosporidium parvum	7200[b]	7200[c]	78[c]	5 – 10[b]

Note: all CT values are for 99% inactivation at 5°C except for *Giardia lamblia* and *Cryptosporidium parvum*.
[a]Values for 99.9% inactivation at pH 6 – 9
[b]99% inactivation at pH 7 and 25°C
[c]90% inactivation at pH 7 and 25°C
ND: no data

Appendix C

Some considerations on hydraulic systemic modelling

A systemic model is a structure of interconnected ideal reactors such as PFRs (Plug Flow Reactors) or CSTRs (Completely Stirred Tank Reactors). Although reproducing satisfactorily the flow dispersion inside the contactor, it provides less information than CFD regarding the flow pattern.
Modelling of oxidation stages can then be achieved using a tool, which solves mass balances of all the chemical species in each of the reactors that constitute the systemic model. Main advantage of solving the problem that way: the computation time is considerably shortened compared to the days (!) necessary to solve the same chemical problem with a CFD hydraulic scheme… Actually, CFD resolutions are heavily dependent on the refinement of the modelling: a fine meshing cell size is crucial. This implies very long calculation times and cannot be applied for on-site simulators (none of the simulators cited in this work performs calculations that way).

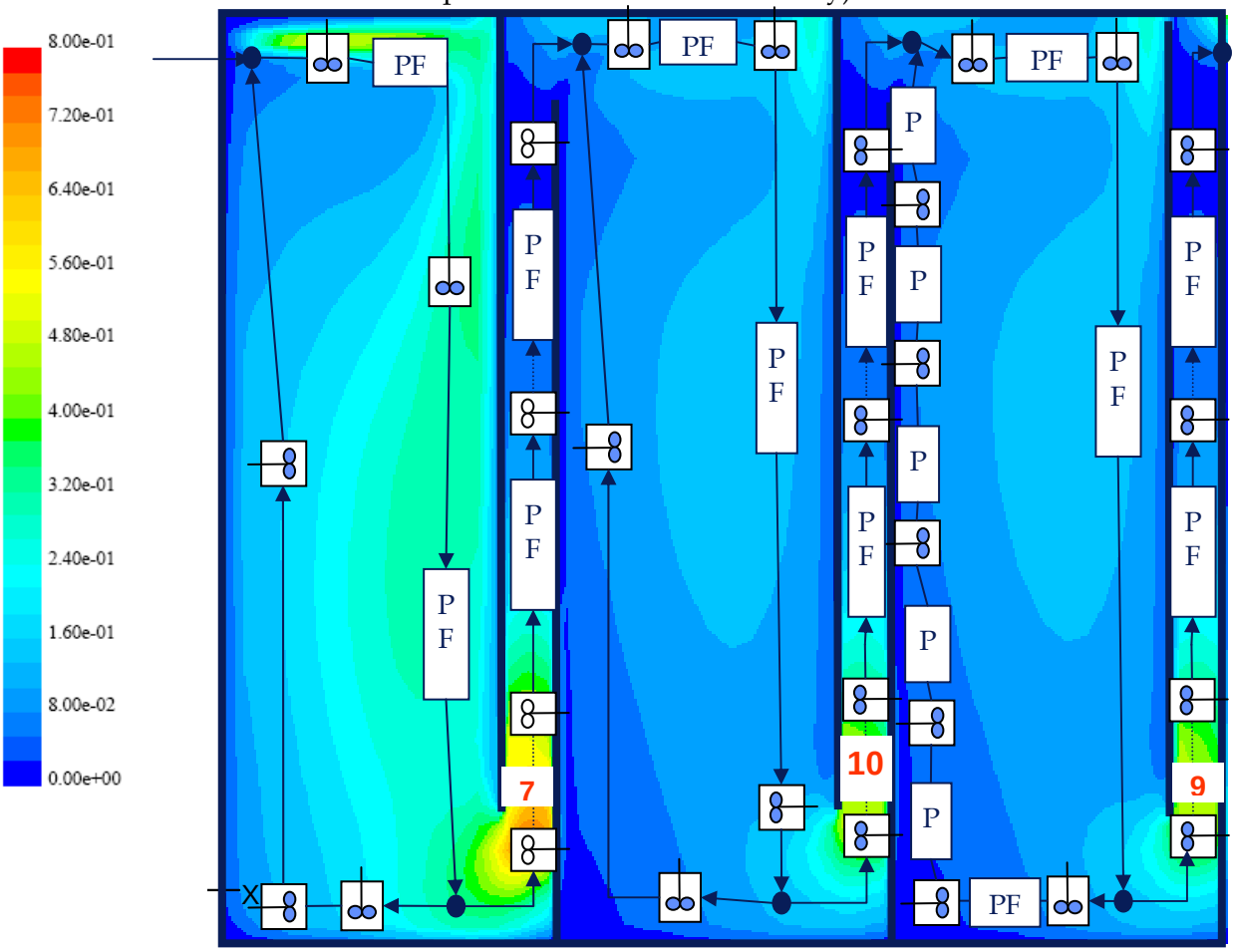

Velocity fields of a chlorination tank obtained with the CFD software Fluent.
Systemic scheme associated.

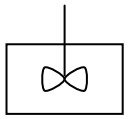

Completely Stirred Tank Reactor

P F

Plug Flow Reactor

Appendix D

ODEs

Ordinary Differential Equations (frequently called "ODEs") are equalities involving a function and its derivatives. An ODE of order n is an equation of the form:

$$F(x, y, y', \ldots, y^{(n)}) = 0 \qquad \textbf{(D.1)}$$

- where y is a function of x, *and only* x. The term "ordinary" is actually used for mathematical quantities that are functions of a single variable
- x is here the independent variable; in most cases, it refers to the time
- $y'=dy/dt$ is the first derivative with respect to x, and $y^{(n)}=d^n y/dx^n$ is the n^{th} derivative with respect to x

Without boundary conditions specification, an ODE is incomplete and cannot be solved. They are therefore essential to ODEs: the number of boundary conditions required is the same as the order of the ODE. Roughly, there are two kinds of problems when solving an ODE with regards to the boundary conditions:

- **Initial Value Problem** – all the boundary conditions are specified at the starting value of the independent variable. Physically, this corresponds to a complete knowledge of the initial state.

- **Boundary Value Problem** – boundary conditions are given at various points. For instance, some boundary conditions may be specified at the initial point and some at one or more other points. So, the problem can be either a two-point boundary value problem or a multipoint boundary value problem.

Explanations on the simplest numerical method to solve ODEs are given in the next appendix. The careful reading is highly recommended if the expression "Euler's method" does not ring any bell in the ones' mind.

Appendix E

Euler's method

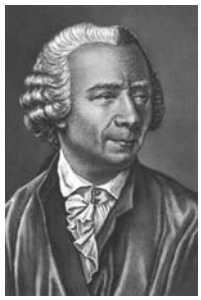

Euler (1707-1783) developed a very simple, yet effective for many problems, numerical method to solve ODEs.

Leonhard Euler (Swiss mathematician who enormously contributed to a wide range of mathematics and physics including analytic geometry, trigonometry, geometry, calculus and number theory)

Let us take a simple example of which solution is hopefully known to everybody, say

$$\frac{dy}{dt} = y \qquad \textbf{(E.1)}$$

$$y(0) = 1 \qquad \textbf{(E.2)}$$

We now suppose being interested in the value of the solution at t=1. How to get a good approximation of it?
Hint: Already noticed that the differential equation also tells us the derivative of the solution at t=0?

$$\frac{dy}{dt}(0) = y(0) = 1 \qquad \textbf{(E.3)}$$

Here comes Euler's intuition: a function behaves similarly to its derivative *around* the point where the derivative was calculated, so why not approximate a function by successive derivatives, calculated at various locations? In other words, this is equivalent to make a linear approximation of a function, assimilating a curve to its tangent.
In our case, one can approximate the solution constructing, step by step, the successive derivatives. Here are the results with increasing numbers of mesh points (steps of evaluation of the derivatives).

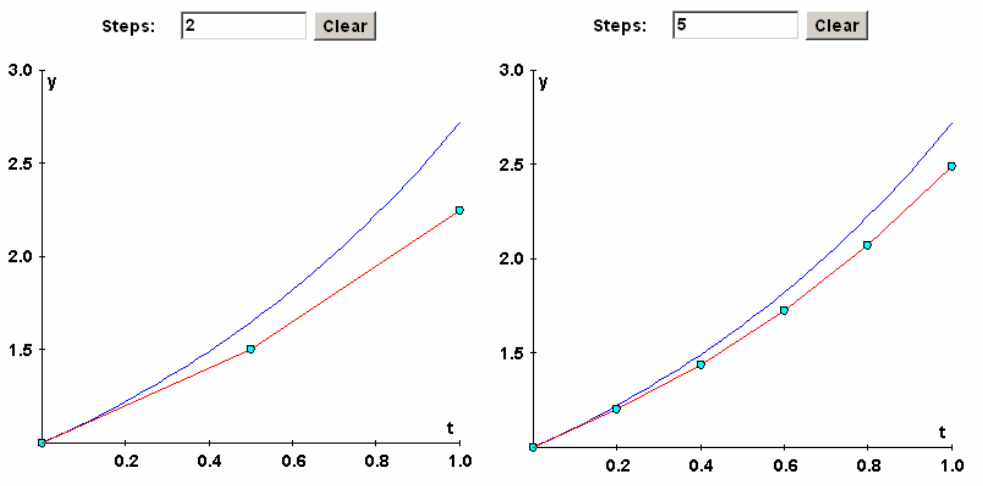

Approximation of the exponential function on the interval [0,1] through use of Euler's method. Graphs generated on the following website: http://www.ugrad.math.ubc.ca/coursedoc/math100/notes/mordifeqs/euler.html

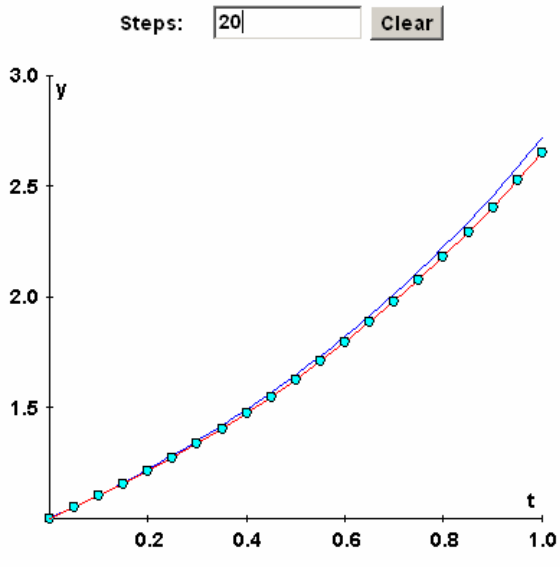

Approximation of y with 20 steps.

Remarks:

1. For each of the approximated functions, the calculations are performed at the mesh points basing on the calculations done at the previous points. It can thus be seen that the approximated functions (red segments) deviate from the solution (blue curve): progressing in the construction of the approximated solution, the method accumulates the errors of the previous steps.
2. Obviously, the graphs give evidence that an increase of the mesh points has positive influence over the final results, i. e. the calculated value at time t=1. This has to be balanced with the increased number of calculations.

Appendix F

Stiff problems

A thorough explanation can be found in various texts. This appendix is largely inspired by the reading of [Ascher et al., 1995].

Many chemical applications involve initial value problems with fast and slow decay rates (just think at chemical constants related to very rapid and very slow reactions). For instance, a solution may look like

$$y(x) = e^{-x} + e^{-1000x}, x \geq 0 \qquad \textbf{(F.1)}$$

With the second component corresponding to much faster time scale than the first. So, for x positive away from 0, the solution behaves essentially like e^{-x} and large step sizes may be taken for good accuracy. Nevertheless, the numerical method may be restricted to using very small steps, in the case that its absolute stability region is limited, because of the presence of a fast time scale in differential equation. This is the problem of *stiffness*. An ODE system of the form

$$y' = f(x, y) \qquad \textbf{(F.2)}$$

which is defined on the interval [a, b], is said to be *stiff* in a neighbourhood of a solution y if there exists a component of y of which variation is large compared to $[b-a]^{-1}$. Often stiffness can directly be related to the eigenvalues of the local Jacobian matrix $\frac{\partial f}{\partial y}(x, y(x))$, viz. to the situation where

$$\min(\mathrm{Re}(\lambda_i))(b-a) << -1$$

Appendix G

Program codes in Matlab™

Unfortunately, due to a computer crash, this appendix is unavailable.